# MODELLING AND TREATING DYSREGULATED FIBROSIS IN PRIMARY OPEN ANGLE GLAUCOMA

By

Lisa Jayne Hill

A thesis submitted to the University of Birmingham for the degree of DOCTOR OF PHILOSOPHY

Molecular Neuroscience Group
Neurotrauma and Neurodegeneration Section
School of Clinical and Experimental Medicine
University of Birmingham
April 2014

## Abstract

### Introduction

A primary risk factor for Primary Open Angle Glaucoma is elevated intraocular pressure induced by reduced outflow of aqueous humour through the trabecular meshwork due to fibrosis, which causes retinal ganglion cell death and loss of vision. This study aimed to: 1), create a rodent model of increased intraocular pressure achieved by the induction of trabecular meshwork fibrosis; 2), evaluate the ability of an anti-fibrotic agent, Decorin, to diminish established trabecular meshwork fibrosis and lower intraocular pressure; 3), correlate these findings to RCG survival and 4), investigate alternative translational methods for delivery of Decorin into the anterior chamber.

### Methods

Fibrotic agents, kaolin or TGF-β, were intracamerally injected in rats to induce fibrosis and intraocular pressure elevation. Following a sustained elevation in intraocular pressure human recombinant Decorin was administered intracamerally. Fibrosis was measured by immunohistochemistry and electron microscopy. Retinal ganglion cell counts were performed from retinal whole mounts. Visual Evoked Potentials were obtained for functional integrity of the visual pathway.

### Results

Kaolin injections did not induce fibrosis. TGF-β injections induced fibrosis of the trabecular meshwork leading to a sustained elevation in IOP and retinal ganglion cell death, thus providing a reliable *in vivo* model of the ocular fibrosis. Decorin reversed the TGF-β induced

fibrosis in the trabecular meshwork, lowered intraocular pressure and indirectly prevented progressive loss of retinal ganglion cells. Decorin was successfully delivered to the anterior chamber in an eye drop formulation.

**Conclusion**

Decorin may be an effective treatment to reverse fibrosis of the trabecular meshwork, lower intraocular pressure and hence prevent RGC death, thereby preserving visual function in patients with POAG.

**Acknowledgements**

I would like to thank my supervisors Professor Ann Logan and Dr Wendy Leadbeater for all their support and input throughout my PhD. Ann has given me countless hours of assistance and her door has always been open when I needed advice or guidance and she is a pleasure to work with. I am also extremely grateful for the unrivalled support from Professor Martin Berry, Dr Richard Blanch and Professor Robert Scott for their intellectual guidance, technical assistance and training in new techniques. I also owe a debt of gratitude to the clinicians, Mr Shabbir Mohamed and Miss Si Rauz, who were always willing to help and advise me with the clinical aspects of glaucoma.

I would also like to thank all the lovely people in our Molecular Neuroscience Group, which has expanded greatly during my time here. I owe many thanks to my former BMedSc students, Ben Mead and Simon Foale, who helped me gather some of the data presented in this thesis. Thanks are also due to our laboratory manager Andy Thewles who gave me technical support and his replacement Carolyn Jones, who has been a joy to work with too. Huge thanks to Hannah Botfield, Felicity de Cogan and Jenna O'Neill who are a dream team when it comes to getting work done in the lab and they have always had time for me and genuinely supported my studies and given me reassurances when needed.

I would like to thank my funding body the Biotechnology and Biological Sciences Research Council, Peter Nightingale for his valuable help with my statistics and all the staff at BMSU for looking after my animals.

Finally, thank you to all my family and close friends for their love and support throughout my PhD.

**Contents**

## List of Figures

## List of Abbreviations

| | |
|---|---|
| ABC | Avidin-biotin complex |
| AC | Anterior chamber |
| ALT | Argon laser trabecularplasty |
| AqH | Aqueous humour |
| BAK | Benzalkonium chloride |
| BSA | Bovine serum albumin |
| CB | Ciliary body |
| CNS | Central nervous system |
| CSF | Cerebrospinal fluid |
| DAB | 3, 3'-diaminobenzidine |
| DAPI | Diaminobenzidine |
| ECM | Extracellular matrix |
| ELISA | Enzyme-linked immunosorbent assay |
| EMT | Epithelial-mesenchymal transition |
| Erk | Extracellular signal-regulated kinases |
| FG | FluoroGold |
| GAG | Glycosaminoglycan |
| GAT | Goldmann applanation tonometry |
| GCL | Ganglion cell layer |
| HRP | Horseradish peroxidase |
| IOP | Intraocular pressure |
| IW | Inner wall |
| JCT | Juxtacanalicular |
| JKN | c-Jun N-terminal kinases |
| LAP | Latency associated protein |
| LGB | Lateral geniculate bodies |
| LGN | Lateral geniculate nucleus |

| | |
|---|---|
| LPS | Lipopolysaccharide |
| MAP | Mitogen-activated protein kinases |
| mmHg | Millimetres of mercury |
| MMP | Matrix metalloproteinases |
| mRNA | Messenger RNA |
| MYOC | Myocilin gene |
| NS | Nanosome |
| OCT | optical coherence tomography |
| OCT | Optimal cutting temperature |
| ON | Optic nerve |
| PAI-1 | Plasminogen activator inhibitor-1 |
| PBS | Phosphate buffered saline |
| PBS-T | PBS containing 0.1% Triton x-100 |
| PFA | Paraformaldehyde |
| POAG | Primary open angle glaucoma |
| PXG | Pseudoexfoliation glaucoma |
| RGC | Retinal ganglion cell |
| RPE | Retinal pigment epithelium |
| TC | Trabecular cells |
| TEM | Transmission Electron Microscopy |
| TGF-β | Transforming growth factor- β |
| TIMP | Tissue inhibitors of metalloproteinases |
| TM | Trabecular meshwork |
| TSP-1 | Thrombospondin 1 |
| VEP | Visual evoked potential |

# Chapter 1

# Introduction

## 1.1 Overview

The role of the eye is to facilitate vision and, when compromised through injury or disease, blindness can occur. Glaucoma is thought to be a multifactorial, progressive chronic neurodegenerative disease leading to retinal ganglion cell (RGC) death and if left untreated, results in irreversible blindness. Currently, there is no cure for glaucoma and restorative therapies and management of the disease is by controlling intraocular pressure (IOP) through eye drops and surgery to slow down the disease process. This introduction will guide the reader through ocular anatomy, the risk factors for developing glaucoma and current treatment options. Experimental models used to research the pathophysiology of glaucoma will also be described. Finally, it is the intention of this chapter to demonstrate that fibrosis within eye is a major contributing factor to the development of glaucoma and, therefore, being able to model this pathological response experimentally provides opportunities to test candidate anti-fibrotic agents, like Decorin, which have shown efficacy as potential treatments for other fibrotic conditions.

## 1.2 Functional anatomy of the mammalian visual system

*"The eye owes its existence to the light. Out of indifferent animal organs the light produces an organ to correspond to itself…" – J.W. von Goethe*

The eye is a sense organ which allows us to detect and regulate light and its intensity from the environment. Light traverses the cornea at the front of the eye through to the retina at the back of the eye, where it is converted into an electrical impulse. From here, the electrical signal is relayed through the RGC axons which make up the optic nerve to the visual cortex located within the occipital lobe of the brain.

The mammalian eye contains two segments, the anterior (to the lens) and posterior (behind the lens) segments. The anterior segment is encapsulated by the cornea and is divided into two chambers, the anterior and posterior chambers and contains the, iris, ciliary body, pupil, zonule fibers and lens (Figure 1.1). Both chambers of the anterior segment are filled with a clear fluid known as aqueous humour (AqH). The cornea is an avascular transparent membrane which forms the most anterior portion of the eye. It consists of the epithelium, Bowman's layer, the substantia proporia, Descement's membrane and endothelium. In humans, the cornea is approx. 0.7mm thick in the periphery and 0.5mm at its centre (Snell, 1998). The cornea's primary function is to act as the most powerful refracting surface of the eye. It also has a protective role and maintains the integrity of the globe. The iris, attached to the anterior surface of the ciliary body, remains suspended in AqH and contains a central

aperture, the pupil. The smooth muscle within iris is able to dilate and constrict the pupil to alter the level of light entering the eye. The iris is a pigmented diaphragm made up of stromal and epithelial cells, approx. 12mm diameter in humans (Snell, 1998) and is located between the cornea and the lens.

The junction at which the cornea and iris converge is known as the iridocorneal angle (Figure 1.1). This anatomical description is used when diagnosing types of glaucoma, based on this angle being “open” or “closed”. The angle width alters the ability of AqH to exit the eye and therefore has consequences for the pressure within the eye. AqH is produced in the posterior chamber, by the ciliary body, and drains through two outflow pathways from the anterior chamber. Of these, the main “conventional” drainage pathway for AqH is through the trabecular meshwork (TM) and Schlemm’s Canal (see section 1.2.1). The other “non-conventional” pathway permits AqH to passively leave the eye through and around tissues including the ciliary muscles, suprachoroidal spaces, sclera and lymphatic vessels. AqH is the main determinant of intraocular pressure (IOP).

The transparent, biconvex lens is contained in a capsule basement membrane, epithelium and fibres (which continually renew themselves). The lens is held in place by zonule fibers. Movement of these zonule fibers permits the lens to focus on near or distant objects and the elasticity of the lens permits accommodation of the eye to focus on near objects. As we age the elasticity of the lens decreases and it becomes harder to accommodate. The lens also becomes densely packed from accumulation of cells (old cells are not removed) and sclerosis, resulting in increased opacity and hence, decreased visual acuity.

The posterior segment of the eye comprises the vitreous body, the choroid, sclera and retina (Figure1.1). The vitreous body lies between the lens and the retina and is attached to these structures from its cortex by suspensory ligaments. The vitreous body is a densely packed gel which contains vast amounts of hyaluronic and amino acids, as well as other proteins and ascorbic acid. Its scaffold consists of collagen fibrils (mostly type II) and small leucine-rich repeat proteins (SLRP) and functions to transmit light whilst helping to maintain the structural stability of the eye. The vitreous gel viscosity decreases with age and becomes more liquefied, increasing the chance of vitreal and retinal detachments and other ocular pathologies to occur. Posterior to the vitreous body is the retina (discussed further in 1.2.3) which is surrounded by a vascularised lining extending from the optic nerve to the ciliary body, known as the choroid. The highly vascularised choroid nourishes the outer layers of the retina.. Covering the choroid is the sclera which is a formed from densely packed collagenous fibers, encapsulating the outer wall of the eye. In addition, the sclera helps to regulate IOP (together with the cornea and AqH) by maintaining eye shape. The sclera also provides structural support for extra-ocular muscles to attach to the eye.

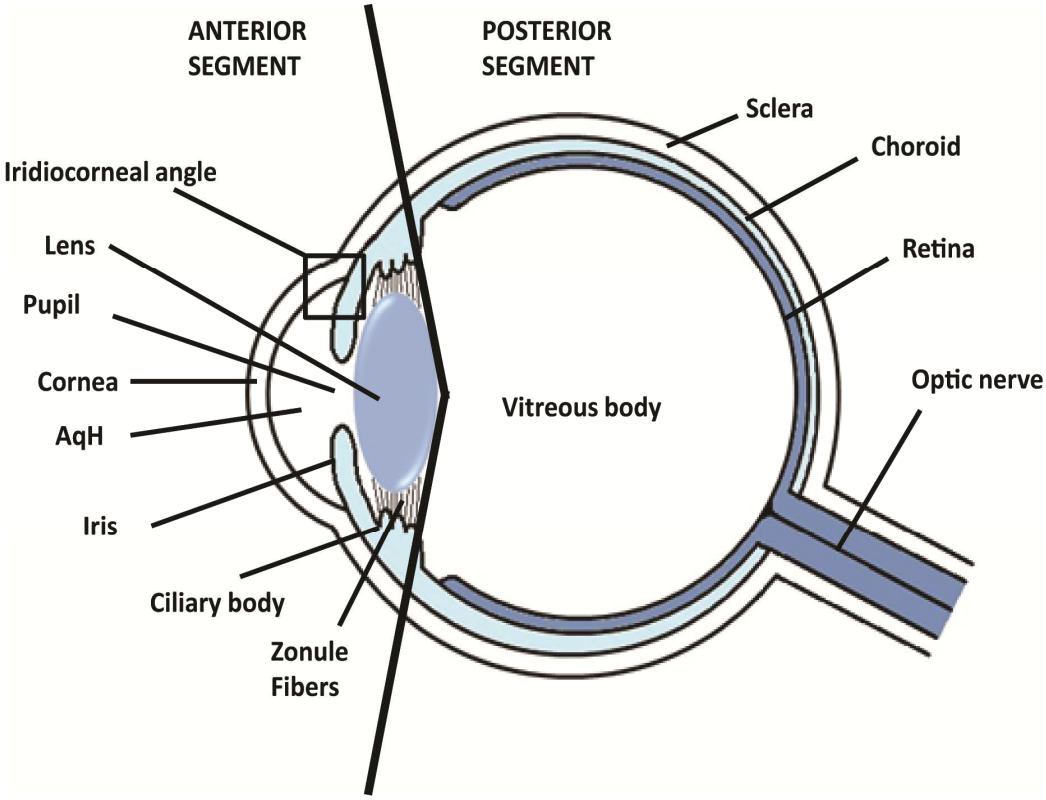


**Figure 1.1 Parasagittal section of the mammalian eye.** Light passes through the transparent cornea at the front of the eye, through the aqueous (AqH) filled chambers and lens across the vitreous body to the retina (the light sensing membrane) at the back of the eye. Here light is converted by photo-chemical transduction to electrical impulses which are transmitted by relay neurons along the optic nerve into the visual cortex for higher cortical processing.

### 1.2.1 Aqueous humour

AqH is found within the anterior segment of the eye. AqH is constitutively produced and secreted from the ciliary epithelium at an average flow rate of 2.75µl/min in humans (Brubaker, 1991) and the rat has an average flow rate of 0.35µl/min due to a much smaller anterior chamber volume (15µl)(Mermoud et al., 1996). AqH functions as a blood/plasma substitute for the avascular lens and cornea, to provide nutrients such as ascorbate to provide antioxidant protection (Ringvold, 1980), amino acids, neurotransmitters and circulation of inflammatory mediators and cells and to remove waste products. AqH also contains low levels of growth factors including Transforming Growth Factor-β (TGF-β) for immunoregulatory functions of the anterior chamber (Cousins et al., 1991). Unidirectional flow of AqH from the posterior chamber to the anterior chamber is thought to occur due to a lower temperature towards the cornea compared to the lens, generating a convective flow pattern (Goel et al., 2010). Normally, the rate of AqH production is matched by its drainage, which occurs at the at the iridocorneal angle. In certain disease states, such as glaucoma, disruption to the production or outflow of AqH can cause elevations in IOP (Kass et al., 1980). From the anterior chamber, the bulk (~90%) of AqH passively leaves the eye through the pressure sensitive TM with the remaining AqH leaving through the uveoscleral pathway (Gonzalez et al., 2000) (Figure 1.2).

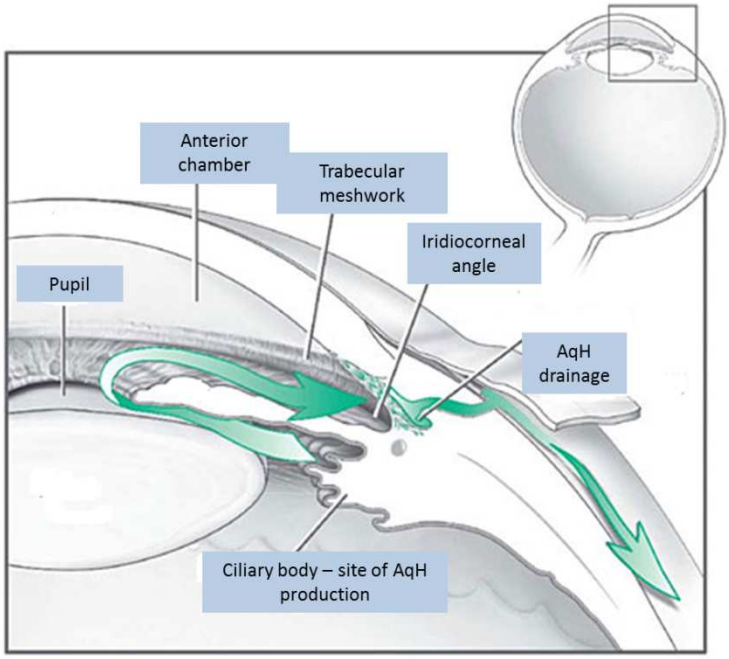


**Figure 1.2 The formation and flow of aqueous humour in the anterior segment.**

Aqueous humour (AqH) is constitutively produced by the ciliary body. From here it flows uni-directionally into the anterior chamber where it exits the eye through the trabecular meshwork.

*Source: Image adapted from the National Eye Institute, National Institutes of Health*

### 1.2.2 The trabecular meshwork

The TM is a composition of avascular tissue which bridges across the base of the angle in the anterior chamber at the point where the ciliary body and iris insert into the sclera (Figure 1.3 panel A). The TM comprises of the uveal and corneoscleral meshworks, juxtacanalicular connective tissue (JCT) and Schlemm's Canal (Figure 1.3 panel B). The uveal meshwork consists of a very porous net-like structure of endothelial cells and is the outermost layer closest to the anterior chamber. Following this, a single layer of endothelial cells is found embedded within the corneoscleral meshwork. This layer has a more compact network of cellular makeup including trabecular cells, and a meshwork of collagen, elastin and basal lamina. Behind this layer is the most densely packed area of the TM, the JCT region, which incorporates the inner wall of Schlemm's Canal and Schlemm's Canal. Schlemm's Canal is an irregular shaped channel containing an endothelial lined lumen with a discontinuous, thin basement membrane. The JCT region in the TM contains an array of endothelial meshworks and connective tissue beams covered with contractile trabecular endothelial cells which make contact with the basement membrane of Schlemm's canal. These cells are embedded within extracellular matrix (ECM) which contains various collagens, glycoproteins, elastins, fibronectin and laminins (Keller & Acott, 2013). The main function of the TM is to regulate the outflow of AqH as it is this area that provides the most resistance and hence determines IOP (discussed in section 1.3). Regulation of AqH outflow occurs through relaxation and contraction of the ciliary muscle and TM. The TM distends as the ciliary muscle contracts resulting in an increase of AqH outflow. Contraction of the TM, through Rho-associated pathways (Nakajima et al., 2005), decreases AqH outflow. In addition, the TM cells are

capable of phagocytosis and are able to keep the area free of debris, bacteria and other particles (Buller et al., 1990).

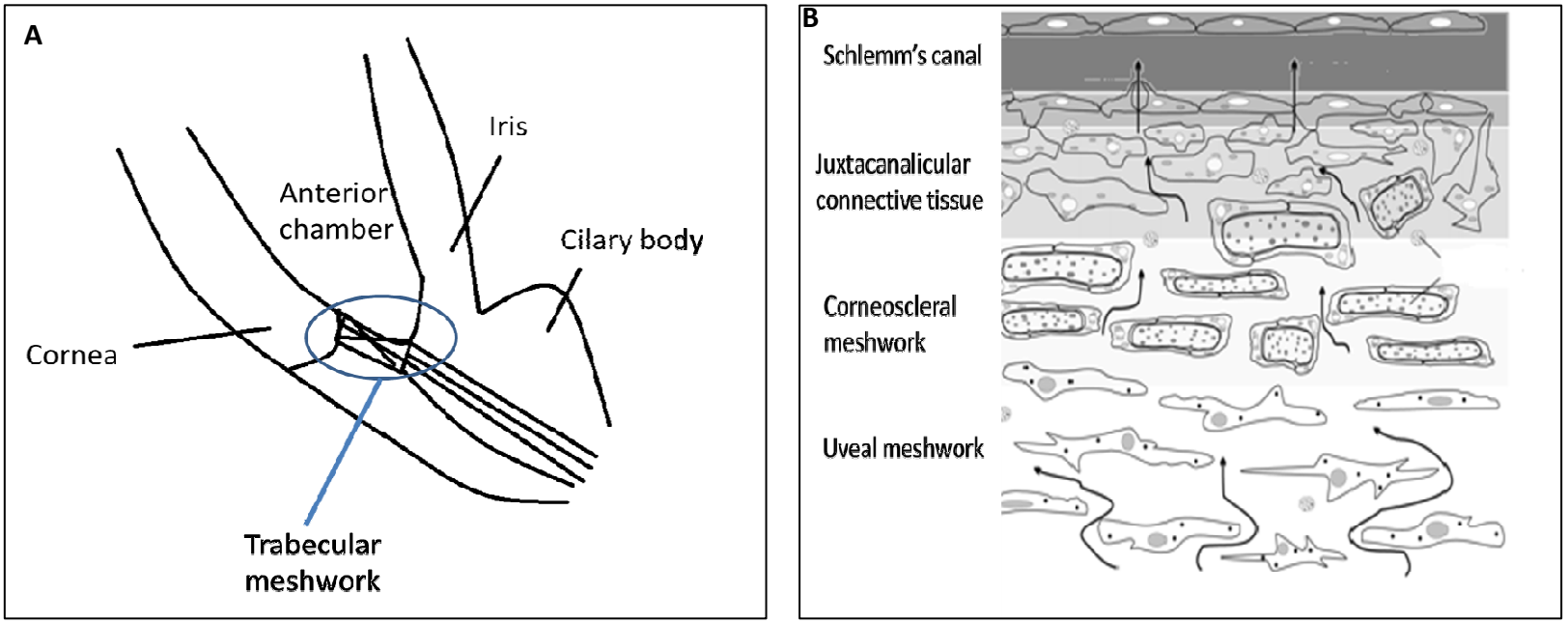


**Figure 1.3 The trabecular meshwork.**

(A) shows the location of the trabecular meshwork (TM) in the iridiocorneal angle within the anterior chamber. (B) Schematic diagram showing the cellular structure of the TM. The arrows show the direction of aqueous humour passage through the TM, across the uveal and corneoscleral meshworks and finally the juxtacanalicular connective tissue into Schlemm's canal where fluid eventually is passed onto the venous drainage systems.

*Source: Image B adapted from Llobet et al., (2003).*

### 1.2.3 The retina, optic nerve and visual pathway

The retina, which is part of the central nervous system (CNS), is the light sensing membrane situated at the back of the eye. Retinal cells are continuous with the optic nerve and the structure lines eye globe with its most anterior edge conjoined to the epithelial cells of the ciliary body and iris. Within the retina light is converted by phototransduction into an electrical signal which is transmitted by the optic nerve to the brain for higher cortical processing and image generation.

The retina is highly structured and composed of ten cellular layers that divide outer pigmented and inner neural structures (Figure 1.4). Light is absorbed and nutrients for the neural retina are metabolised by the outer pigmented layer, commonly known as the retinal pigment epithelium (RPE). Below the RPE lies the neural retina, which comprises (from outside in) the photoreceptors (rods and cones), bipolar cells and RGC, along with horizontal and amacrine cells. In addition, Müller glia radially span the retina and their processes form the external and internal limiting membranes. Light passing through the vitreous traverses the retinal layers converging on the photoreceptors. From here light is transduced and relayed as an electrical impulse through bipolar interneurons to the RGC. The RGC form both single and multiple ganglion cell layers (GCL) depending on their location within the retina and synapse with bipolar and amacrine cells. Their axons are non-myelinated within the retina and exit the eye at the optic disc where they form the optic nerve. After the RGC axons pass through the sclera to leave the eye they become myelinated by oligodendrocytes after the lamina cribosa.

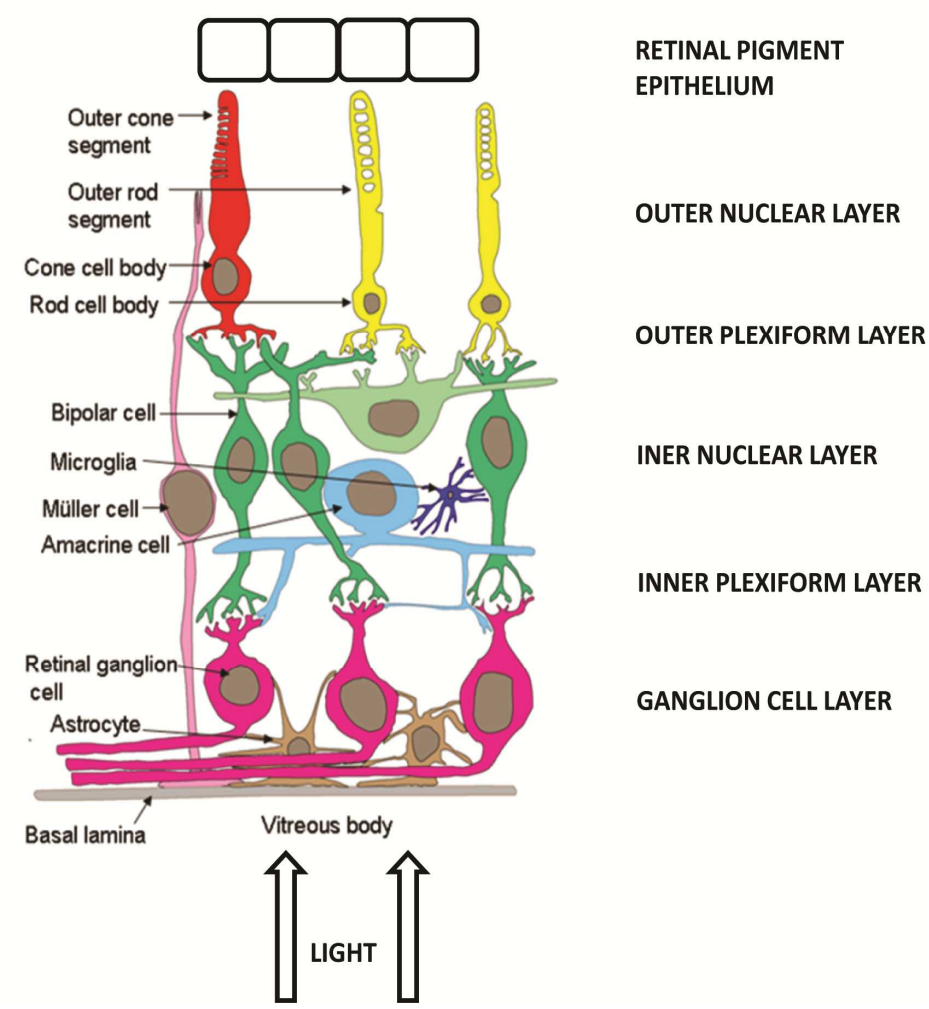


**Figure 1.4 The mammalian retinal layers**. Light is transmitted through the retinal layers to the photoreceptors. Light energy is transduced into electrical signals which are relayed through the retina to the RGC *via* the bipolar cells and then onto the brain *via* their axons which fasciculate as they leave the back of the eye to form the optic nerve.

*Source: Image modified from Berry et al. (2008)*

Once departed from the retina, electrical impulses travel along axons in the optic nerve onto the optic chiasm after decussating at the optic tracts, to make their first synapse at the lateral geniculate bodies (LGB) or superior colliculus from where they pass the signal onto and to the visual cortex (Figure 1.5). At the level of the optic chiasm, retinal axons from

(50% and 95% of axons in humans and rats, respectively) decussate so that they are projected through the contra-lateral optic tract. The remaining axons project ipsilaterally. Testing, for example, measuring visual evoked potentials (VEP), can be used both clinically and experimentally to assess function of the retina and visual pathways. High IOP damages the retina by various mechanisms that causes RGC loss, leading to irreversible blindness as seen in, for example, some forms of glaucoma (discussed in section 1.4).

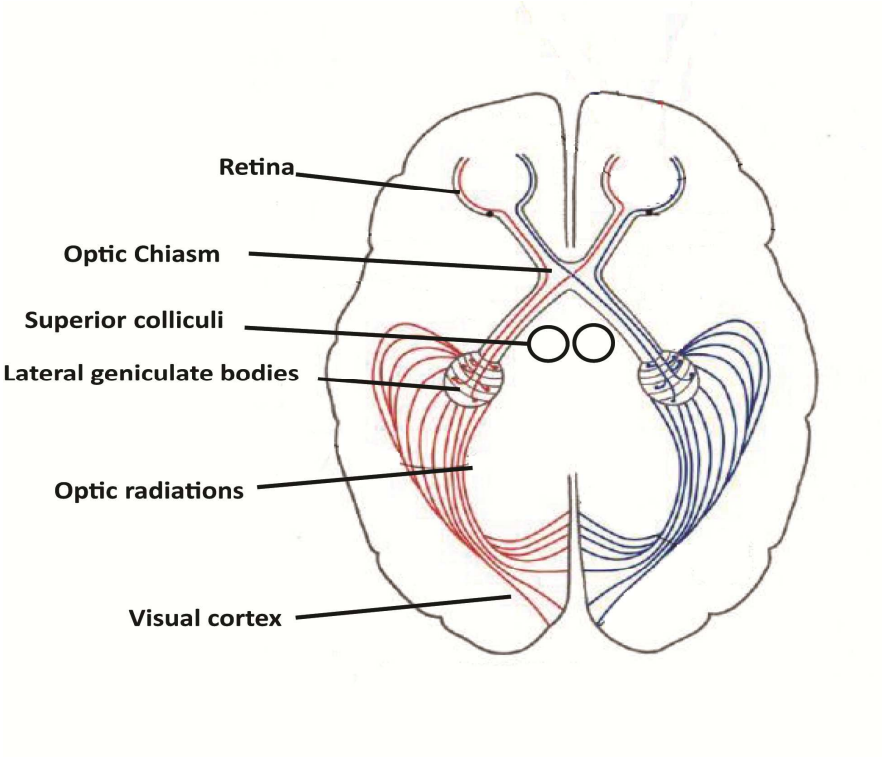


**Figure 1.5 The visual pathway.** From the retina, electrical impulses travel along axons in the optic nerve onto the optic chiasm after decussating at the optic tracts, to make their first synapse at the lateral geniculate bodies or superior colliculus, from where they pass the signal onto and to the visual cortex.

*Source: Image modified from Haines (2013)*

## 1.3 Intraocular pressure

### 1.3.1 Factors influencing IOP

Normal IOP for humans ranges between 10-20mmHg (Murgatroyd & Bembridge, 2008) with a median of 16-17mmHg (Brubaker, 1998); in the rat the normal IOP can vary depending on the species, method of IOP measuring and use of anaesthetics. As previously described the main determinant of IOP is balance between the rate of production and outflow of AqH. IOP in humans fluctuates throughout a 24 hour cycle (Henkind et al., 1973; Asejczyk-Widlicka & Pierscionek, 2007) and studies have suggested that IOP tends to peak mid-morning and decrease during the afternoon and evening time (Liu et al., 1998); this is due to the rates of AqH production following a circadian rhythm (Reiss et al., 1984). Diurnal variations in IOP have also been noted in the rat (Krishna et al., 1995). IOP, under normal physiological conditions, will tend to increase slightly with age. Certain factors such as blood pressure (Klein et al., 2005), diseased states for example, having Diabetes mellitus (Hennis et al., 2003), and exercise can alter IOP. Another important factor both clinically and experimentally is that use of general anaesthetics e.g. Isoflurane have been demonstrated to decrease IOP in humans (Mirakhur et al., 1990) and rodents (Jia et al., 2000). Certain medications for instance the corticosteroid dexamethasone (Weinreb et al., 1985) and anti-cholinergics (Razeghinejad et al., 2011) may also lead to increases in IOP that can be very problematic in patients undergoing ocular surgery.

Other factors such as age, gender, ethnicity may also lead to differences in IOP which, in turn, may exacerbate pathological conditions, the most notable disease being glaucoma

(discussed further in section 1.4). The Beaver Dam Eye Study demonstrated a significant increase in IOP correlated with increasing age (Klein et al., 1992) and it could be that age related biological changes within the eye affect the production and outflow of AqH thereby not isolating age itself as a direct factor for determining IOP. The Barbados Eye Study showed that females were more likely to have higher IOP than men. This study also indicated that higher body mass index, darker skin and smoking were all correlated with higher measurements in IOP (Wu and Leske, 1997).

### 1.3.2 Measuring IOP

Clinical and experimental measurements of IOP must provide reproducible and accurate readings in order to monitor levels accurately across a certain time period. It is particularly useful clinically to evaluate and monitor people at risk of, or with, glaucoma. The gold standard method used clinically and experimentally is tonometry, an indirect and non-invasive method to obtain IOP (normally expressed in mm of mercury (mmHg)). Clinically, the most reliable IOP measurements are provided using Goldmann Applanation Tonometry (GAT) (Bhan et al., 2002). This tonometer can be added to a slit lamp or used as a hand-held device and is based on measuring the force applied to applanate the cornea (Murgatroyd et al., 2008). Also used in the clinic and in experimental settings is the TonoPen tonometer, which uses the same principle as GAT but requires applanation of a smaller region of the cornea. Research has shown this method to be as reliable as GAT (Lester et al., 2001), although for IOP measuring in experimental studies using rodents, studies have shown rebound tonometry to be more reliable (Kontiloa et al., 2001; Goldblum et al., 2002). The

TonoLab Rebound Tonometer is based upon a lightweight probe touching a small area of the cornea to measure IOP and is specifically designed for use with rodents. Rebound tonometry is widely used in experimental settings and is shown to provide an accurate and sensitive reading (Morrison et al., 2009).

## 1.4 Glaucoma

### 1.4.1 Glaucoma definition, epidemiology and risk factors

Glaucoma is a chronic neurodegenerative disease affecting the retina and optic nerve and is the second leading cause of blindness worldwide following cataracts (Rieck, 2013). However, unlike cataracts, if left untreated glaucoma results in irreversible blindness (Weinreb and Khaw, 2004). Currently up to 70 million people have glaucoma worldwide (Williams et al., 2013), with 8.4 million being permanently blind in both eyes from this disease (Subak-Sharpe et al., 2010). Rates of glaucoma are set to increase by 2020 to an expected incidence of 80 million and, of those, 11 million people will be bilaterally blind from the disease (Quigley & Broman, 2006). Glaucoma, collectively termed the Glaucomas, are a multifactorial and heterogeneous group of neurodegenerative diseases. Broadly, they can be acute or chronic and are normally classified into i) primary, where there is no known cause; ii) secondary, where there is an underlying cause such as injury or infection; or iii) developmental, which is present in infants usually by the age of one. Primary glaucomas can be further classified into two main types based on the anterior chamber anatomy, namely from the presence of an "open" or "closed" iridiocorneal angle (see section 1.2). Closed angle glaucoma is normally

acute and needs to be surgically dealt with while open angle, where there is still some flow is regarded as chronic. Primary angle-closure glaucoma occurs when the anterior chamber angle closes preventing AqH from draining through the TM. People with a narrow anterior chamber can develop a pupillary block which is the most common cause of angle closure glaucoma. Pupillary block occurs when there is an increased pressure gradient causing the iris to move forward and cover the TM. Those from Asian ethnic groups (Seah et al., 1997), being of older age (Foster, 2002), having a positive family history or being female (Congdon et al., 1992) are more prone to angle-closure glaucoma.

The most prevalent form of glaucoma in the western world is Primary Open Angle Glaucoma (POAG) (Kroese & Burton, 2003). In POAG, there is progressive loss of RGC leading to retinal nerve fibre layer thinning together with elevated IOP. Clinically, this can manifest as thinning of the neuro-retinal rim at the optic disc (referred to as optic disc cupping), retinal degeneration or thinning of the retinal nerve fibre layer on optical coherence tomography (OCT) and decreases in vision using visual field or functional testing. Risk factors for developing POAG are IOP elevation (Quigley et al., 1980; Sommer et al., 1991), a thinner central corneal thickness (Gordon et al., 2002), being of older age (Gordon et al., 2002), being of African origin (Gordon et al., 2002) and having a family history of the disease (Tielsch et al., 1994) (Figure 1.6). Gender as a risk factor is still under debate, as some studies for POAG prevalence have determined that men were more at risk (Leske et al. 1995; Gordon et al., 2002; Rudnicka et al., 2006), whereas other studies suggested that women were more at risk (Mitchell et al., 1996) or that there was no gender difference in rates of POAG (Klein et al., 1992). An array of genetic and environmental factors contribute to the

onset of glaucoma and many glaucoma associated genes have now been identified. Further genetic risk factors are being identified through genome-wide association studies (GWAS) showing that mutations in specific genes carry a very high risk of developing POAG (Fingert, 2011). GWAS is a robust method to identify common variants in genes from thousands people with and without glaucoma. Admixture mapping is another method used for tracking genes associated disease progression within certain populations (Mendoza-Reinoso et al., 2012). There are many different affected genes associated with glaucoma including the Myocilin (MYOC), Optineurin (OPTN) and WDR36 genes. Mutations in MYOC lead to early onset POAG and patients and is believed to lead to TM dysfunction although the exact mechanism of this is still debated. Kwon et al., (2009) suggests that protein trafficking and mis-folding leads to protein accumulation whereas, Stamer et al., (2011) suggested altered exosome release into AqH changes paracrine and autocrine signalling within the TM disrupting normal TM homeostasis. OPTN is not generally associated with increasing IOP but is thought to induce premature RGC death by altering pro-apoptotic factors (Morton et al., 2008). WDR36 is widely expressed throughout the eye and mutations are associated with axonal growth in the optic nerve (Chi et al., 2010) and absence of WDR36 from TM cells can lead to apoptosis (Gallenberger et al., 2011).

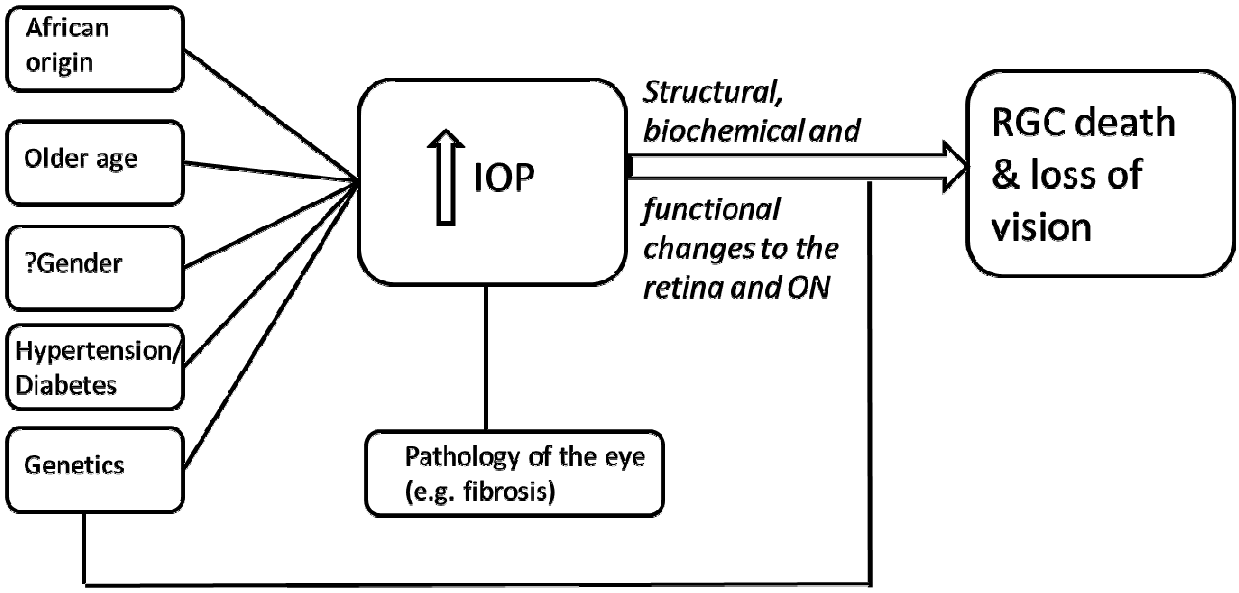


**Figure 1.6 – Outline of risk factors for elevation in IOP and the development of POAG.** Glaucoma is a multifactorial disease with those of certain ethnic origins, age, family history of glaucoma being more at risk of developing glaucoma. However, the main risk factor is increased IOP which leads to damage and death of the retina. The aetiology of IOP elevations are still not completely understood but it is thought that fibrosis within anterior chamber could be a factor.

### 1.4.2 Pathobiology of POAG

Despite POAG being multifactorial, elevated IOP is a highly significant and, currently, the only modifiable risk factor for the development of POAG treated by surgery or pharmacologic therapies. IOP as a risk factor for developing POAG have been extensively described in the literature and it is accepted that IOP increases within the eye are caused by reductions in AqH outflow (Grant, 1951; Johnson and Kamm, 1983; Tripathi et al., 1994).

Grant (1951), using organ perfusion studies, showed reduced outflow of AqH in glaucomatous human eyes. Johnson and Kamm (1983) showed that most resistance to outflow occurred in the inner wall of Schlemm's Canal (which can be considered part of the JCT region of the TM). Interestingly, in cohorts of patients with high IOP, the patients with glaucoma had higher levels of outflow resistance than those without glaucoma (Johnson and Kamm, 1983) suggesting there is a pathological process occurring in glaucomatous eyes causing outflow resistance. It has been demonstrated that higher levels of pro-fibrogenic cytokines, including TGF-β, are found within the AqH of glaucoma patients and this may lead to excess deposition of ECM in the drainage portal (Tripathi et al., 1994) thus changing the cellularity of the TM and reducing outflow (discussed further in section 1.5.2).

Studies have shown that lowering IOP helps to preserve visual function in humans with POAG (Heijl et al., 2002; Maier et al., 2005) and in experimental rodent models of glaucoma, (Morrison et al., 1998) that high levels of IOP can lead to death of RGC. The mechanisms by which increases in IOP can lead to RGC death have been under much investigation. Many experimental studies have investigated the structural, biochemical and functional changes within the retina and ON which lead to RGC death after IOP elevation, and some of those when induced experimentally mimic the pathological aspects of the human condition (Quigley et al., 2000; Levkovitch-Verbin et al., 2002; Kim et al., 2004; Urcola et al., 2006). Nickells (2007) proposed a staged hypothesis for elevated IOP causing changes in glia around the optic nerve head, leading to RGC axonal death by compromising the neurotrophic support to RGC that in turn causes RGC to undergo apoptosis. Death of RGC may then release neurotoxic substances, such as glutamate, which can further damage neighbouring

RGC. Unmyelinated axons arising from the RGC are most vulnerable at the level of the optic nerve head and it is this region that is susceptible to damage in glaucoma (Quigley et al., 1981; Roberts et al., 2010; Dai et al., 2012). In humans and primates the optic nerve head contains tough connective tissue known as the lamina cribrosa and it has been suggested that mechanical forces in this region lead to axonal damage and RGC death (Quigley et al., 1981).

There is increasing evidence that increases in IOP leads to glaucomatous damage to the optic nerve head through damage and loss of astrocytes which, in turn, leads to RGC death through the lack of structural and metabolic support from the astrocytes (Dai et al., 2012). Death of RGC is permanent and correlates with the degree of blindness. Our understanding of the different mechanisms involved in the development of POAG and RGC death, namely resistance to AqH outflow through the TM and elevated IOP, provide promising targets for therapeutic interventions. Currently though, the only available treatment options for patients are based around lowering IOP through surgery or drugs.

### 1.4.3 Current treatments for POAG

The aim of treatment for POAG is to reduce IOP and protect the retina and optic nerve from further damage. Treatment for POAG can be difficult because patients often present when the disease has progressed to an advanced stage, usually when vision is already significantly impaired. In the UK, there are now guidelines for screening patients in the community by optometrists.

The most common, and first line, treatment for glaucoma is the topical administration of IOP lowering agents in the form of eye drops (McKee et al., 2004). To date there are no medications available to directly protect RGC death although some medications, e.g. Brimonidine, have shown some neuroprotective efficacy (Cantor, 2006). Eye drops prescribed to patients work by either increasing outflow or decreasing production of AqH. They are broadly categorised by their active ingredients and include prostaglandin analogues (Tamada et al., 2001) e.g. latanoprost (trading from Pfizer as Xalatan), to increase outflow through the uveoscleral pathway by altering pressure gradients and cellular permeability, and carbonic anhydrase inhibitors (Lippa et al., 1992) and β-blockers (Johnson et al., 2010), e.g. Timolol, to decrease AqH production by the ciliary body.

Eye drops enter the eye through the cornea and conjunctiva, usually by passive diffusion, to become mixed in with AqH. The cornea contains both lipids and water in its stroma enclosed within a layer of epithelium and endothelium. The presence of lipids and water in the cornea makes the delivery of some drugs across this barrier difficult. Many glaucoma drops contain preservatives, such as benzalkonium chloride (BAK), to break down tight junctions located within the epithelium of the cornea. However, there has been a wave of negative literature about the use of BAK in eye drops as it can increase levels of ocular surface disease in patients (Becquet et al., 1998; Noecker, 2001; Leung et al., 2008). Newer preservative-free drops are now on the market (Rouland et al., 2013).

To date there are no eye drops used to target the main pathology, which is fibrosis of TM, (where most resistance to AqH outflow occurs). Most procedures to increase AqH drainage

are carried out through surgical means. There are various laser therapies or surgical options to increase AqH drainage. Argon laser trabecularplasty (ALT) is the use of a green wavelength laser at 700-100mW delivered at the iridiocorneal angle altering the cellular environment in the TM and inducing changes in trabecular cells to express certain factors, such as matrix metalloproteinases (MMP), that remodel the TM reducing resistance to AqH outflow (Johnson, 2007). There is some TM cell death using ALT through apoptosis and necrosis, but this is balanced by activation of the TM cells that survive (Johnson, 2007). However, like all surgery ALT is not without its risks. ALT often starts to fail throughout the treatment course in patients. It is thought that the repeated use of ALT causes cellular sheets within the TM to fibrose as a result of excess cellular activation and subsequent release of pro-fibrogenic factors that increase resistance of outflow through the TM (Alexander & Grierson, 1989).

Glaucoma filtration surgeries, such as trabeculoectomies, are often performed in patients when IOP lowering eye drops fail to work. In a trabeculoectomy the angle is surgically opened up so that AqH can drain directly through the sclera, bypassing the TM. One of the main complications after this type of surgery is fibrosis of the opening, and this too can prevent AqH from leaving the eye (Stahnke et al., 2012). Drainage implants, composed of a silicone tube connected to a drainage plate can also be used to drain AqH from the anterior chamber into the sub-tenons space. The implantation of a drainage device causes microtrauma to tissue and therefore can lead to scarring from fibroblast activation within and around the newly created AqH outflow pathway (Yoon & Singh, 2004).

Experimental studies have been successful in combating post-operative fibrosis of ocular tissue using anti-fibrotic agents, and in particular agents that antagonise TGF-β, thereby improving the outcome in experimental glaucoma filtration surgery in rabbits (Mead et al., 2003; Wong et al., 2003; Grisanti et al., 2005) suggesting that reducing fibrosis controls IOP and prevents further glaucomatous disease progression.

## 1.5 Fibrosis in Glaucoma

### 1.5.1 Fibrosis

Dysregulated fibrosis is considered by some as an impaired healing response (Mutsaers et al., 1997) and is a leading cause of mortality and morbidity in patients (Leask & Abraham, 2004). Chronic fibrotic disease occurs in many tissues throughout the body, including lung (Crouch, 1990), cardiac (Lijen et al., 2000) renal (Liu, 2006) and ocular tissue (Wang et al., 2009) and is currently very difficult to treat. Of relevance to this project, fibrosis within the eye, in particular the TM, is thought to contribute to the pathology occurring in POAG (Tamm & Fuschshofer, 2007). These fibrotic conditions all have common pathological features including chronic inflammation, the presence of myofibroblasts and excessive accumulation of ECM in the microenvironment of affected tissues. Abnormal ECM deposition leads to tissue dysfunction, often by perturbing the normal contractility/motility of cells.

Following disruption of tissue integrity through infection, chemical insults, ageing or accumulation of debris, increased levels of pro-fibrogenic cytokines and growth factors

attempt to heal the compromised tissue. However, this healing response is often inappropriately perpetuated by an abnormally sustained release of cytokines, including pro-fibrogenic TGF-βs, resulting in the development of fibrotic lesions and tissue dysfunction. It is widely accepted that TGF-βs are key cytokines that orchestrate acute and chronic fibrotic responses (TGF-β will be discussed further in Section 1.6). One of the main cell types in stromal tissues responsible for repair and remodelling of the local microenvironment are fibroblasts. In the diseased TM, for example, local cells are transformed to a fibroblast phenotype and assist in remodelling the compromised tissue. For example, local epithelial cells can be transformed into myofibroblasts, *via* TGF-β signalling, so that they lose their cellular adhesions and become motile and deposit ECM (including collagen, fibronectin and laminin) at sites of tissue damage (McAnulty, 2007).

### 1.5.2 Trabecular meshwork cells and extracellular matrix

TM cells are a heterogeneous group that have secretory, contractile, proliferative, motile and phagocytic capabilities and play an important role in TM tissue homeostasis (Polansky et al., 1984). TM cells are key regulators of ECM turnover (Fuchshofer & Tamm, 2009), responding to shear and mechanical stresses to regulate AqH outflow by altering local ECM deposition/degradation and releasing cytokines that modulate the ECM. The ECM contains collagens (the most abundant matrix molecule), fibronectin, laminins and glycoproteins, along with various adapter proteins that modulate matrix interactions with cells (Hann et al., 2001; Ueda et al., 2002) (Figure 1.7). Many types of collagen are found within the TM including the fibril-forming (types I, III and V) basement membrane collagen (type IV),

filament-forming (type VI) and network-forming collagens (type VIII). Together these collagens provide strength and resilience throughout the meshwork (Weinreb et al., 1996). Fibronectin is another major component of the ECM. Fibronectin is a dimeric high molecular weight (450kDa) glycoprotein secreted by fibroblasts within the JCT and on the inner wall of Schlemm's canal. Laminins are heterotrimeric glycoproteins which are present in basement membrane and are used to connect basement membrane to other cell layers.

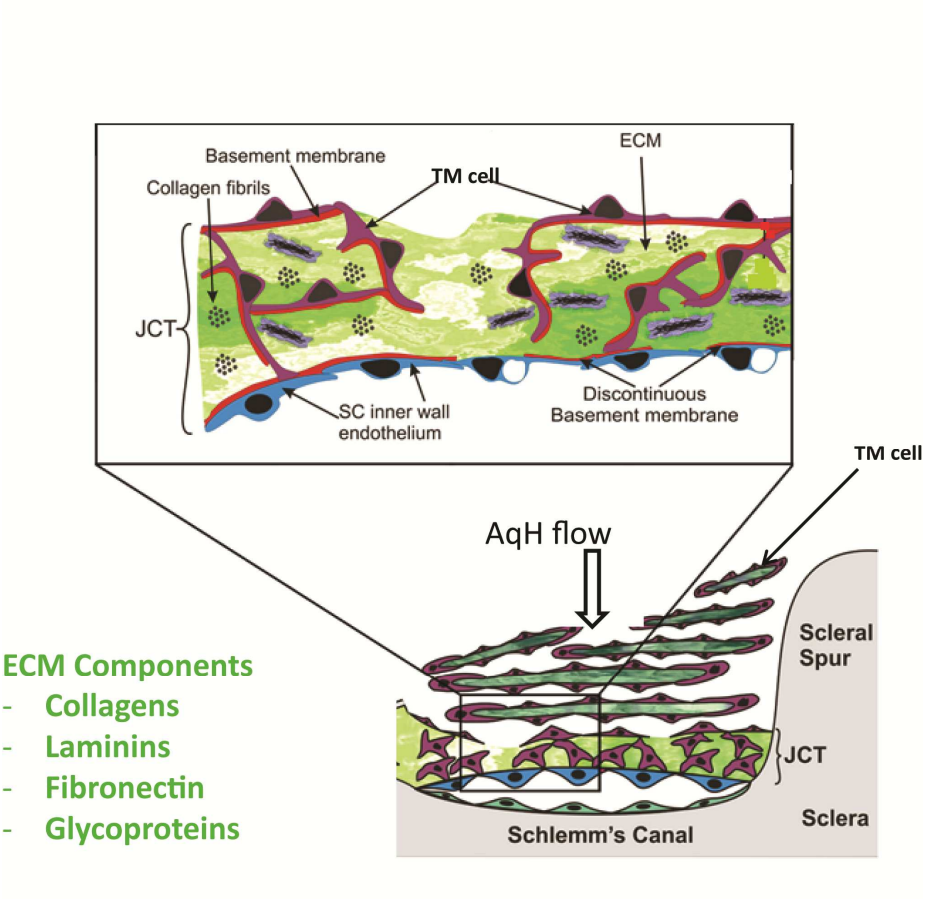


**Figure 1.7 Schematic representation of the TM.** This image shows the outflow pathway through the TM, with particular emphasis on the presence of TM cells embedded with ECM. The insert highlights the JCT region cells interspersed and ECM conjugated to the inner wall of Schlemm's canal.

*Source: Image adapted from Acott & Kelley (2008)*

### 1.5.3 Fibrosis in the TM and POAG

There is much evidence that fibrosis within the TM is a contributing factor to the pathobiology of POAG by decreasing AqH outflow, causing increased IOP (Tamm and Fuchshofer, 2007). The TM is a dynamic structure which is intimately linked to the endothelial lined inner wall of Schlemm's Canal (Figure 1.7) and is anchored to the ciliary muscle. Contraction of the ciliary muscles distends the TM, reducing outflow of AqH, whereas TM relaxation opens the meshwork and leads to an increase in AqH outflow (Weiderholt et al., 2000). Resistance to outflow through the TM is necessary to maintain the IOP and most resistance is supplied by the ECM within JCT region and around Schlemm's Canal (Lütjen-Drecoll, 1999). Regulated ECM turnover by TM cells also provides resistance to AqH outflow by the production of ECM and degrading proteases in response to stress or mechanical forces provided by the IOP (Sanka et al., 2007; Acott & Kelley, 2008). Therefore, any alteration in the cellularity or matrix of the TM will alter ECM dynamics and hence the resistance that it provides to outflow. In POAG there is no clear pathological pathway leading to raised IOP but there have been studies showing a loss of TM cell function (Alvarado et al., 1981; Stamer et al., 1995). In addition to loss of cell numbers, cells lose smooth muscle (actin) cell function in terms of contraction and synthesis. The loss of TM cells with age is profound. Human studies have estimated that in youth the eye has in the region of 800,000 of these cells, while in a normal 80 year old this will have reduced to 400,000 (Grierson et al., 1987) but in an 80 year old with open angle glaucoma the numbers are far fewer (Alvarado et al., 1984). Due to the active phagocytic and migratory activity of TM cells it is possible that their proliferation capacity is limited, hence, the decrease in

numbers over a lifetime (Calthorpe & Grierson, 1990). The increase in debris accumulation within the anterior chamber may cause more TM cells to detach in order to try and remove this. Loss of TM cells will alter the local microenvironment and the levels of ECM. Over time the TM cells also alter their phenotype to become less motile and more productive of ECM, shown experimentally through decreases in actin and increases in collagen synthesis (Millard et al., 1987; Porter et al., 2012). In addition to alterations in ECM and cell contractility, the higher levels of mechanical stress also lead to TM cells releasing various cytokines including TGF-β (Liton et al., 2005), which can in turn lead to more ECM deposition through its fibrogenic signalling pathways.

### 1.6 TGF-β

The TGF-βs are a family of growth factors that are important regulators of cellular actions, including differentiation, proliferation, migration, cell death, ECM production and modelling, immune cell modulation and growth factor production. The response and actions of TGF-β are dependent on the cell type and location within the body and, because of this, TGF-β can have opposing biological actions depending on context. Three main isoforms of TGF-β exist, TGF-β1, TGF-β2 and TGF-β3. Cloning studies have shown that TGF-β1 and 2 are 71% identical, yield similar biological activity and are of the same size but contain different amino acids at the amino-terminal end (Marquardt et al., 1987). The TGF-β3 isoform is 78% similar to TGF-β2 isoform and its structure is identical to TGF-β2 (Cox, 1995). Although TGF-β expression may be different to that of the TGF-β1 and TGF-β2 isoforms, studies have demonstrated that TGF-β3 is often co-expressed with the TGF-β1 and TGF-β2 isoforms (Cox,

1995). TGF-β3 is an important growth factor during development, with its expression found in high levels within most tissues in the developing embryo (Cox, 1995).

### 1.6.1 TGF-β bioactivity

TGF-β bioactivity is tightly regulated by two proteins, a latent TGF-β binding protein (LTBP) and a latency associated protein (LAP) that confer latency. Secretion of TGF-β in a latent form enables optimal concentrations of TGF-β to be achieved at the designated site of action. The mature latent TGF-β is linked by two disulphide bonds. Dissociation of the complex is required for TGF-β to become active and bind to its cognate receptors to initiate intracellular signalling (Figure 1.8). Dissociation of the complex to liberate TGF-β in its active form can be achieved experimentally through acidic conditions. Biologically, liberation is achieved through proteases e.g. elastase (Nathan, 2002) and plasmin (Munger et al., 1997), thrombospondins (Crawford et al., 1998), integrins (Annes et al., 2004) and free radicals (Barcellos-Hoff & Dix, 1996). Binding of Thrombospondin-1 (TSP-1) leads to a conformational change in the LAP, also resulting in release of the active TGF-β cytokine. Oxidative activation can cause to a conformational change in the LAP, releasing the active form of TGF-β (Khalil, 1999).

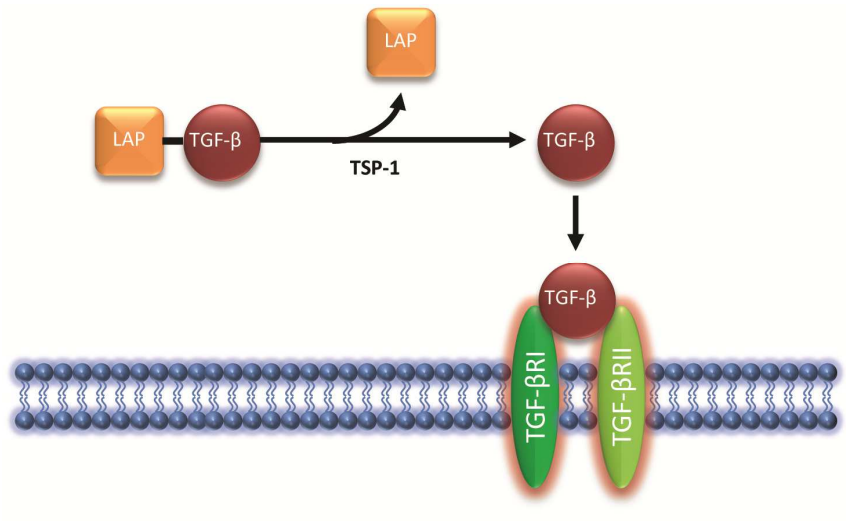


**Figure 1.8 TGF-β bioactivity.** The mature TGF-β is in an inactive form which associated to its binding proteins (LAP). Binding of TSP-1 dissociates the LAP and releases the active cytokine to bind to its cognate receptors.

### 1.6.2 TGF-β signalling

Once active, the TGF-β initiates intracellular signalling through interactions with transmembrane serine-threonine kinase type 1 and type 2 receptors (Figure 1.9) and through the TGFBR3 (betaglycan) co-receptor. TGF-β signalling is dependent on the receptor complexes forming. Betaglycan is able to regulate TGF-β signalling at the receptor level to both enhance (Blobe et al., 2001) or down-regulate (Chen et al., 2003) TGF-β signalling. Betaglycan is able to regulate TGF-β signalling through its ability to bind the core protein of TGF-β and regulate its release to the type 2 receptor. Binding of TGF-β leads to a unidirectional phosphorylation of the type I receptor. This phosphorylation activates the

Smad intracellular signalling cascade. Smad2/3, once phosphorylated by the type 1 receptor, translocates to form a complex with Smad4 and, from there, relocates as a complex to the nucleus. Within the nucleus, Smads and their co-transcriptional factors are able to up- and down-regulate gene expression. Although Smads are required for most of TGF-β effects, there are other intracellular pathways that are used in conjunction with Smad signalling, for example, activation of the MAP kinase pathway (which includes Erk, JKN and the p38 MAP kinases) is essential for apoptosis (Chang & Karin, 2001), for epithelial-mesenchymal transition (EMT) (Zavadil & Böttinger, 2005) and ECM production (Chiquet et al., 2003). Smad-independent signalling also occurs *via* Rho GTPases (which includes RhoA, Rac1 and Cdc42) which lead to cytoskeletal reorganisation permitting cell motility and EMT. These pathways are not exclusive, MAP kinase pathways can lead to Smad activation and thereby alter gene transcription. This complex interaction of intracellular kinases across multiple pathways demonstrates the plethora of biological actions that TGF-β can have on gene expression.

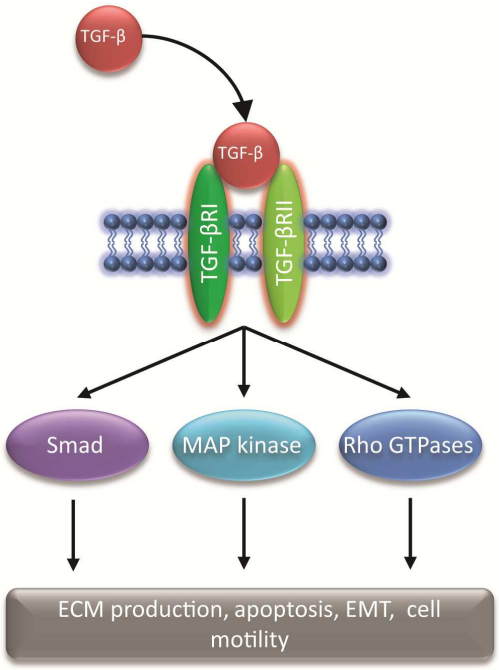


**Figure 1.9 TGF-β signalling.** Binding of active TGF-β to its receptors activates intracellular signalling through the Smad, MAP kinase or Rho GTPase pathways to regulate ECM production, cell death, cell proliferation and differentiation through gene expression.

### 1.6.3 TGF-β and fibrosis

Many experimental and human studies have demonstrated TGF-β as being the most potent cytokine to induce tissue fibrosis within the body (Leask & Abraham, 2004). TGF-β activates epithelial cells, fibroblasts and macrophages and other cells that contribute to fibrotic scarring. In addition to producing an array pro- and anti-inflammatory mediators from various cells, TGF-β can induce its own release from cells. The autocrine ability of TGF-β is regulated by expression of its receptors. For example, TGF-β-induced differentiation of epithelial cells leads to a down-regulation of TGF-β receptors, thus reducing the downstream effects. This autocrine regulation is partly achieved by TGF-β inducing inhibitor proteins (e.g

Decorin) that bind and sequester activated TGF-β. Importantly, TGF-β orchestrates the deposition and reduced degradation of ECM by upregulating gene expression of collagens, fibronectin and laminins and reducing gene expression of MMP, whilst upregulating MMP inhibitors (TIMP), resulting in a net accumulation of ECM and, thereby regulating tissue fibrosis. There are different effects on scarring within each of the TGF-β isoforms. It is well known that TGF-β1 and TGF-β2 are associated with increasing fibrosis and scar formation, however, TGF-β3 has shown anti-scarring in wound healing models whereby exogenous TGF-β3 administered to cutaneous wounds reduced scarring compared to controls (Shah et al., 1995)

### 1.6.4 TGF-β in the eye

TGF-βs are normally found within AqH where it is helps maintain the immune privilege within the anterior chamber (Cousins et al., 1991). Although both TGF-β1, TGF-β2 and TGF-β3 are present, the predominant form normally found within the eye is TGF-β2. TGF-β2 is secreted by ciliary and lens epithelium (Allen et al., 1998), platelets found within the inner wall of Schlemm's Canal (Hamanaka & Bill, 1994) and TM cells. TGF-β is able to induce macrophages with immune deviating capabilities and is therefore considered imperative for induction of anterior chamber-associated immune deviation (ACAID; Wilbanks et al., 1992). ACAID is achieved partly through the immunoregulatory properties of the AqH. Co-culture studies have demonstrated that the presence of AqH inhibits proliferation of antigen presenting cells and T cells. The first significant immunomodulatory factor in AqH to be discovered was TGF-β (Wilbanks et al., 1992). In addition to a direct role of TGF-β from AqH inhibiting T cell proliferation (Cousins et al., 1991), Takeuchi et al. (1998) demonstrated the

role of TGF-β in ACAID whereby exogenous TGF-β2 prevented antigen presenting cells (macrophages) activating T Cells by lowering levels of IL-12. TGF-β1 is also found stored within the ECM of the TM. Once activated, TGF-β1 and TGF-β2 is released and binds to cell surface receptors, some of which are present on TM cells, suggesting an autocrine action. Mechanical stress of TM cells induces TGF-β release, providing further evidence of its role in TM functioning (Liton et al., 2005; Liton et al., 2009). In the same way that aberrant levels can cause fibrosis in other organs, dysregulated TGF-β signalling has been implicated as a major factor for fibrosis of the TM in POAG.

### 1.6.5 TGF-β in POAG

TGF-β1 and TGF-β2 have been implicated in the pathogenesis of glaucoma and TGF-β2 in particular, has been extensively investigated with regards to TGF-β signalling and development of TGF-β induced fibrosis of the TM, in patients with POAG. The ability of TGF-β to transform TM cells into myofibroblasts through its actions on α-smooth muscle actin has been shown in culture studies (Tamm et al., 1996). The decrease in TM cell numbers observed in patients with POAG is attributed to TGF-β's inhibitory effects on cell proliferation (Borisuth et al., 1992) and its ability to promote phagocytosis (Cao et al., 2003). Together with its ability to increase ECM deposition, the data makes TGF-β a prime target for investigation into its role in increasing outflow resistance and hence POAG pathobiology.

Enzyme-linked immunosorbent assay (ELISA) of the AqH from patients with POAG reveals higher levels of total (i.e. TGF-β bound to LAP) and active (i.e. liberated from LAP) TGF-β2

when compared to age-matched controls (Tripathi et al., 1994). Another study, by Ochiai & Ochiai (2000), also using ELISA to determine TGF-β2 levels reported that total TGF-β2 levels were similar between POAG patients and controls, and that only the active TGF-β2 levels were significantly higher in POAG patients. In addition to higher levels of active TGF-β2 in the AqH of POAG patients, these studies and others report negligible active TGF-β1 found in AqH, despite both isoforms being potentially able to modulate ECM. The levels of TGF-β isoforms found within AqH can vary depending on the type of glaucoma; for example TGF-β1 levels increase in neo-vascular glaucoma (Yu et al., 2007) and Pseudoexfoliation glaucoma (PXG) (Schloetzer-Schrehardt et al., 2001). In light of the above, TGF-β2 in the anterior chamber has been the focus of studying POAG (Tripathi et al., 1994; Ochiai & Ochiai, 2000; Ozcan et al., 2004).

One area of particular focus is the effects of TGF-β2 on proteases within the TM, namely, the MMP family. Net accumulation of ECM in the TM results from both TGF-β2-induced ECM deposition and TGF-β2 induced down regulation of proteases which degrade ECM. TM cells express MMP2 and MMP9 enzymes that are secreted in a pro-form, like TGF-β, and need to be activated through cleavage by serine proteases including plasmin. Culture studies have shown increases in plasmin inhibition, *via* PAI-1, that leads to a marked decrease in MMP2 function (Fuchshofer et al., 2003). This study demonstrated no alteration in MMP2 levels in cells after TGF-β treatment but it does highlight that, although TGF-β can induce MMP secretion, it may be a failure of MMP activation that contributes to the fibrotic pathology seen in POAG. TGF-β is also known to increase expression on TIMPs, thus providing a mechanism for further inhibition of MMP (Leivonen et al., 2013).

TGF-β1 has similar fibrotic effects to TGF-β2 in cultured TM cells and, although studies investigating AqH content of TGF-β isoforms find very little TGF-β1 compared to TGF-β2 (Jampel et al., 1990), TGF-β1 is found within the TM cells. Gene expression studies have demonstrated an increase in ECM proteins and alterations in redox processes within the cultured TM cells treated with both TGF-β1 and TGF-β2 (Zhao et al., 2004). Hence, the gene profiling in the study by Zhao et al., (2004) suggests that increased levels of TGF-β are responsible for changes observed in the TM of patients with POAG. Further evidence for TGF-β1 expression by TM cells has been obtained through TM cell culture experiments that demonstrate constitutive expression TGF-β1 mRNA and, like TGF-β2, the auto-activation of gene expression in an autocrine manner (Li et al., 1996).

Interestingly, TSP-1 is a potent regulator of TGF-β as it dissociates the LAP, liberating the active form of TGF-β. TSP-1 is normally found within the JCT region of the TM and its levels are increased in POAG, with the hypothesis of higher levels of TSP-1 leading to higher levels of TGF-β and hence, more ECM deposition (Khalil, 1999). A study by Flügel-Koch et al (2004) demonstrated higher levels of TGF-β1-induced expression of TSP-1, thereby reinforcing the increasing levels of active TGF-β within the TM in glaucomatous eyes compared to normal controls.

### 1.7 Anti-fibrotic agents

Having identified that TM fibrosis is part of the pathology of POAG, it is evident that there are still no treatments available to target this aspect of the disease. There are many IOP lowering agents available, but they work through other mechanisms, namely by increasing

outflow through the uveoscleral pathway or reducing production of AqH (see section 1.4.3). Trabeculectomy and laser surgery provide therapeutic efficacy in managing uncontrolled POAG but have associated complications as the surgery itself can cause fibrosis, warranting further medical intervention. The use of anti-fibrotic agents, such as mitomycin C, has shown to improve surgical success rates (Scott et al., 1998). Gristanti et al., (2005) showed that sub-conjunctival injections of Decorin, a naturally occurring TGF-β inhibitor, was able to significantly reduce post-operative scarring in the surgical area and also lower IOP. Another study by Mohan et al. (2011) demonstrated that adenoviral gene expression of Decorin prevented corneal fibrosis in rabbits providing further evidence for the anti-fibrotic actions of the glycoprotein.

Despite there being much investigation into the use of anti-fibrotic agents in ocular surgery, they are not currently used in patients with POAG to directly target the TM. Being able to lower IOP through reversing established and/or preventing further fibrosis in the TM would provide a promising avenue for more curative treatments. Decorin, through is ability to interact with TGF-β and other ECM molecules to inhibit fibrogenesis, as well as having immunomodulatory functions, is potentially an effective anti-fibrotic treatment for a number of diseases emanating from a fibrotic pathology and hold promise as a new agent to treat POAG.

## 1.8 Decorin

### 1.8.1 Structure and function

Decorin is naturally occurring, extracellular leucine rich secreted glycoprotein and is part of the chondroitin-dermatan sulphate family of proteoglycans (Figure 1.10). Human Decorin is approx. 70kDa (Brandan et al., 1992), is encoded by the DCN gene on chromosome 12q21.33 and contains 359 amino acids (Grover et al., 1995). Binding of proteins to the concaved shaped Decorin occurs through its 12 leucine-rich repeat core, and its functionality is conferred though its associated chondroitin sulphate glycosaminoglycan chains (GAG) attached to the cysteine rich N-terminus (Scott et al., 2004). Decorin was so-called through its ability to decorate, or arrange, collagen through its binding of collagen fibrils to its protein core. This interaction is required for normal functioning of collagen to provide strength and order (Weber et al., 1996). The structure-function relationship between Decorin regulating collagen have been confirmed in experiments whereby Decorin null mice presented with abnormal collagen fibril formation and weakness in their skin structure (Danielson et al., 1997). Decorin can be found in most organs which are rich in collagen such as heart, lung, liver and spleen (Hocking et al., 1998). Decorin is also thought to be the primary regulator of fibril formation during development of the cornea (Zhang et al., 2009). Recently, the non-structural functions of Decorin have become apparent in terms of its immunomodulatory, anti-angiogenic, anti-proliferative and anti-fibrotic functions through its ability to bind to various growth factors and their receptors.

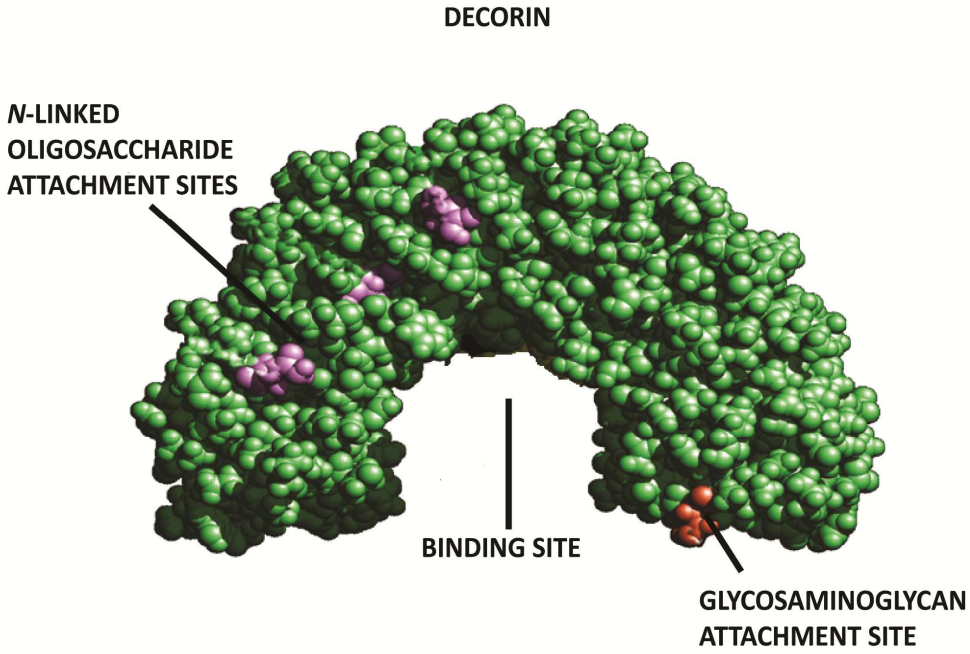


**Figure 1.10 Decorin structure and collagen binding.** Decorin has a concave shape, with its inner surface for ligand binding.

*Source: Image modified from Weber et al., (1996)*

### 1.8.2 Decorin and TGF-β

Decorin's ability to bind directly to and sequester TGF-β was first demonstrated using Chinese hamster ovary cells in a cell proliferation study by Yamaguchi et al. (1990). This study followed a similar study that identified Decorin's ability to attenuate cell proliferation (Yamaguchi & Ruoslahti, 1988). Decorin is able to bind to TGF-β1 and TGF-β2, preventing its binding to receptors and subsequent intracellular signalling. However, reports of Decorin increasing TGF-β activity in extracted bone matrix have also been noted in the literature (Takeuchi et al., 1994). These contradictory findings may be due to different bioactivity in different cells, and/or other ECM protein interactions. Increases in TGF-β production generally leads to increases in expression of Decorin (on ECM), which then is able to

modulate TGF-β levels in a negative feed-back loop mechanism. Decorin is also able to interact with other ECM molecules through its core protein (Schmidt et al., 1991), e.g. fibronectin, and ECM proteases, thus having a direct effect on ECM turnover in conjunction with TGF-β signalling.

### 1.8.3 Decorin and fibrosis

Fibronectin fibril formation plays a big part in producing thick fibrous strands within the TM and contributes to the tensile strength of TM cell necessary when stretching and contributing to AqH outflow resistance (Vittal et al., 2005). Decorin modulates MMP activity by increasing levels of plasminogen (Davies et al., 2006), favouring higher turnover of ECM and leading to ECM degradation. A recent study using Decorin after spinal cord injury in rodents demonstrated that Decorin enhanced levels of MMP2 and MMP9 and reduced levels of fibronectin and laminin over 21 and 35 days (Ahmed et al., 2013). Other wound healing models in the CNS have demonstrated the use of Decorin to decrease matrix deposition, including the deposition of laminin basement membranes and scar formation (Logan et al., 1999; Davies et al., 2004). The use of Decorin in disease where fibrosis is a major cause of morbidity has been established. For example, Decorin has shown a reduction in fibrosis in many pathological conditions including proliferative vitreoretinopathy (Nassar et al., 2011), renal fibrosis (Isaka et al., 1996), lung fibrosis (Giri et al., 1997) and juvenile communicating hydrocephalus (Botfield et al., 2013). The study by Botfield et al. (2013) used the aluminium silicate, kaolin, to replicate the inflammatory response in the subarachnoid space causing significant fibrosis, and perturbed CSF drainage, modelling the human condition of

hydrocephalus. In this model Decorin attenuated inflammation and fibrosis and prevented the development of ventriculomegaly. The increasing evidence of Decorin as an effective anti-fibrotic agent through its actions on TGF-β and its ability to alter ECM turnover provide a promising avenue for use to combat the fibrotic pathology seen in POAG. As with other pathological conditions investigating the pathobiology and development of new treatments require the use of experimental models and, for complete biological effects, the most useful modelling comes from *in vivo* experimentation.

### 1.9 Modelling POAG in rodents

POAG is a multifactorial disease, therefore modelling the disease experimentally is not straightforward. Most rodent models serve to investigate a certain aspect of the disease and, not replicating the human condition perfectly, they can be very useful in terms of identifying compounds that alter the cardinal features of POAG, which include IOP elevation and RGC death. Rats in particular are suitable for studying POAG as the anterior chamber anatomy is very similar, in terms of outflow pathways, to humans (Bouhenni et al., 2012) and they are inexpensive and are easily maintained within a laboratory setting. Mice are also often used for their ease of genetic manipulation to create transgenic models. The most popular genetic alteration is that of the myocilin gene (MYOC) (Gould et al., 2004). Patients with glaucoma have demonstrated higher levels of MYOC expression and this has been modelled in mice. Interestingly, point mutations (leading to increased expression) of MYOC leads to open angle glaucoma in mice, and dexamethasone and TGF-β increases MYOC expression leading to POAG (Tamm et al., 1999; Senatorov et al., 2006).

MYOC is also known to associate with ECM proteins and glycoproteins including Decorin (Ueda et al., 2002). Similar to rats, mice are inexpensive and easy to maintain. However, from a surgical point of view, the mouse eye is a lot smaller than that of a rat making intraocular injections more difficult. Studies using rodent models demonstrate IOP elevations and retinal and ON changes similar those shown in POAG patients (reviewed by Johnson &Tomarev, 2010).

Most models of POAG are based around methods to cause IOP elevation, as this is the main risk factor for the development of POAG in humans. In rats, the most commonly used experimental methods used for IOP elevation include giving intracameral injections of viscoelastic substances (Benozzi et al., 2002) or micro-beads to occlude TM drainage (Sappington et al., 2010), using lasers to damage cells within the TM (Levkovitch-Verbin et al., 2002) and ligation of episcleral vessels (Yu et al., 2006). Although reliable and useful for studies to manipulate IOP, these models of IOP elevation are not ideal for investigations of TM fibrosis and would not be suitable for testing anti-fibrotic agents such as Decorin. However, they are very useful in terms of testing neuroprotective and IOP lowering agents. Agents known to cause fibrosis in other experimental models of fibrotic disease e.g. TGF-β (Sime et al., 1997), Dexamethasone (Fingert et al., 2001) and kaolin (Botfield et al., 2013) may be useful in modelling fibrosis in the TM and hence, be more suitable to assess the effectiveness of anti-fibrotic agents.

### 1.9.1 Intracameral injection of substances to increase IOP

A study by Benozzi et al. (2002) demonstrated that a single injection of hyaluronic acid (a viscoelastic substance routinely used during ocular surgery) into the anterior chamber of rats led to an increase IOP from a baseline reading of 12mmHg up to 22mmHg, which lasted for five days before decreasing towards baseline due to degradation of the hyaluronic acid . This study also showed that multiple injections of hyaluronic acid led to significantly higher IOP levels over 10 weeks. These effects were followed in another study that showed similar results in terms of IOP elevation (Moreno et al., 2005). These hyaluronic-induced IOP increases, which are thought to cause direct blocking of the TM outflow pathways, were reduced with the application of IOP lowering drops including latanoprost (which increase outflow through the uveoscleral pathway).

Sappington et al. (2010) designed a novel method for increasing IOP by intracamerally injecting polystyrene microbeads to occlude AqH outflow. This produced a rapid increase in IOP which lasted weeks and resulting in a moderate 30% increase in IOP, which is comparable to the modest increase seen in patients who develop POAG. This model, however, is not suitable for investigating TM fibrosis.

Reproducibility of these models are very favourable and many are useful to assess candidate neuroprotective agents as they successfully model RGC death. However, the invasive nature and severity from hyaluronate injections on the IOP elevation pose some disadvantages by it not being able to cause subtle IOP increases over a period of time. This issue was addressed

in the microbead occlusion model that provided the most sustained increases in IOP, however, none of these models are useful to assess fibrotic changes within the TM.

### 1.9.2 Laser photocoagulation POAG model

Application of a laser beam either directly or indirectly onto the TM causes IOP elevations in rats and is one of the main methods used to elevate IOP experimentally (reviewed by Johnson &Tomarev, 2010). This method serves to reduce AqH outflow by creating cellular disorganisation and deposition of cell debris within the TM. Levkovitch-Verbin et al. (2002) optimised the use of laser in the anterior chamber to create a reliable model of glaucoma in rats using translimbal photocoagulation. They demonstrated abnormalities in the TM cellular arrangement, scarring within the angle and the presence of red blood cells. They also observed complications, including corneal injuries and hyphema (presence of blood) in the chronic studies, but these were avoided in their acute models. A previous study which also used also lasers directly on the TM showed similar changes in the TM with increased ECM deposition, debris and the presence of macrophages (Ueda et al., 1998). Here, carbon particles from India ink injections accumulated in the TM and, hence, permitted localised argon laser treatment.

Despite their complications, laser photocoagulation models are reliable models of creating elevations in IOP, and they do mimic cellular changes within the TM which could be useful for studies of fibrosis. However, these studies require specialist laser equipment and can

damage other ocular structures. Laser ablation may also represent a more severe response than that which naturally occurs in patients with POAG.

### 1.9.3 Episcleral vein injections and ligation POAG models

In addition to laser photocoagulation, the injection of saline into, or ligation of, the episcleral veins is a popular experimental method to reliably elevate IOP in rats (Morrison et al., 1995). Injections of saline or ligation lead to sclerosis of the episcleral veins through disruption of venous return from the anterior chamber, causing IOP elevations (which can remain high for months) and this is correlated with RGC death. Zhong (2013) managed to achieve an 81% increases in IOP over 24 weeks, leading to 60% death of RGC using injections of saline into the episcleral veins. Yu et al. (2006) demonstrated an elevation in IOP within 24 hours of ligation, that lasted for several months. Garcia-Valenzuela et al. (1995) were able to demonstrate elevations in IOP following cauterization of two limbal veins, with the highest IOP being achieved within the first week. Ligation or cauterization of the episcleral veins can reliably elevate IOP and is relatively inexpensive to perform, however, Morrison et al. (2005) raised some interesting questions about this model, showing RGC loss from the periphery of the retina when most other glaucoma models show preferential loss of RGC proximal to the optic nerve head. Another confounding factor with ligation or cauterization is the risk of ischemia (Goldblum & Mittag, 2002).

### 1.9.4 TGF-β gene-transfection model of glaucoma

A recent study by Robertson et al. (2010) demonstrated the effects of TGF-β1 over-expression in the anterior segment of rat eyes using adenoviral gene transfer. In these experiments raised levels of TGF-β1 led to proliferation of corneal endothelial cell and changes in TM actin and ECM accumulation, in addition to ocular hypertension. A study by Shepard et al. (2010) demonstrated similar results, namely elevations in IOP and decreased AqH outflow, after adenoviral gene expression of active TGF-β2 in both mouse and rat eyes. There was however, a reduction in IOP after 8 days the rat eyes and the authors suspected the short-lived transgene expression and rapid IOP decreases may have been due to immune responses to the virus. However, there are limited models available to investigate TM fibrosis but the research to develop these models is now being found in the literature. The most notable study came from Junglas et al., (2012) who were able to successfully demonstrate a mouse model of TM fibrosis through up-regulation of the TGF-β signalling pathway.

## 1.10 Hypothesis and aims

### 1.10.1 Hypotheses

It is widely accepted that TGF-β levels are increased in AqH of patients with POAG compared to patients without POAG, and patients with elevations in IOP are more at risk for developing POAG. IOP elevations are correlated with RGC death in patients and in experimental models of glaucoma. POAG develops due to fibrosis of the TM preventing AqH from leaving the eye. The build-up of AqH results in IOP elevations and death of RGC. TGF-β is the main cytokine that orchestrates fibrosis. TGF-β through up-regulation of ECM deposition and prevention of degradation, results in ECM accumulation in the TM. In addition, TGF-β leads to altered phenotypes of TM cells so that they become phagocytic and motile thus decreasing the cellularity of the TM.

Hence, it is hypothesised that intracameral TGF-β injections will result in excess ECM deposition and reduced ECM degradation at the TM and, as a consequence, IOP will be elevated enough to cause RGC death and; thatDecorin, through its actions on TGF-β and on the ECM, will demonstrate therapeutic efficacy by attenuating established fibrosis and reducing elevated IOP and, through its IOP lowering actions, Decorin will promote RGC survival.

### 1.10.2 Aims

1) To develop a reproducible *in vivo* model of TM fibrosis using fibrotic agents to mimic the fibrotic pathology seen in patients with POAG.

2) To assess the effects Decorin in the developed *in vivo* model of TM fibrosis and its potential as a treatment to attenuate TM fibrosis, raised IOP and RGC loss.

3) To evaluate novel drug delivery mechanisms for Decorin into the eye for future translational studies.

# Chapter 2

# Materials and Methods

## 2.1 In vivo procedures described in Chapters 3-6

### 2.1.1 Surgery and anaesthetic

After formal training from Professor Martin Berry, all of the surgical procedures used in this study were performed by myself at the Biomedical Services Unit at the University of Birmingham in accordance with the Home Office guidelines and the 1986 Animal Act (UK). The work was performed under a Home Office project license PL30/2720. Male Sprague Dawley rats 175g-200g (Charles River, Kent UK) were used for all *in vivo* experiments and housed with free access to food and water, under a 12hr dark/light cycle. All ocular surgical procedures, electrophysiology, optical coherence tomography (OCT) and IOP measurements were performed under general anaesthetic using 2-5% Isoflurane/95% $O_2$ (VetTech, Cheshire, UK) at a flow rate of 1.5L/min. Local anaesthetic, 0.4% Oxybuprocaine, was used in study 1 (Figure 2.1). All intracameral injections of treatment agents were administered unilaterally with contralateral eyes as control injections, unless specified. The initial corneal incisions with the $15^{o}$ blade on 0d induced a very small amount of AqH leakage. The subsequent intracameral injections using glass micropipette did not induce any AqH leakage. After surgery, rats were administered 0.1mg/kg Buprenorphine (if required) placed in cages in a recovery room and monitored by trained animal welfare technicians daily. Rats were killed using rising concentrations of $CO_2$ at various time points. The experimental groups, treatments, experimental time course and end points in addition to the relevant experimental chapters are described in Figure 2.1.

| Study | *n* | Treatment regime | Control groups | Experimental Time course | Endpoint | Chapter |
|---|---|---|---|---|---|---|
| Kaolin pilot study | 8 eyes | 1.25% Kaolin (n=1)<br>3.5% Kaolin (n=1)<br>5% Kaolin (n=1)<br>10% Kaolin (n=1)<br>20% Kaolin (n=1)<br>(Injected only on 0d and 5d) | Intact (n=2 eyes)<br><br>PBS (n=1 eye) | 0d-21d | IOP<br>OCT<br>IHC | 3.2.1<br>3.3.1 |
| Kaolin+LPS study | 8 eyes | Kaolin+LPS (n=4)<br><br>(Injected 0d only) | Kaolin+PBS (n=4) | 0d-28d | IOP<br>OCT<br>IHC | 3.2.2<br>3.3.2 |
| Effects of anaesthetic on IOP (Study 1) | 6 eyes | Isoflurane<br>General anaesthetic<br>(n=3) | Oxybuprocaine eye drop anaesthetic<br>(n=3) | 1 single IOP recording session per week (=3 sessions over 3 weeks) | IOP | 4.2.1<br>4.3.1 |
| TGF-β1 dosing (Study 2) | 6 eyes | 3.5µl 0.5ng/µl active TGF-β1<br>3.5µl 5ng/µl active TGF-β1<br>(n=3) | 3.5µl PBS<br>(n=3) | 0d-45d | IOP | 4.2.2<br>4.3.2 |
| TGF-β1 Latanoprost (Study 3) | 16 eyes | 3.5µl 5ng/µl active TGF-β1<br>(n=8)<br>(Latanoprost drop, n=4)<br>(PBS drop, n=4) | 3.5µl PBS<br>(n=8)<br>(Latanoprost drop, n=4)<br>(PBS drop, n=4) | 0-45d<br><br>(30-45d) | IOP | 4.2.3<br>4.3.3 |
| TGF-β1 (Study 4) | 18 eyes | 3.5µl 5ng/µl active TGF-β1<br>(n=6)<br>3.5µl 5ng/µl active TGF-β1 then PBS (n=6) | 3.5µl PBS (n=6) | 0d-30d | IOP<br>IHC<br>RGC-Death | 4.2.4<br>4.3.4 |
| TGF-β2 (Study 5) | 24 eyes | 3.5µl 5ng/µl active TGF-β2<br>(n=12) | 3.5µl PBS (n=12) | 0d-30d | IOP<br>VEP<br>EM<br>IHC<br>RCG-DEATH | 4.2.5<br>4.3.5 |
| TGF-β1 Decorin study | 6 eyes | 3.5µl 5ng/µl active TGF-β1 then Decorin (n=3) | 3.5µl 5ng/µl active TGF-β1 then PBS (n=6) | 0d-30d | IOP<br>IHC<br>RGC-DEATH | 5.2.1<br>5.3 |
| TGF-β2 Decorin study | 12 eyes | 3.5µl 5ng/µl active TGF-β1 then Decorin (n=12) | TGF-β2 study 5 | 0d-30d | IOP<br>VEP<br>EM<br>IHC<br>RCG-DEATH | 5.2.2<br>5.3 |
| Nanosome eye drop study | 24 eyes | Covalent NS+Decorin (n=4)<br>Electrostatic NS+Decorin<br>(n=4) | Intact (n=4)<br>NS+PBS (n=4)<br>NS only (n=4)<br>Decorin only (n=4) | 10 min | OCT<br>ELISA | 6 |

Key
d – day;
ELISA – Enzyme-linked immunosorbent assay; LPS – Lipopolysaccharide; RGC – Retinal ganglion cell
EM – Electron Microscopy; NS – Nanosome; TGF-β – Transforming Growth Factor-β;
IHC – Immunohistochemistry; OCT – Optical Coherence Tomography;
IOP – Intraocular Pressure; PBS – Phosphate Buffered Saline; VEP – Visual Evoked Potential

**Figure 2.1 Overview of experimental design.** The study, number of eyes (n), treatment, controls, duration of experiment, end points and relevant experimental chapters are described.

### 2.1.2 Intracameral Injections of Kaolin

One self-sealing incision was made through the cornea into the anterior chamber using a 15° disposable blade (BD Systems, Warwickshire, UK) enabling repeat 3.5µl injections of 1.25%, 3.5%, 5%, 10% and 20% w/v Kaolin (Sigma, Dorset UK) in phosphate buffered saline (PBS) on 0d and 5d to determine the optimal concentrations of Kaolin to induce fibrosis (see Figure 2.1).

### 2.1.3 Intracameral Injections of TGF-β1, TGF-β2 or Decorin

On 0d, one self-sealing incision was made through the cornea into the anterior chamber using a 15° disposable blade enabling repeat 3.5µl injections for 30 days of either PBS (Sigma Poole) ($PBS_{0\text{-}30d}$), active TGF-β1 or TGF-β2 (5ng/µl; Peprotech, London, UK) ($TGF\text{-}\beta_{0\text{-}30d}$), TGF-β (5ng/µl) 0-17d then PBS 21-30d (5mg/ml; Catalent Pharma Solutions, Philadelphia, USA) ($TGF\text{-}\beta_{0\text{-}17d}/PBS_{21\text{-}30d}$) or TGF-β (5ng/µl) 0-17d then human recombinant Decorin 21-30d (5mg/ml; $TGF\text{-}\beta_{0\text{-}17d}/Decorin_{21\text{-}30d}$) and using a sterile glass micropipette produced in-house from a glass capillary rod (Harvard, Kent UK) (see Figure 2.2). An injection regime of TGF-β from 0-17d was determined from the IOP data gathered in the initial TGF-β 0-30d experiments. By 17d the IOP had increased and was maintained at a higher level compared to controls, therefore 21d was considered a suitable time point to inject Decorin/PBS treatments. No injections were given between 18-20d to ensure IOP remained at raised levels by 21d after cessation of TGF-β injections at 17d.

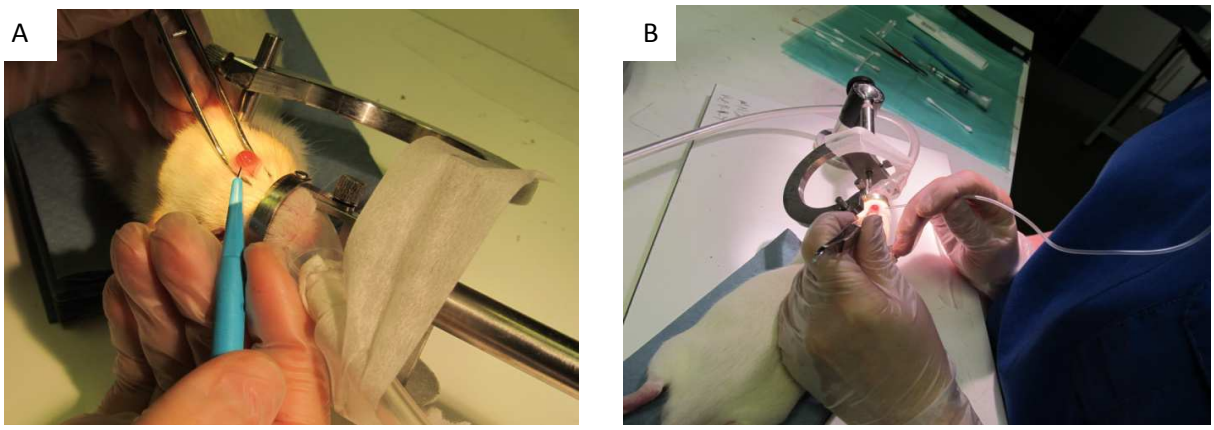


**Figure 2.2 Intracameral injections**. (A) Intracameral injection using a disposable 15$^{o}$ blade. The two-step incision is made through the cornea to promote a self-sealing wound suitable for repeat injections. (B) Intracameral injection of agents using a glass micropipette.

### 2.1.4 TGF-β model validation using latanoprost eye drops

Latanoprost (trading under Xalatan™ Pfizer) eye drops (VetTech, Cheshire, UK) were administered to assess its IOP lowering abilities in the TGF-β model of elevated IOP. Studies with Latanoprost were conducted as part of the TGF-β model development (Figure 2.1 study 3). Administration of latanoprost would be used to assess if the TGF-β model is able to respond with a well-known IOP lowering agent and validate the IOP increases observed in the TGF-β1 group. Latanoprost or control PBS drops were administered once a sustained elevation in IOP had occurred by 30d until the end of the experiment at 45d.

### 2.1.5 In vivo nanosome procedures described in Chapter 6

This study investigated the use of an oligioarginine cell penetrating peptide nanosome as a potential drug delivery system into the eye. All peptide synthesis was performed by Dr Felicity de Cogan and *in vivo* testing carried out by myself. Briefly, nanosome peptide sequence were synthesised using standard Fmoc solid phase support synthesis methods. To form the electrostatic drop, nanosome peptides and Decorin were mixed at a 1:1 (v/v) and incubated for 5 min. Covalent Decorin/nanosome drops were synthesised using a maleimide linker to crosslink the amine group of the nanosome with a thiol group on the Decorin protein sequence. An Fmoc Ahx linker was added to allow effective addition of a 5/6-carboxyfluorescein label to fluorescently label the nanosome.

Electrostatic, covalent or control Decorin and PBS drops were placed bilaterally onto the cornea in awake, manually restrained, rats and left for 10 min when rats were killed using increasing concentrations of $CO_2$. Following death, 10-20µl of AqH was removed and stored at $4^oC$ ready for analysis of Decorin levels by ELISA (Figure 2.1). A patent has been filed relating to the nanaosome preparations (UK Patent Application Number 1401453.4).

## 2.2 Rebound Tonometry

### 2.2.1 Principles of Rebound Tonometry

The measurement of IOP is essential to monitor the progression of glaucoma in patients and for this project IOP was one of the main outcomes to assess the validity of the acute and chronic model of raised IOP. There are different types of tonometers available for use clinically and experimentally, most of which are calibrated for millimetres of mercury (mmHg). For human (in particular children and uncooperative patients) and animal experiments, rebound tonometers are ideal (Moreno-Montañes et al., 2011) and widely used to provide non-invasive intraocular pressure measurements in animals. The TonoLab™ (ICare, Helsinki, Finland) is a tonometer specifically designed for rodents and its accuracy and reliability for measuring IOP has been demonstrated in previous studies (Pease et al. 2011). The hand-held, calibrated, device relies on a looped coil wrapped around a metallic core, creating a force to propel the 1.8mm diameter plastic ended steel probe against the cornea. The probe (which is held in place by an electromagnetic field) deceleration is measured and used to calculate IOP in mmHg and the speed of deceleration is inversely proportionate with IOP.

### 2.2.2 Protocol for Rebound Tonometry

Monitoring of IOP using the Tonolab rebound tonometer was carried out at intervals for the duration of the experiment, to provide reliable and reproducible readings to ascertain if there are any pressure differences between treatments. All IOPs were recorded between 9-11am to avoid the diurnal variations (which also occur in both humans and rodents; Moore

et al., 1996). The TonoLab was placed at a 90$^{o}$ angle against the central part of the cornea (to reduce IOP measurement variability of corneal thickness) of anaesthetised rats (Figure 2.3) and 6 rebound measurements are taken to give an average IOP measurement in mmHg (calibrated by the device). For all graphical data points described in the experimental chapters, 3 readings (of 6 rebounds each) were taken and averaged to ensure a reproducible measurement (Tsuruga et al., 2012). Since anaesthetic is known to lower IOP (Jia et al., 2012) all anaesthetic exposure times were constant for all IOP readings avoid confounding IOP measurements.

A

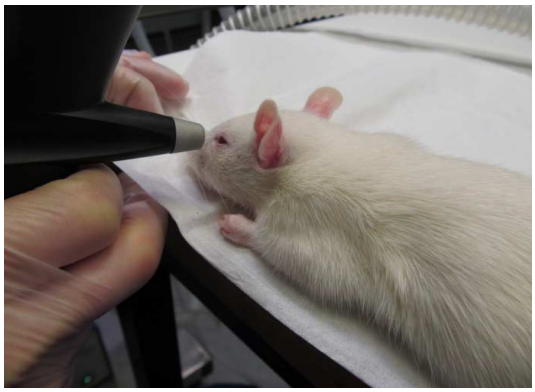

B

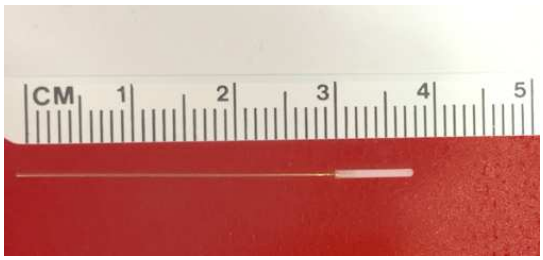


**Figure 2.3 Rebound tonometry.** Rats were anaesthetised and placed flat on the surgical table. The tonometer (the black hand-held machine to the left of the image) was placed horizontally towards the centre of the cornea and held in place for IOP readings to be taken (A). Size of the probe used in the Tonolab tonometer (B).

## 2.3 Functional assessment using VEP for experiments described in chapters 4-5

### 2.3.1 Principles of visual evoked potential recordings

The visual evoked potential (VEP) is a quantitative electrophysiological assessment that is used clinically to detect and monitor glaucomatous damage to the visual pathway and experimentally to assess and monitor neuroprotective compounds *in vivo*. It measures the functional integrity of RGC and the optic projections through the optic chiasm and optic tracts, through the LGN to the visual cortex. Different stimuli allow assessment of different aspects of visual function. Flash VEP are recorded after a flash of light to the eye and which is measured by electrodes placed over the occipital cortex and the latency and intensity of particular aspects of the recorded waveform are assessed (e.g. shown in Figure 2.4). Previous studies have shown reduced VEP amplitude to correlate with axonal loss after 6 days in a rat model of optic neuritis (You et al., 2011) and VEP is used clinically to assess optic nerve function (Holder, 2004). Studies in optic neuritis (You et al., 2011) have demonstrated evidence to suggest that amplitude on VEP reflects the number of functional optic nerve fibers and, in these models, latency reflects the state of myelination. Similar studies show that decreases in amplitude on VEP correlates with decreasing RGC numbers being able to transmit signals to the brain (Heiduschka, et al., 2010). Nomenclature for VEP are based on peaks, for example, P1 representing the first peak, and negative deflections, for example, N1 representing the first negative deflection (Figure 2.4). Reductions of amplitude have previously been reported at N1-P1, P1-N2, and N2-P2 (Zhang et al., 2013) and was measured in the studies presented in Chapter 4.

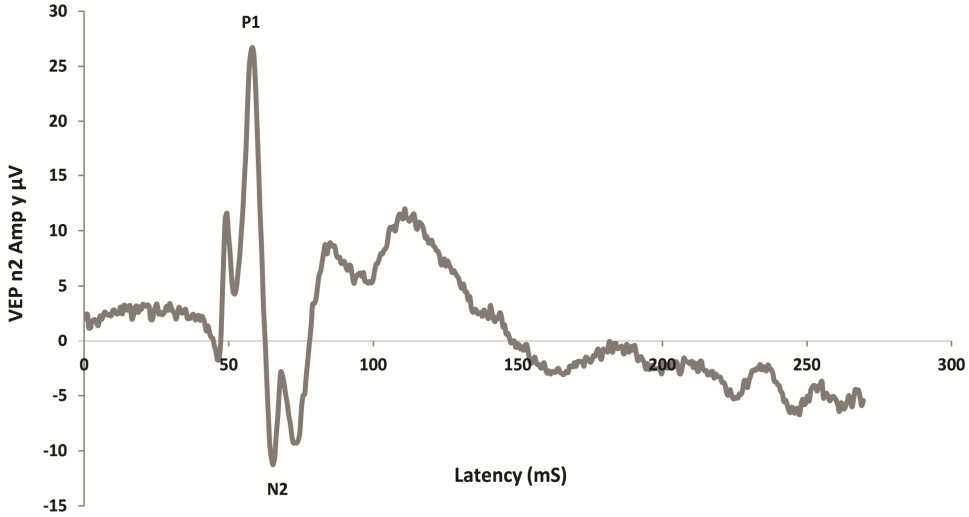


**Figure 2.4 VEP trace with selected parameters.** Amplitude and latency will be analysed from P1 to N2.

### 2.3.2 Protocol for visual evoked potential recordings

Five days prior to VEP recordings stainless steel screws were implanted at 7mm posterior to begma, 3mm lateral to the midline at a depth of 0.5mm into the skull to connect the positive recording electrodes. The reference (negative) skull screw electrode was placed on the midline, 3mm anterior to bregma. The skin was sutured around the screws. For VEP recordings on experimental day 30, rats were dark-adapted overnight and VEP recordings were carried out using HMsERG (Ocuscience) in a light sealed room with preparation under dim red light. Rats were anaesthetised using 2% Isoflurane for the duration of recordings and readings were taken in a 37$^{o}$C temperature controlled Faraday cage to reduce electrical interference (kindly made and supplied by Maj Richard Blanch, Molecular Neuroscience Group). A needle ground electrode was placed in the midline dorsal subcutaneous tissue at the base of the tail. Electrode impedance was measured and kept below 2k Ω. A mini-

Ganzfeld stimulator was used with increasing stimulus intensities of 300, 3000 and 25,000mcd/s/m2, which were averaged 100 times at each intensity with a recording duration of 250ms and an inter-stimulus interval of 1s. VEP from each eye were recorded separately by uniocular occlusion. The amplitude of VEP was measured from the first peak (P1) to the second negative peak (N2) in ERGView (Ocuscience) by an observer blinded to the identity of the treatment groups.

## 2.4 Ocular imaging using Optical Coherence Tomography for experiments described in chapters 3 and 6

### 2.4.1 Principles of Optical Coherence Tomography

Optical Coherence Tomography (OCT) is an imaging technology used routinely in clinical and experimental settings to analyse various ocular structures. OCT functions by using a near infra-red light to construct a high resolution cross sectional image of the retina and/or anterior segment of the eye (cornea and iridiocorneal angle). It is similar to ultrasound, whereby it collates distance from the time delays of reflected signals, however, unlike using sound it uses optical waves to produce cross sectional imaging of the retina.

### 2.4.2 OCT Protocol

Anterior chamber imaging was conducted using a Heidelberg SPECTRALIS Spectral Domain Optical Coherence Tomography (SD-OCT) with the SPECTRALIS Anterior segment Module (Heidelberg Engineering, Heidelberg, Germany). Rats were anaesthetised with 2-2.5% Isoflurane and placed on the imaging stage. Multiple images of the anterior segment were taken manually for qualitative analysis.

## 2.5 Retrograde labelling of RGC and retinal wholemount preparation

Optic nerves were injected with 2µl of a 4% solution of FluoroGold (FG-hydroxystilbamidine) retrograde tracer (Cambridge Bioscience, Cambridge UK), 2mm from the lamina cribosa. This is a reliable and validated method for labelling RGC (Dong et al., 1996; Chui et al., 2008), widely used to identify and quantify RGC by immunofluorescence (FG fluoresces under blue excitation of 300-400nm). FG diffuses into axons and is retrogradely transported by lysosomal transport (Wessendorf, 1991) RGC somata. Rats were killed 48h after FG injections using increasing concentrations of CO2. The cornea, iris, lens and vitreous were removed and the retina and associated sclera were fixed in 4% paraformaldehyde (PFA, Sigma, Poole) in PBS for 2 hours fixation at room temperature. After 2hr, the retina placed on a glass slide, flattened after radial incisions divided the retina into quadrants (Figure 2.5) and mounted with Vectamount media (Vector Labs, Peterborough, UK) and stored at $4^{o}$c before immunofluorescence imaging (see section 2.9).

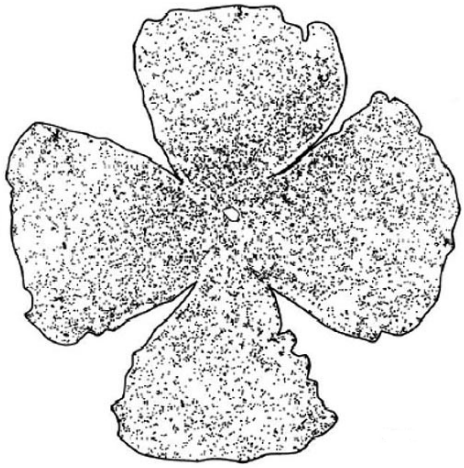

**Figure 2.5 Retinal wholemount preparation.** The retina is flattened after radial incisions divided the retina into quadrants for immunohistochemical analysis.

*Source: Image modified from Vidal-Sanz et al. (1991)*

## 2.6 Tissue processing for immunohistochemical analysis

Animals were killed using increasing concentrations of $CO_2$ and perfused using 4% paraformaldehyde (PFA) in PBS. Eyes were post fixed by immersion with PFA 4% for 2 hours at 4$^{o}$C before cryoprotection. The eyes were cryoprotected by sequential immersion in 10%, 20%, 30% sucrose in PBS at 4$^{o}$C for 24 hours each before embedding in optimal cutting temperature (OCT) embedding medium (Thermo Shandon, Runcorn, UK) in peel-away mould containers (Agar Scientific, Essex, UK). The tissue embedded in OCT was rapidly frozen in crushed dry ice and stored at -80°C. Eyes were allocated a block number to blind the user of from treatment or control groups and sectioned in the para-sagittal plane at -22°C using a Bright cryostat microtome (Bright, Huntingdon, UK) at a thickness of 20µm, mounted on positively charged glass slides (Superfrost plus; Fisher Scientific, Pittsburgh, USA) and stored at -20$^{o}$C until use.

## 2.7 Immunohistochemistry

### 2.7.1 Principles of Immunohistochemistry

Immunohistochemistry is a technique to identify proteins and their localisation within tissue using antibodies to bind their specific antigens on the protein of interest. These studies used the indirect immunofluorescent method (Figure 2.6) and the avidin-biotin complex (ABC) method (Figure 2.7). For indirect immunofluorescent labelling tissue samples are were incubated with a primary antibody which binds to the antigen of interest and then the primary antibody is bound by a fluorescently tagged secondary antibody (raised in the same species as the primary antibody). Multiple secondary antibodies can bind to the primary

antibody providing signal amplification which is detected using an epi-fluorescent microscope. The fluorescently labelled secondary antibody absorbs and emits light at specific wavelengths which can then be detected by the fluorescent microscope. In the ABC method of immunostaining, biotin that is conjugated to the secondary antibody binds to the preformed ABC complex. ABC is already bound to HRP catalyses oxidation of added DAB yielding brown staining of the primary antibody binding site. ABC immuostaining is visualised under a light microscope.

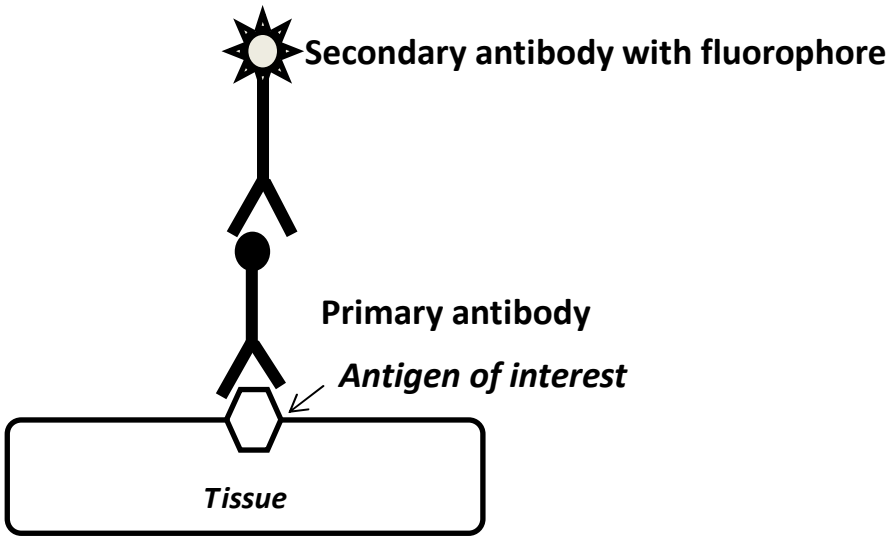


**Figure 2.6 Indirect immunofluorescence.** The antigen of interest is bound by a primary antibody. The primary antibody is bound by a secondary antibody which is conjugated to a fluorescent dye. The light emission from the fluorescent dye can be detected with a fluorescent microscope.

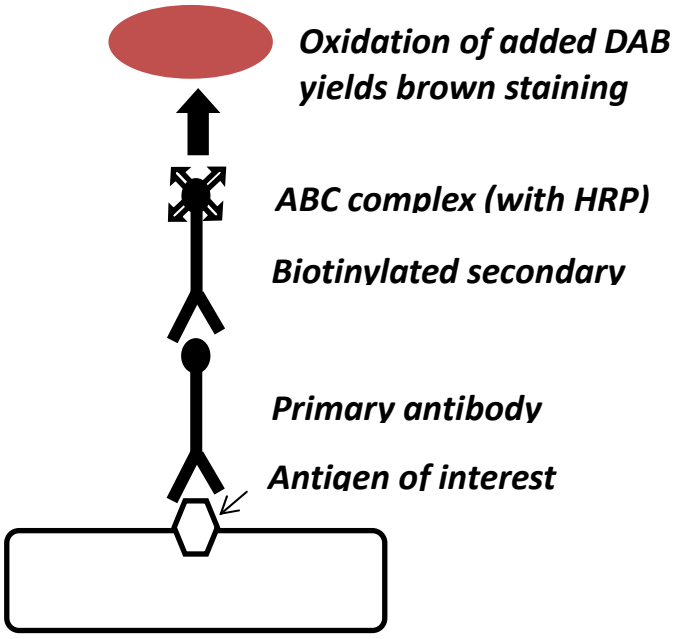


**Figure 2.7 ABC method of immunohistochemistry.** The antigen of interest is bound by a primary antibody. The primary antibody is bound by a biotinylated secondary antibody which binds to preformed ABC complex. HRP within the ABC complex, reacts with added DAB yielding a brown coloured stain where the primary antibody bound to the antigen of interest.

### 2.7.2 Protocol for immunofluorescence staining

Thawed frozen sections were washed 2 X 3 min and permeabilised with PBS containing 0.1% Triton x-100 (PBS-T; Sigma, Poole UK). In order to keep reagents localised over the tissue, a hydrophobic barrier was placed around each section using an ImmEdge™ pen (Vector Laboratories). Slides were blocked for 30 min in 0.5% bovine serum albumin (BSA; Sigma, Poole, UK) and 15% normal goat serum (Vector Laboratories) in PBS-T. BSA prevented non-specific binding of the primary and secondary antibodies. However, goat serum was also used as an additional blocking step to prevent non-specific binding of the secondary antibody specific to the species it was raised in. Tissue sections were incubated with primary antibody (Figure 2.8) for either 1hr at room temperature or 24 hr at $4^{O}$C in a humidified chamber before being washed 3x5 min. Sections were then incubated for 1hr with secondary antibody at room temperature. After incubation, the excess secondary antibody (Figure 2.8) was removed by 3x5min washes with PBS-T. Finally, slides were mounted in Vectorshield mounting medium containing the nuclear marker, DAPI (Vector Laboratories), and stored in a light-proof container at 4°C. Incubation of tissue sections with secondary antibody alone were used for reagent controls.

### 2.7.3 Protocol for immunoperoxidase

Thawed frozen sections were washed 2 X 3 min in distilled water and incubated for 30 min in 0.3% $H_20_2$ in 70% methanol (diluted in PBS) and after, were washed 2 X 3 min in PBST. In order to keep reagents localised over the tissue, a hydrophobic barrier was placed around each section using an ImmEdge™ pen. Slides were blocked for 30 min in 0.5% bovine serum

albumin (BSA; Sigma, Poole, UK) and 15% normal serum (Vector Laboratories) in PBS-T. Tissue sections were incubated with primary antibody (Figure 2.8) for 24hr at 4$^{o}$C in a humidified chamber before being washed 3x5min in PBST. Sections were then incubated for 30min with the biotonylated secondary antibody at room temperature. After incubation, sections were washed 3x5 min in PBS-T and incubated for a further 30 mins in the ABC complex. Sections were washed in PBST, 3x5 min, and diaminobenzidine (DAB; Vector Laboratories) substrate was added. Finally, slides were mounted in Vectorshield mounting medium (Vector Laboratories) ready for analysis using the light microscope.

| Antibody | Species | Dilution | Marker For | Supplier | Catalogue Number |
|---|---|---|---|---|---|
| TGF-β1 | Rabbit | 1/200 | TGF-β1 | Santa Cruz Biotechnology, Texas, Usa | Sc-146 |
| Laminin | Rabbit | 1/200 | Laminin | Sigma-Aldrich, Dorset, Uk | L9393 |
| Fibronectin | Rabbit | 1/200 | ECM | Sigma-Aldrich, Poole, UK | F3648 |
| ED1(Cd68) | Mouse | 1/400 | Macrophages | Serotec, Oxford, Uk | Mca341r |
| BIII-Tubulin | Mouse | 1/400 | Neuronal marker | Sigma-Aldrich, Poole, UK | T8660 |
| Decorin | Mouse | 1/400 | Human Decorin | Abcam, Cambridge, UK | Ab54728 |
| MMP2 | Rabbit | 1/100 | MMP2 | Abcam, Cambridge, UK | Ab37150 |
| MMP9 | Rabbit | 1/100 | MMP9 | Merck Millipore, USA | Ab804 |
| TIMP2 | Rabbit | 1/100 | TIMP2 | Santa Cruz, USA | SC-5539 |
| Biotinylated Anti-Rabbit IgG | Goat | 1/1000 | Rabbit IgG | Vector Laboratories. Peterborough, UK | BA1000 |
| Alexa Fluor 594 | Goat | 1/500 | Rabbit IgG | Life Technologies, Paisley, Uk | A11037 |
| Alexa Fluor 488 | Goat | 1/500 | Mouse IgG | Life Technologies, Paisley, Uk | A11029 |

**Figure 2.8 Antibodies used for immunostaining.**

## 2.8 Image analysis and quantification

### 2.8.1 Semi-quantitative image analysis for TM fibrosis

After immunofluorescence staining, sections were viewed on a Zeiss Axioplan 2 epi-fluorescent microscope (Zeiss, Germany) and images captured using a Zeiss AxioCam HRc. Images were quantified using the Java based Image J software (National Institutes of Health).

For evaluation of immunofluorescence staining, region of interest of the same set size for all eyes/treatments were selected to make sample counts within the TM and the percentage of immunofluorescent pixels above a set background threshold were calculated using ImageJ software. The levels of brightness were altered to include all stained areas of the TM on intact eye sections to determine the threshold level for test group analysis. Images were then saved as randomised numbers to ensure treatment groups were anonymised for quantification. These methods to quantify immunofluorescence staining have been used previously (Botfield et al., 2013).

### 2.8.2 RGC survival

FG-filled RGC were counted under a Zeiss fluorescence microscope with an UV filter (365/420 nm) at x20 magnification and photographed using an Axiocam HRc camera coupled to Axiovision software (Zeiss Ltd, Hertfordshire, UK). Images were captured from 3 different areas of each quadrant (Figure 2.9) and images assigned a random number to blind the counter from treatment groups. RGC counts expressed as RGC/$mm^2$±SEM (Ahmed et al., 2011) performed using ImagePro (Media Cybernetics, MD, USA).

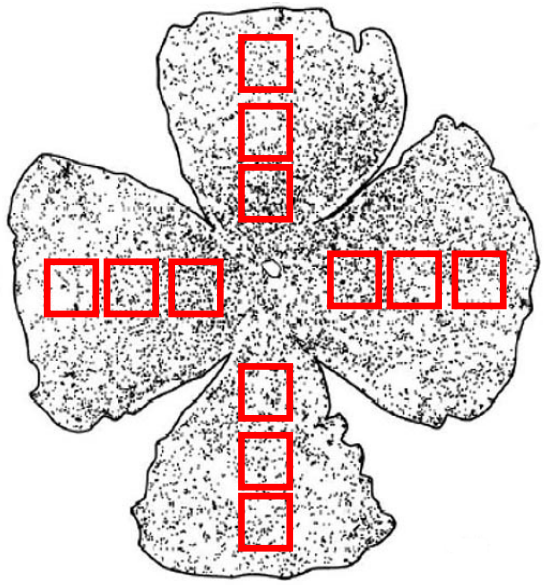

**Figure 2.9 RGC counting.** Red squares show the areas in which RGC were actually counted. In each retina 3 different areas of 0.6mm x 0.5mm from each quadrant were imaged and counted using Zeiss Axiovision software.

*Source: Image modified from Vidal-Sanz et al. (1991)*

## 2.9 Enzyme-linked immunosorbent assay

### 2.9.1 Principles of enzyme-linked immunosorbent assay

Enzyme-linked immunosorbent assay (ELISA) is a biochemical assay quantifying protein levels by detection of antigens using antibodies. Samples in solution are placed into a 96 well plate previously coated with antibodies to capture the antigens of interest. An additional detection antibody (biotinylated) is added to bind to the same antigen in the sample (using a different epitope to the capture antibody). Hence, the antigen of interest is sandwiched between the capture and detection antibodies. HRP-Conjugated Streptavidin binds the detection antibody. The addition of a substrate permits oxidation of HRP and yields a colourmetric change detectable and quantified using a microplate reader of optical density, which is positively correlated with the antigen concentration in the sample (Figure 2.10). Optical density for known (standard) concentrations of antigen is then used to determine the sample concentration.

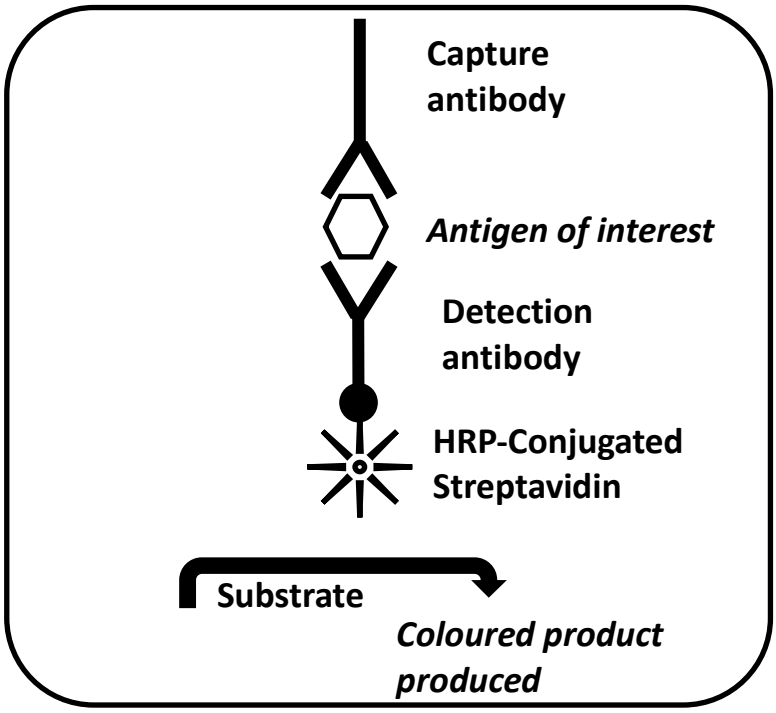


**Figure 2.10 ELISA assay steps**

The sample is added to wells coated with capture antibody. A biotinylated antibody is then used to detect the antigen. The HRP conjugated with Streptavidin binds to the detection antibody and the addition of a substrate oxidises HRP creating a coloured product.

### 2.9.2 Protocol for Decorin ELISA of Aqueous humour samples

ELISA was used to detect levels of Decorin in AqH. All ELISA experimental protocols were performed using the R&D Systems human Decorin DuoSet ELISA kit (Catalogue DY143, R&D systems, Abingdon UK). All reagents were supplied in the kit.

Mono-clonal mouse anti-human Decorin capture antibody (2µg/ml) was added to both standards and sample allocated wells on a 96 well plate and was incubated overnight at room temperature. Wells were washed in PBS containing 0.05% Tween®20 (pH7.2-7.4) before placing in blocking solution of 1% BSA in PBS (pH7.2-7.4), to block non-specific binding, for 1hr at room temperature. Wells were washed again and human Decorin standards (serial dilutions up to 2000pg/ml; supplied by R&D) and aqueous humour samples (1/2 dilutions) in duplicate were incubated for 2hr at room temperature, then washed and incubated in biotinylated mouse anti-human Decorin detection antibody (250ng/ml) for 2 hr before being washed again. Streptavidin-HRP (1/200 dilution) was then added to each well and incubated for 20 min at room temperature and kept away from direct light. After further washing wells were incubated in 1:1 $H_20_2$ and tetramethylbenzidine substrate solution in the dark. After 20 minutes the 2N $H_2SO_4$ stop-solution was added and the optical density was read on a microplate reader at 450nm. Blank values subtracted from all readings.

## 2.10 Transmission Electron Microscopy of the TM

### 2.10.1 Principles of Transmission Electron Microscopy

Electron microscopy visualises cellular ultrastructure using electron beams to acheive resolution (e.g. x200,000) of cellular ultrastructure. The electron source emits electrons through a vacuum column which focus on the specimen through an electromagnectic lens, through the specimen onto a fluorescent screen (visualised by the user).

### 2.10.2 Tissue processing and sectioning for Transmission Electron Microscopy

Eyes were fixed in 4% glutaraldehyde in 0.1M phosphate buffer (TAAB, Berks UK) for 48 hours, bisected in the sagittal plane and 3 radial sections of tissue including cornea, TM and ciliary body were isolated from one half globe for embedding using Vanna's scissors. The remaining half globe was stored in glutaraldehyde. Tissue was washed in 0.1M Phosphate buffer pH 7.0 for 30min and fixed in 1% Osmium (ElectronMicroscope Sciences, Hatfield) for 45 min at room temperature, then tissues washed 3x in 0.1M Phosphate Buffer and dehydrated through increasing concentrations of ethanol from 50%-100% diluted in distilled water for 10 min at each concentration. Tissue was then placed in pure propylene oxide to remove ethanol residue for 2x10 min and immersed in resin for 24hr (Electron Microscope Sciences, Hatfield UK) at room temperature. Resin blocks were labelled with eye number and incubated at $56^{O}$C for 24hr before being stored at room temperature. For analysis under the TEM, resin blocks were trimmed and semi-thin (1um thick) sections cut using a glass knife and stained with 1% toluidine blue (Agar Scientific) in 1% sodium borate (Fischer Scientific) by heating over a paraffin flame for up to a minute before rinsing in distilled

water. The sections were then viewed under a light microscope to identify the area of interest (the TM).

With technical assistance from, ultra-thin sections, using a diamond knife, were cut by Theresa Morris (EM technician, Centre for EM, University of Birmingham). Once the resin block face was cut down to approx. 0.5-0.75mm$^2$ a diamond knife was used to cut gold (80-90nm) sections and placed on a Formvar-coated copper mesh grid (Agar Scientific). Grids were stained with uranyl acetate for 5 min, rinsed in deionised water x 3 and placed on filter paper to dry before staining with Lead citrate for 8 min and washing in deionized water x 3 and stored at RT in a grid box for later TEM.

### 2.11 Statistics

All statistical analyses were performed using SPSS 20 (IBM, USA) with assistance from Dr. Peter Nightingale, Statistician at University Hospital Birmingham. Normal distribution tests were carried out to determine the most appropriate statistical analysis to use to compare treatments. Statistical significance was determined as $p<0.05$. The NC3Rs resource equation was used to determine a suitable number of animals for experiments. The resource equation is used to determine sampling sizes in a hypothesis driven experiment and usually requires smaller sampling sizes to ascertain differences between treatments compared to power calculations, which are generally required to estimate parameters of treatments. IOP data were measured using the within-subjects repeated measured design or generalised estimated equations. TM fibrosis, RGC survival and ELISA data were tested for significance using Student t test or 1-way ANOVA for >2 group comparisons ±SEM. VEP data were analysed using the Generalised Estimated Equations (autoregressive correlation matrix).

# Chapter 3

# Modelling Trabecular Meshwork Fibrosis using Kaolin/LPS

### 3.1 Rationale

The aim of this pilot study was to assess the efficacy of two well-known pro-inflammatory and fibrogenic agents, lipopolysaccharide (LPS) and kaolin, to cause fibrosis in the trabecular meshwork (TM) and sustained IOP elevations after injections into the anterior chamber of the rat eye. If successful, these models could be used to investigate candidate anti-fibrotic agents to combat these pathological aspects of glaucoma. Intracameral injections of LPS, a potent bacterial wall endotoxin, has been used to model the ocular inflammatory disorder, uveitis in rats, by inducing macrophage infiltration into the anterior segment of the eye (Sakimoto et al., 2009). Macrophages release pro-inflammatory cytokines which transform local trabecular cells into fibroblasts causing fibrosis. Basal cistern injections of kaolin, an aluminium silicate, increases endogenous levels of TGF-β from meningeal fibroblasts and macrophages leading to tissue fibrosis in the sub-arachnoid space blocking CSF drainage portals and inducing ventriculomegaly (Botfield et al., 2013). Fibrosis of the TM seen in POAG probably arises, in part, from abnormally high levels of TGF-β in the aqueous humour (AqH) acting on cells within the TM (Tamm et al., 2007).

Based on the observation that LPS induces macrophage infiltration and pro-inflammatory cytokine release together with the fibrogenic properties of kaolin, it was hypothesised that intracameral injections both of LPS and kaolin would lead to a sustained elevation in IOP through restriction of AqH outflow from TM fibrosis.

To test this hypothesis, a pilot study was designed to; (1) determine optimal concentration of kaolin to inject into anterior chamber to achieve maximal TM fibrosis; (2) intracamerally injected kaolin, with and without LPS, to cause fibrosis of the TM; (3) quantify ED1+ macrophages, laminin and fibronectin deposition in the TM in LPS and LPS+kaolin treated eyes; and (4) determined changes in IOP.

**3.2 Experimental design**

3.2.1 Pilot study to determine if intracameral kaolin increases levels of laminin and fibronectin in the TM and elevates IOP

To assess the optimal TM fibrosis inducing kaolin concentration, a single eye from male Sprague Dawley rats (175-200g) was intracamerally injected with 5µl of 1.25%, 3.5%, 5%, 10% or 20% w/v kaolin diluted in 10mM PBS on 0d and 5d. A vehicle of PBS alone (0% kaolin) was used as a sham injection for one eye. IOP measurements and TM tissue architecture were also analysed in two intact eyes (which received no injections) as negative controls. The concentrations of kaolin tested in this study were estimated from those used by Botfield et al. (2013) who demonstrated that a 20% w/v of kaolin was sufficient to induce inflammation and fibrosis within the brain. Single session IOP measurements were taken throughout the 21d experiment. At 21d anterior segment OCT imaging visualised the angle to detect residual kaolin. Following OCT imaging, all rats were killed using increasing concentrations of $C0_2$, perfused with 4%PFA and the eyes removed and parasagittal sections of the eye immunohistochemically qualitatively analysed for TM fibrosis.

### 3.2.2 Pilot study to determine if LPS with and without kaolin elevates IOP and increases levels of laminin and fibronectin in the TM

On 0d, 8 male Sprague Dawley rats (n=4 eye/group) received a single unilateral 6µl intracameral injection composed of 3µl of 0.1g/L LPS and a 3µl 30% w/v kaolin in PBS (LPS+kaolin), or, a single unilateral 6µl intracameral injection of 3µl 0.1g/L LPS and 3µl intracameral injection of PBS (LPS+PBS). The LPS+PBS group served as a control to assess the effects of LPS alone. The concentration of LPS was extrapolated from methods previously described (Tsuji et al., 1997; Rosenbaum et al., 2011). Single session IOP measurements were taken at regular intervals throughout the 28d experiment. At 28d all rats were killed using increasing concentrations of $C0_2$, perfused with 4%PFA and eyes removed for immunohistochemical analysis of TM fibrosis determined from parasagittal sections of the eye. Anterior segment OCT imaging was conducted on at 0d and 28d to observe any residual presence of kaolin. IOP data were analysed for significance using a repeated measures ANOVA. ED1 counts were analysed for significance using Student's *t* test ($p<0.05$).

## 3.3 Results

### 3.3.1 Pilot study to determine if kaolin can cause IOP elevation and increase levels of laminin and fibronectin in the TM

#### *3.3.1.1 Kaolin (1.25-20% w/v) did not cause a sustained elevation of IOP*

Intracameral injection of kaolin at a concentration (w/v) of 1.25% (Figure 3.1a), 2.5% (Figure 3.1b), 5% (Figure 3.1c), 10% (Figure 3.1c) or 20% (Figure 3.1d) did not achieve sustained increases in IOP from the baseline measures (8-12mmHg) recorded from 0% (PBS) and intact control eyes. After Intracameral injection of 1.25% kaolin the IOP peaked at 21d at 13.7mmHg. The average IOP peaked at 13mmHg at 1d for the concentration of 2.5%. Eyes injected with 5% w/v kaolin, spiked at 2d reaching 28mmHg and similar single spikes were observed with 10% and 20% w/v kaolin, reaching 19mmHg by 6d and 17.3mmHg at 1d, respectively. This pilot data suggests that the kaolin concentrations ranging from 1.25%-20% were able to induce transient increases in IOP but were not suitable for causing sustained elevations in IOP.

A

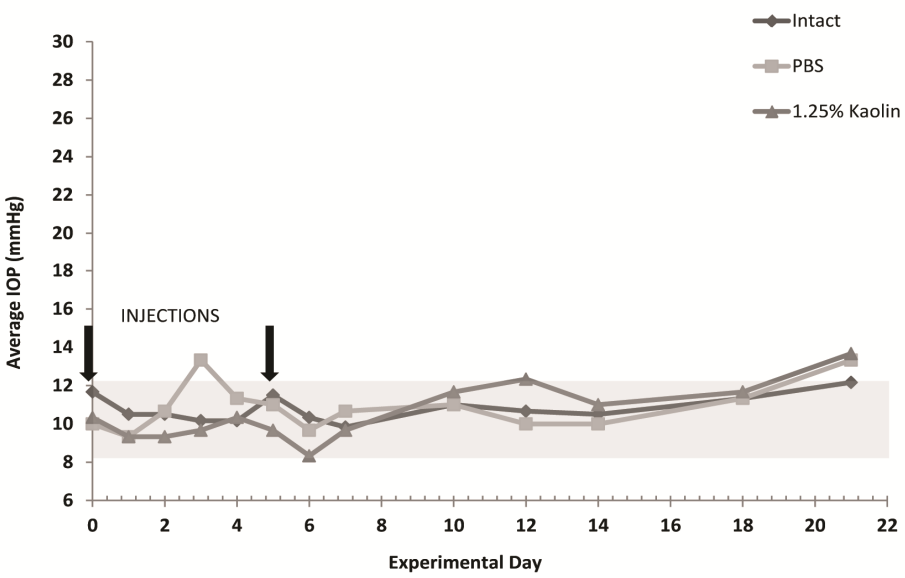
Intact
PBS
1.25% Kaolin
Average IOP (mmHg)
INJECTIONS
Experimental Day

B

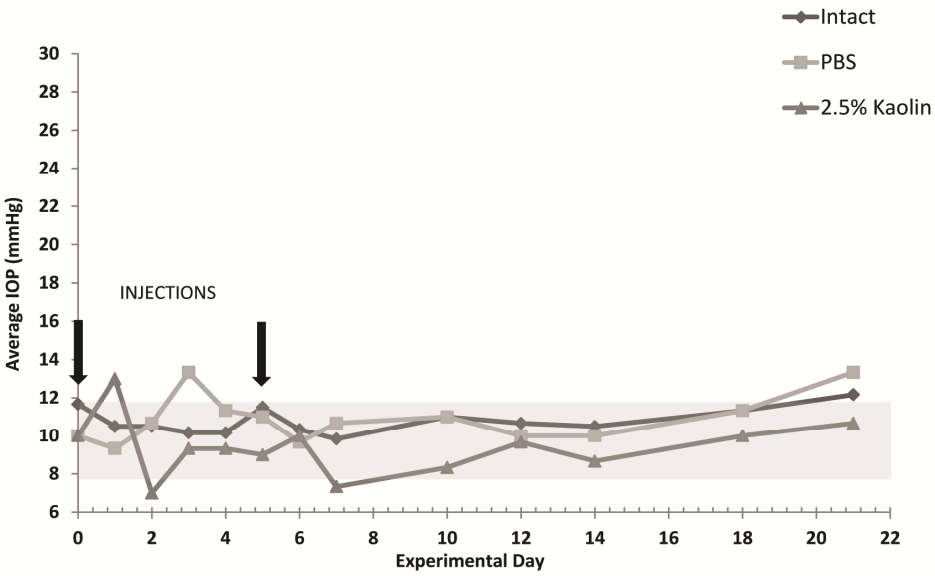
Intact
PBS
2.5% Kaolin
Average IOP (mmHg)
INJECTIONS
Experimental Day

C

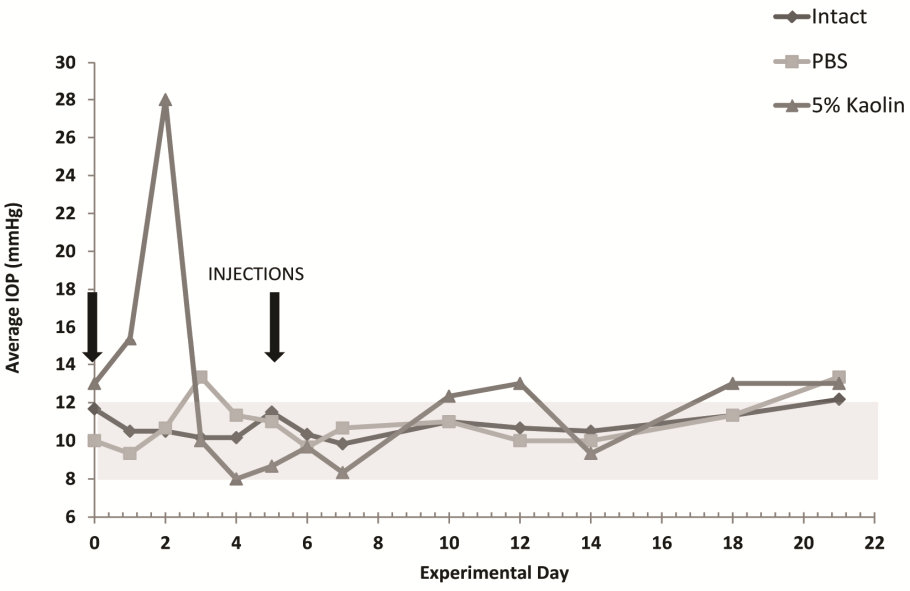
Intact
PBS
5% Kaolin
Average IOP (mmHg)
INJECTIONS
Experimental Day

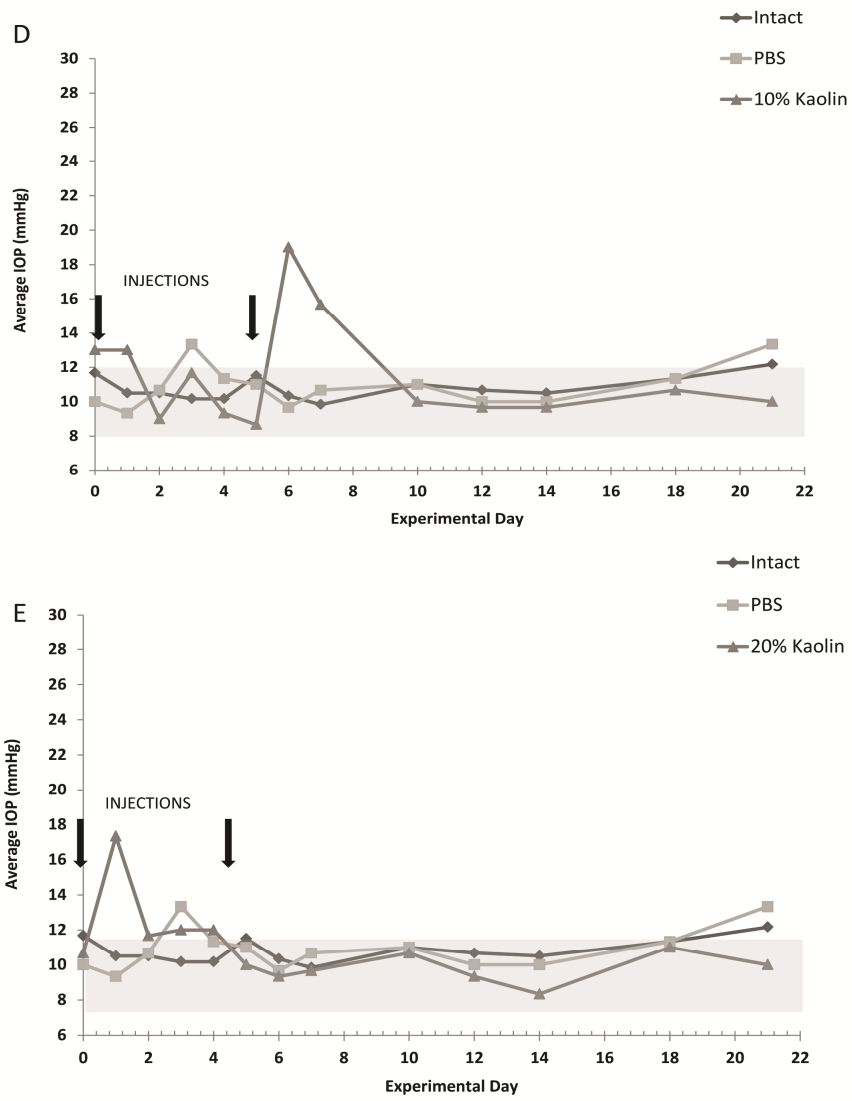


**Figure 3.1 IOP after intracameral injections of kaolin.** The average IOP is displayed as a single point on the graph. The shaded area depicts the normal IOP range. The arrows represent the time point of injection at 0d and 5d. IOP for injections of (A) 1.25%, (B)2.5%, (C) 5%, (D) 10% and (E) 20% kaolin were measured. No sustained elevations in IOP were observed at any concentration of kaolin over the 21d (A-E). Instead there were transient increases in IOP observed in the (C) 5%, (D) 10% and (E) 20% but all IOP measurements were at similar levels to the intact and PBS control eyes by 21d.

*3.3.1.2 Kaolin (20%) accumulation in the iridiocorneal angle*

The presence of kaolin in the anterior chamber was observed macroscopically and on anterior segment OCT imaging (Figure 3.2). Twenty one days after the 20% kaolin injection at 0d and 5d, kaolin accumulated in the anterior segment and appeared as opacities in the TM in the OCT image. From one eye it was observed that kaolin accumulated towards the inferior aspect of the anterior chamber suggesting a gravitational effect had occurred (Figure 3.2 B Inset). Kaolin accumulation in the angle suggests that the transient kaolin-induced IOP spikes observed in the 5%, 10% and 20% eyes may have resulted from temporary obstruction of AqH outflow. This contention is supported by the observation that all other kaolin concentrations that had no spikes showed no kaolin accumulation upon macroscopic evaluation with demonstrably clear angles within the anterior chamber on OCT by 21d (data not shown).

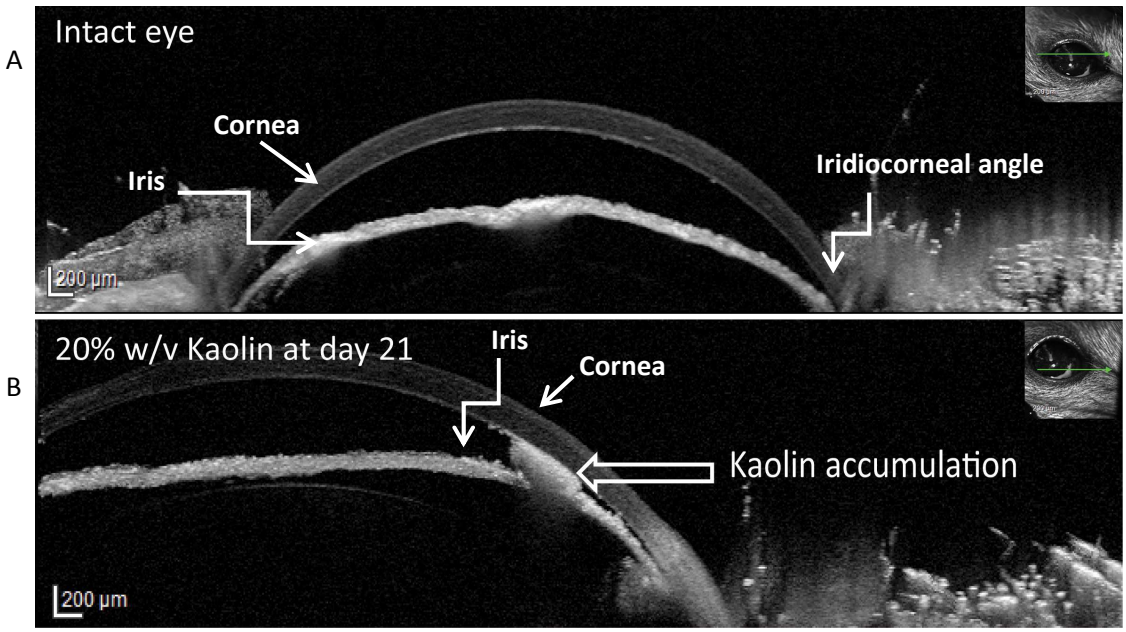


**(***Figure 3.2 legend on next page)*

**Figure 3.2 Anterior segment OCT imaging of 20% kaolin at 21d**

OCT imaging at 21d of (A) intact eye and (B) eye injected with 20% kaolin at 0d and 5d. The intact eye (A) shows normal anterior chamber with a clear angle. The eye injected with 20% kaolin (B) shows the white opacities characteristic of an accumulation of kaolin in the angle. Inset shows meridian of OCT section.

#### *3.3.1.3 Kaolin did not alter TGF-β, laminin or fibronectin levels in the TM compared to intact or PBS controls*

Qualitative analysis (performed by two independent observers) of total TGF-β immunoperoxidase staining of 8-12 sections from the vertical meridian of each eye detected no changes in staining between the intact eye and eyes injected with 0% (PBS only), 5% or 20% kaolin concentrations (Figure 3.3). Cytoplasmic TGF-β staining was localised within the ciliary body, iris , TM and sclera. These data show that increasing concentrations of kaolin did not alter the endogenous levels of total TGF-β within the angle. Laminin staining was also present at similar levels across all groups (Figure 3.4). Laminin was observable as long thin strands within the TM and at varying thickness in a discontinuous fashion around Schlemm's canal. Fibronectin levels were very low in all eyes and no observable differences were apparent between groups (data not shown).

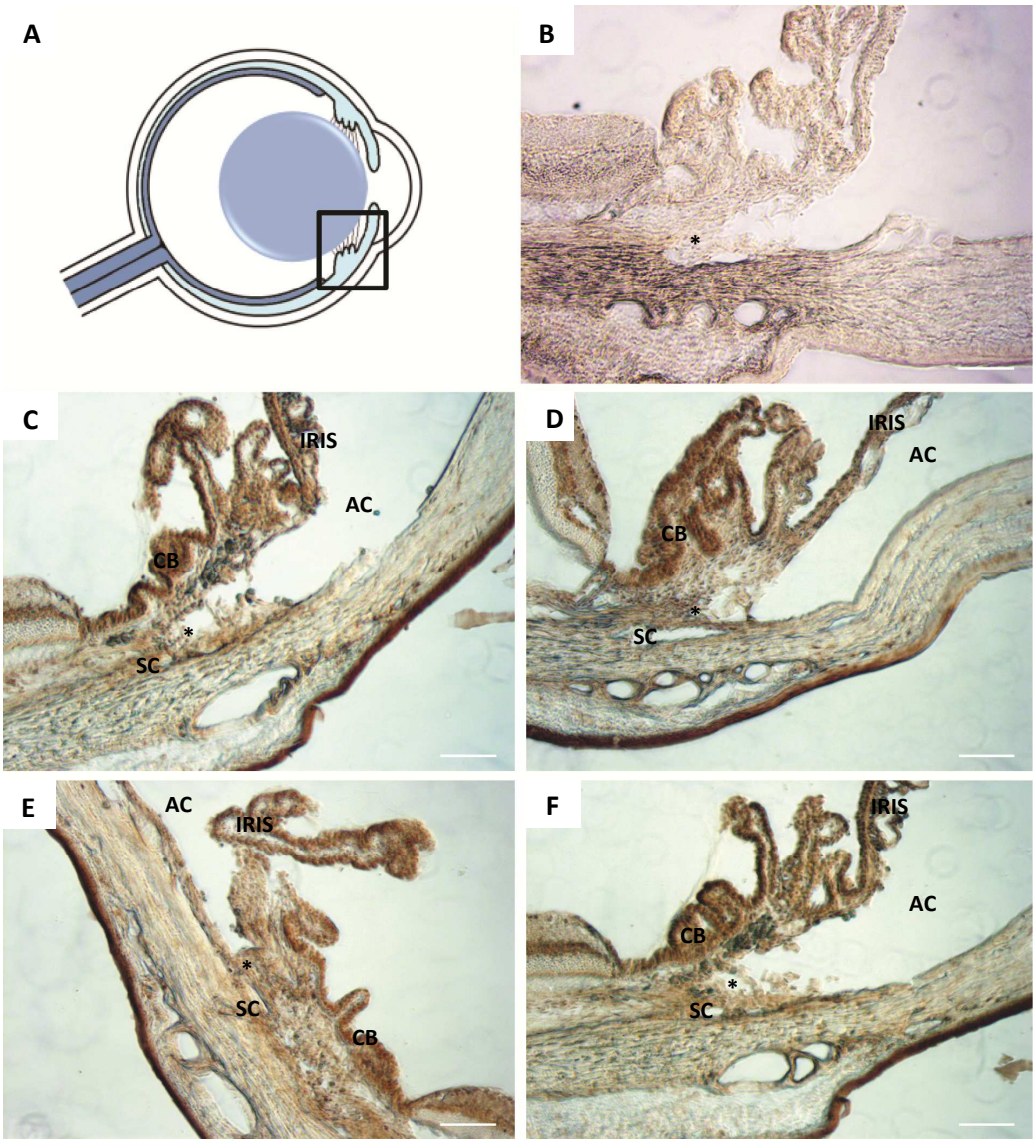


**Figure 3.3 TGF-β staining at experimental 21d.**

Parasagittal eye sections illustrating total TGF-β staining in the iridiocorneal angle of the anterior chamber (AC). (**A**) Diagram to show region of interest. (**B**) Negative reagent control (no primary antibody). (**C-F**) Representative images of TGF-β staining in the kaolin injected eyes. There was intense cytoplasmic staining in the ciliary body (CB) and iris in the intact (**C**) 0% (**D**) 5% (**E**) and (**F**) 20%. Lower levels of staining were observable in all groups in the TM. There were no differences in total TGF-β levels between the groups (**C-F**). Scale bar – 100µm; CB – Ciliary body; SC – Schlemm's Canal; AC – anterior chamber; * trabecular meshwork.

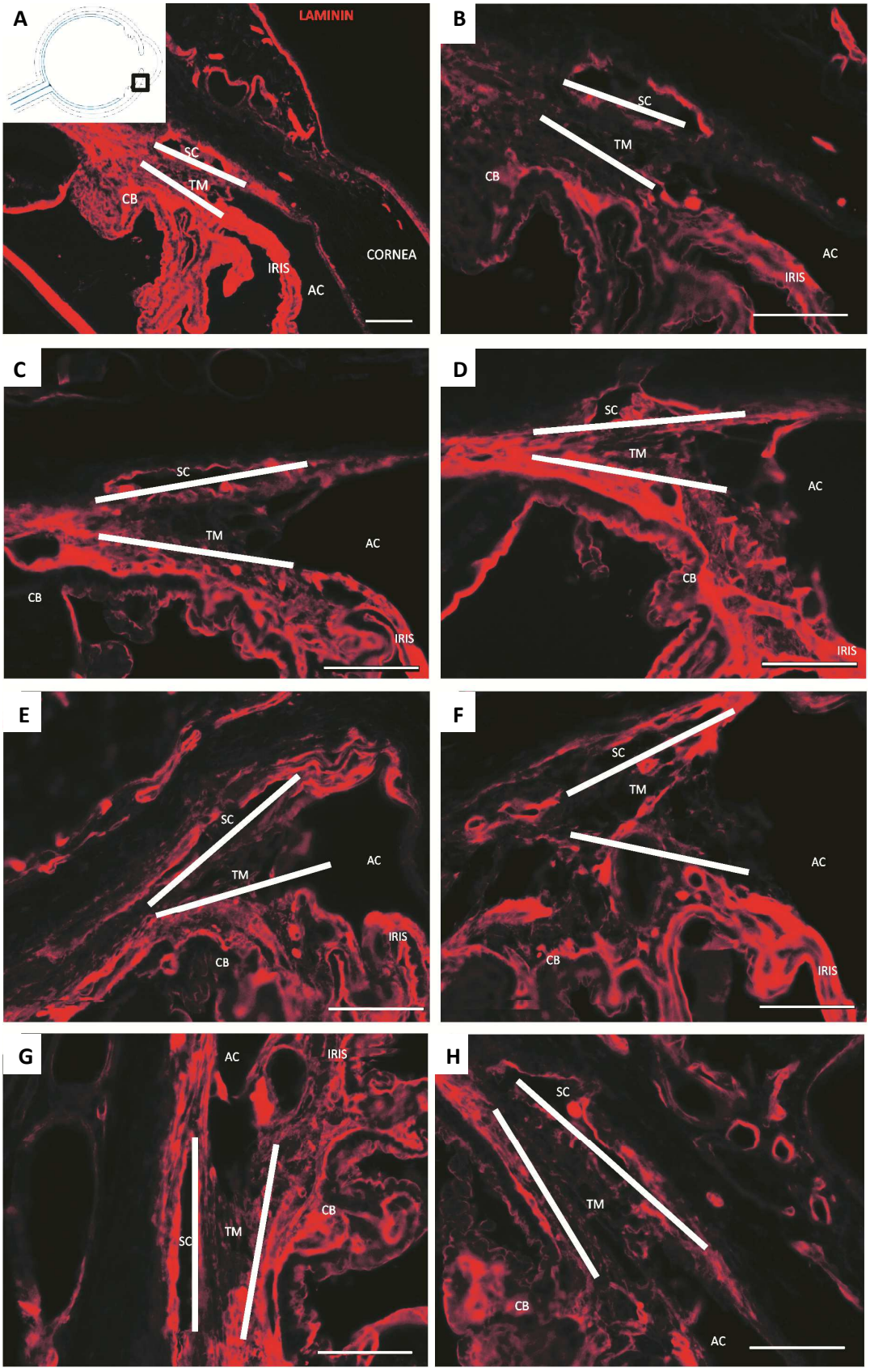


***(Figure 3.4 legend on next page)***

**Figure 3.4 Laminin deposition in the TM.** Parasagittal eye sections illustrating laminin staining (red) in the iridiocorneal angle of the anterior chamber (AC). (**A**) over exposed image to show the angle containing the TM and Schlemm's canal (located between white lines). (**B-H**) Representative images of laminin staining in the kaolin injected eyes. Similar levels of laminin staining (red) were observed within the ciliary body (CB), TM, cornea and iris in the **(B)** intact and (**C**) 0%, (**D**) 1.25%, (**E**) 2.5%, **(F)** 5%, **(G)** 10% and **(H)** 20% kaolin injected eyes. In all groups (**B-H**), laminin deposition around Schlemm's canal was discontinuous and was less visible on the inner wall (towards the TM) compared to the outer wall. Scale bar – 100µm; CB – Ciliary body; SC – Schlemm's canal; TM – trabecular meshwork; AC – anterior chamber.

### 3.3.2 Pilot study to determine if LPS±kaolin(30%) can cause IOP elevation and increase levels of laminin and fibronectin

#### *3.3.2.1 Intracameral injection of LPS+kaolin(30%) induced transient increases in IOP compared to LPS+PBS but not a sustained an elevation in IOP*

Intracameral injection of LPS+30%kaolin transiently increased IOP between 1d and 7d (Figure 3.5). A single intracameral injection of LPS+30%kaolin significantly elevated IOP ($p<0.05$) compared to the LPS+PBS group reaching an average of 20±0.9mmHg at 1d and 2d. By 3d the average IOP was lower at 11.3±1mmHg, similar to the IOP in the LPS+PBS group. By 4d IOP significantly increased again to 21.8±1.7mmHg ($p<0.05$) and remained elevated until 7d at a mean IOP of 21.2±mmHg. After 7d the IOP returned to baseline levels of 10.1±0.5mmHg and stayed there until 28d. The LPS+PBS group remained within normal levels throughout the 28d period, varying between 8.25±0.2mmHg and 11.42±0.4mmHg. Interestingly, the IOP data were significantly higher ($p<0.05$) in the LPS+kaolin group compared to LPS+PBS from transient peaks but both values were within the normal range at the end of the experiment.

These data suggest that LPS+30%kaolin induced acute spikes in IOP, which was compared to the lower concentrations of kaolin used in the pilot study, in which a sustained increase in IOP was not achieved.

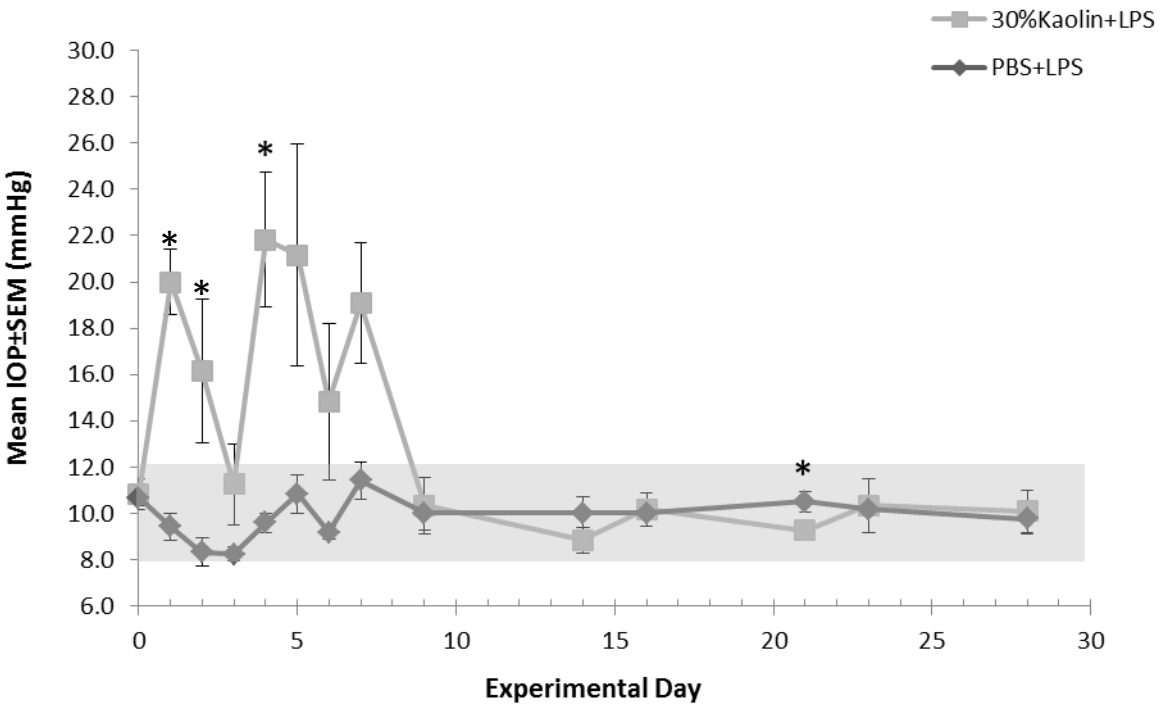


**Figure 3.5 IOP measurements after LPS+30%kaolin and LPS+PBS.** The average IOP±SEM is displayed here as a single point on the graph. The shaded area represents normal IOP range. Intracameral injections were given on 0d. Compared to PBS+LPS, transient elevations in IOP were observed between 1d and 7d in the LPS+30%kaolin group with a return to normal IOP measurements between 7d and 28d. IOP were significantly higher ($p<0.05$) in the LPS+kaolin(30%) compared to the LPS+PBS group on 1d, 2d, 4d and 21d. Mean IOP values remained within the normal range for the eyes injected with PBS+LPS.

### *3.3.2.2 Anterior segment OCT imaging detected 30%kaolin in the angle*

Before injections the anterior chamber angles were clear on OCT images (Figure 3.6A). At 28d after LPS+30%kaolin injections, the presence of kaolin in the anterior chamber was observed macroscopically (not shown) and on anterior segment OCT imaging in 2 out of 4 eyes (Figure 3.6B). All eyes injected with LPS+PBS were devoid of opacities in the angle on OCT (data not shown). The presence of kaolin in the angle 28ds after injection shows that it is not completely cleared from the eye and thus could have attributed to the acute IOP spikes observed between 1d and 7d (Figure 3.5). However, as the IOP levels returned to baseline, any resistance to outflow was most likely restored through the movement of kaolin from the drainage site so that AqH outflow was normalised.

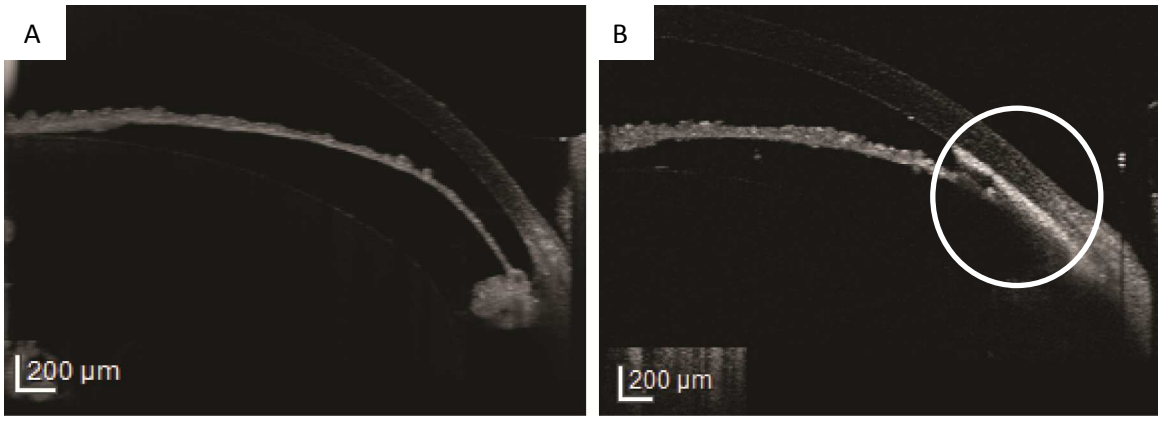


**Figure 3.6 Anterior segment OCT imaging of LPS+30%kaolin at 28d**

Anterior segment OCT imaging (A) before intracameral injection showing the normal anterior chamber with a clear angle and (B) 28d after intracameral injection of 30%kaolin+LPS showing an accumulation of white opacities of kaolin (circled on image) in the angle.

#### *3.3.2.3 LPS+30%kaolin did not alter TGF-β, laminin or fibronectin levels in the TM but did increase the number of ED1+ cells compared to LPS+PBS*

Qualitative analysis of total TGF-β immunoperoxidase staining detected no apparent change in levels of staining between LPS+30%kaolin and LPS+PBS groups (Figure 3.7). As with the kaolin pilot data (Figure 3.3), intense cytoplasmic TGF-β staining was localised within the ciliary body and iris and less intensive staining was observed in the TM and sclera. Non-specific staining was found in both groups in the form of dark brown spherical cellular deposits localised to inflammatory cells. These data suggest that the addition of kaolin to LPS injections did not alter the endogenous levels of total TGF-β within the angle. Laminin was present within the ECM at similar levels in both LPS+PBS and LPS+30%kaolin groups (Figure 3.8), observable as long thin strands within the TM and at varying thickness in a discontinuous fashion around Schlemm's canal. Similar low extracellular fibronectin levels were seen in LPS+30%kaolin and LPS+PBS groups (data not shown).

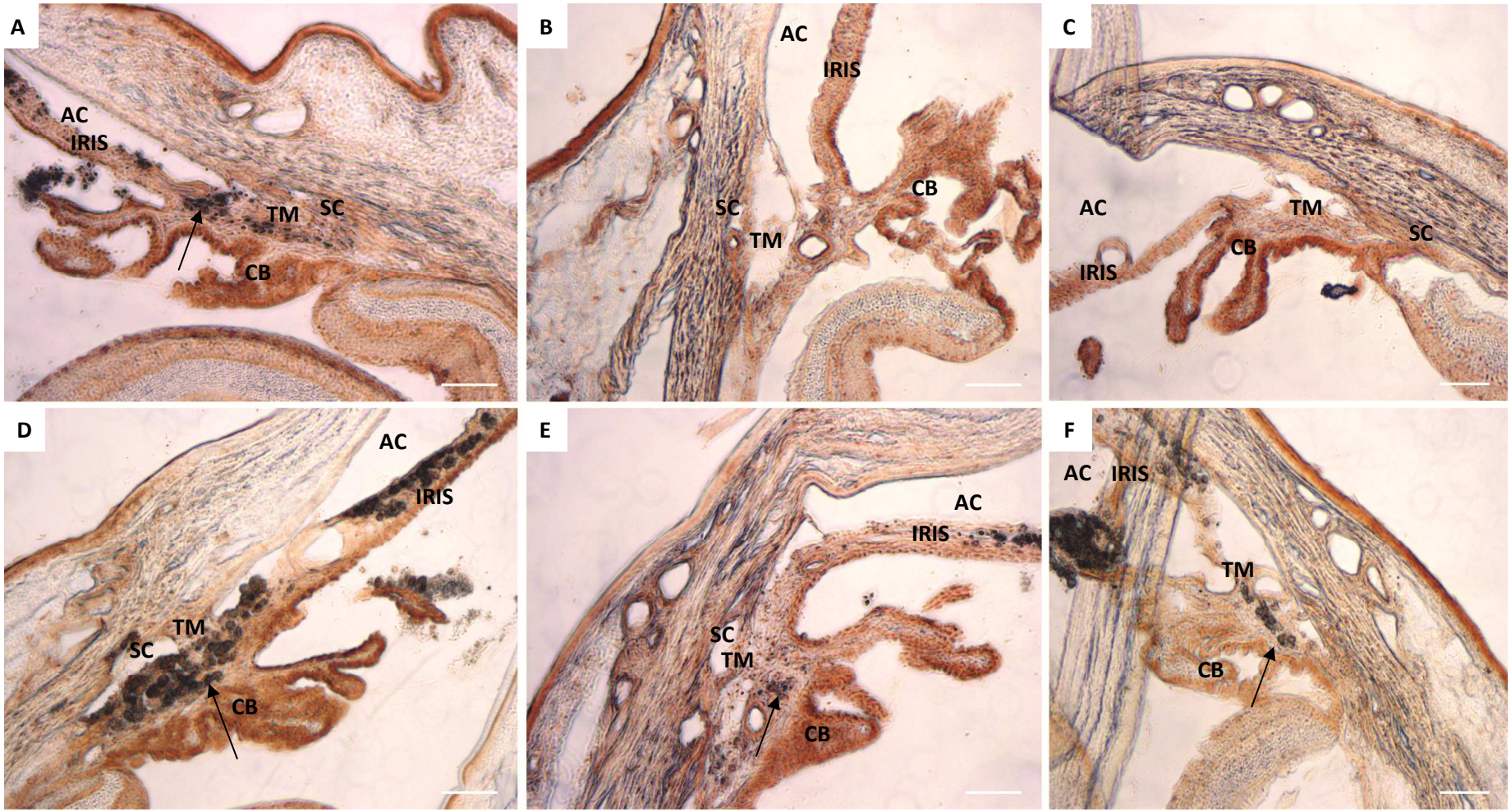


**(Figure 3.7 legend on next page)**

**Figure 3.7 TGF-β staining at experimental 28d.** Parasagittal eye sections illustrating TGF-β staining of the anterior chamber (AC) iridiocorneal angle. **(A-C)** Representative images of TGF-β staining in the LPS+PBS injected eyes, and **(D-F)** in the LPS+kaolin(30%) injected eyes. There was intense cytoplasmic staining in the ciliary body (CB) and iris in the intact and lower levels of staining was observed in all groups in the TM but no differences between the groups were identified. Dark brown spherical staining was also observed in both groups (illustrated by the arrow in panels A, D, E and F) possibly associated with the presence of macrophages. Scale bar – 100µm; CB – Ciliary body; SC – Schlemm's canal; TM – trabecular meshwork; AC – anterior chamber.

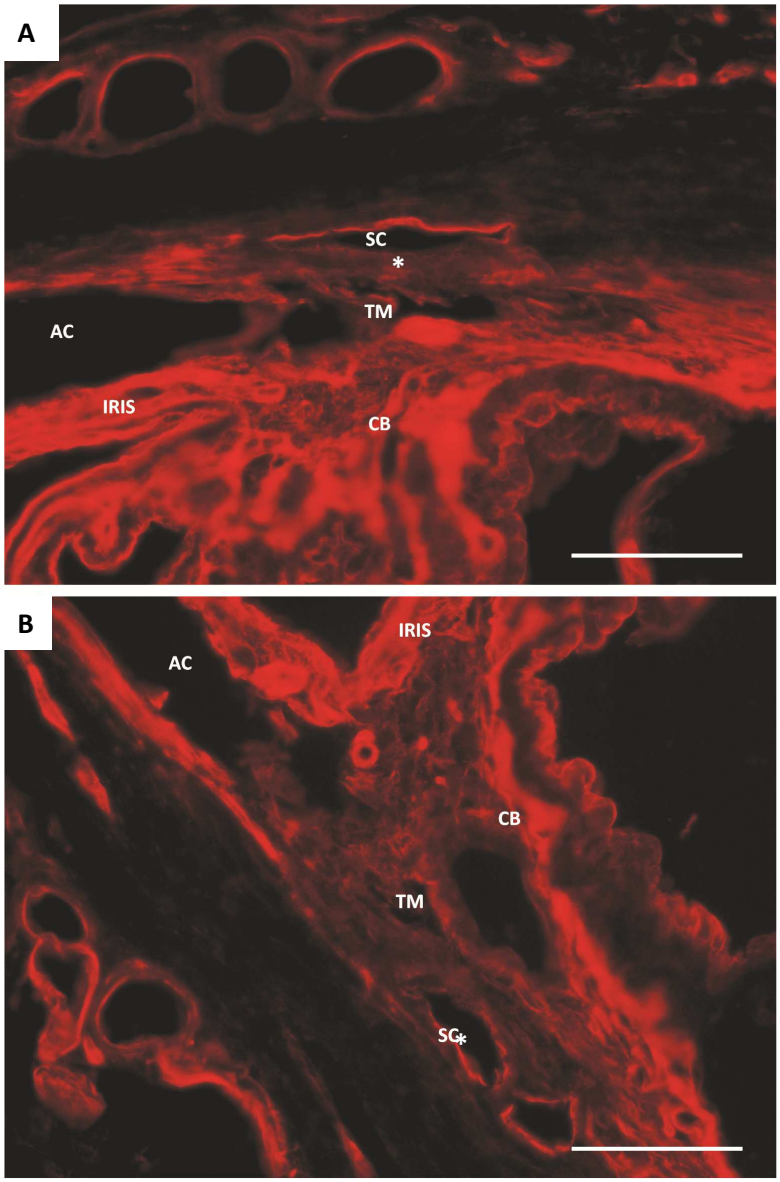


**Figure 3.8 Laminin deposition in the TM at 28d.** Parasagittal eye sections illustrating laminin staining of the anterior chamber (AC) in the iridiocorneal angle. Representative images of laminin (red) staining in the **(A)** LPS+PBS and **(B)** LPS+30%kaolin injected eyes. Similar levels of laminin staining were observed within the ciliary body (CB), TM and iris in both groups. In addition, both groups showed discontinuous laminin deposition around Schlemm's canal (SC) with less intense laminin in the wall juxtaposed to the TM compared to that opposed to it (*). Scale bar – 100µm; CB – Ciliary body; SC – Schlemm's canal; TM – trabecular meshwork; AC – anterior chamber.

Interestingly, in one LPS+30%kaolin eye there was a mass accumulation of particles and cells that were positive for fibronectin in their cytoplasm, shown by a circular staining pattern around the nucleus (Figure 3.9A). Extracellular laminin staining was also shown with in the particulate mass (Figure 3.9A). The IOP for this eye were particularly high (>25mmHg) within the first 7d after injection. TGF-β staining was also observed within this accumulation of cells/particles as dark brown/grey mass with a circular cell shape (Figure 3.9 B). This suggests that in this animal a large residual kaolin deposition was present in the anterior chamber in at 28d. It is important to note that the mass accumulation seen here was an isolated incidence and was not seen in the other eyes on OCT.

There was an significant ($p<0.05$) increase in the number of ED1 cells in the TM seen in all eyes in the LPS+30%kaolin group compared to LPS+PBS group (Figure 3.9C-E) suggesting that the combination of LPS and 30%kaolin caused more inflammation than LPS alone.

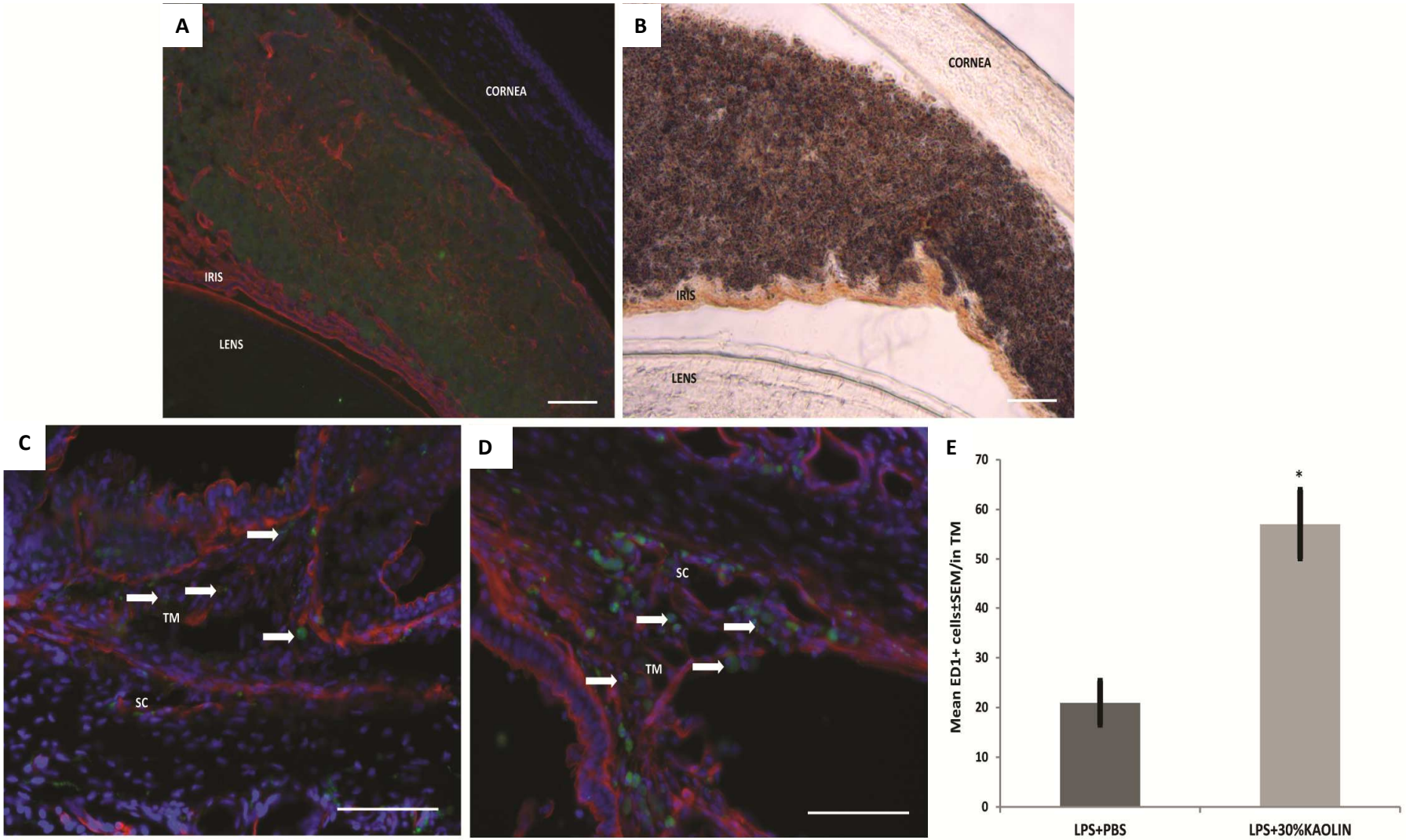


***Figure 3.9 legend on next page***

**Figure 3.9 Effects of LPS+30%kaolin on ED1 macrophage infiltration.** Parasagittal eye sections of the angle showing mass infiltration of cells in the LPS+30%kaolin identified by: **(A)** cellular fibronectin (green), extracellular laminin staining (red) and DAPI staining was used to identify cell nuclei (blue); and **(B)** Total TGF-β staining is seen as brown/grey particulate in the same region. **(C)** Representative image showing $ED1^+$ cells (green) in the angle of the LPS+PBS group and **(D)** LPS+30%kaolin group. White arrows show example of positive cells. **(E)** Graphical representation showing there were significantly more $ED1^+$ cells in the TM after LPS+30%kaolin injections compared to LPS+PBS injection groups ($p<0.05$, $n=4$). Scale bar – 100µm; SC – Schlemm's canal; TM – trabecular meshwork.

In summary, these data suggest that the injection of LPS to 30%kaolin led to early peaks in IOP that returned to normal levels after the first week. The addition of LPS caused an infiltration of $ED1^+$ exacerbated specifically by 30% kaolin compared to LPS alone. However, despite inducing an inflammatory microenvironment, fibrosis within the TM was not established and there were no sustained increases in IOP.

## 3.4 Discussion

### 3.4.1 Kaolin pilot study

The aim of this study was to develop a sustained increase in IOP after inducing TM fibrosis using intracameral injections of kaolin. Kaolin injections into the basal cisterns induces endogenous raised levels of TGF-β causes fibrosis in the sub-arachnoid space in the rat brain (Botfield et al., 2013) and therefore this suggested that it would be a suitable candidate fibrogenic agent in the eye. To find the concentrations favourable to induce TM fibrosis, a number of concentrations up to the 20% used by Botfield et al. (2013) were intracamerally injected and IOP was monitored. In addition to its fibrogenic properties, kaolin may also act as a plug and obstruct AqH from draining through the TM. The aim of the study was to induce fibrosis of the TM using kaolin at a concentration which avoids obstructions of TM drainage and increases in IOP, so lower concentrations were tested than those by Botfield et al. (2013). A sustained increase in IOP was not induced at any of the kaolin concentrations up to 20%, although there were random peaks in IOP within the 2-3d after injections in the eyes injected with 5%, 10% and 20% kaolin probably caused by kaolin temporarily blocking outflow, an assertion supported by macroscopic and OCT imaging of kaolin opacity in the anterior chamber. In addition, the rapid return of IOP to normal range suggested there were no permanent changes to AqH outflow, indicative of TM fibrosis. The nature of AqH dynamics results in its very high turnover rate, therefore it is possible that kaolin was completely cleared from the anterior chamber before it caused any noticeable inflammation or fibrosis within the angle. However, there was slight an accumulation of residual kaolin within the angle at 21d in the 20% kaolin eye despite the IOP being within normal range. This

suggests that the kaolin concentrations used in this study were not enough to cause inflammation. This failure of kaolin >20% at these concentrations to cause sustained elevations in IOP correlated with an absence of fibrosis of the TM. It was expected that endogenous levels of TGF-β would increase following administration of kaolin (as shown with Botfield et al., 2013) and this increase in TGF-β would, in part, lead to fibrogenesis in the TM through increasing deposition of ECM proteins including laminin and fibronectin. Only total TGF-β levels were measured in this study, therefore, levels of active TGF-β may have altered with injections of kaolin and/or LPS. Measuring active TGF-β levels would be required in future studies to demonstrate any changes. However, the failure of TGF-β, laminin or fibronectin levels to change between the intact eyes and the eyes injected with kaolin demonstrated that fibrosis within the TM had not occurred. Thus kaolin was not a suitable TM fibrogenic agent because in an immune privileged area such as the eye, it may be that kaolin is inert. Therefore it was hypothesised that administration of LPS (a potent immune cell activator) combined with an increased concentration (30%) of kaolin would induce a more robust inflammatory response, evidenced by increases in total TGF-β and other pro-inflammatory cytokines and TM fibrosis. TM fibrosis would also be reflected by a sustained elevation in IOP.

### 3.4.2 LPS±30%Kaolin pilot study

LPS alone or combined with 30%kaolin did not induce a sustained increase in IOP and did not result in fibrosis of the TM. The combination of LPS and 30%kaolin did show an increased number of $ED1^+$ macrophages, compared to LPS alone, suggesting that kaolin did exacerbate the inflammatory response in this model. However, the increase in $ED1^+$ macrophages in

this group was not enough to cause a sustained rise in IOP. This suggests that the increase in macrophage numbers was not sufficient to alter the resistance of the TM enough to reduce AqH outflow.

As with the kaolin pilot studies, transient increases in IOP occurred within the first week after the single intracameral injections at 0d. OCT imaging detected the presence of residual kaolin within the anterior chamber of some eyes, despite IOP returning within the normal range by the end of the experiment at 28d. The reason for the transient increases in IOP was unclear but could be attributed to the clearance of kaolin.

Another consideration is the vascular permeability alterations induced by LPS. LPS causes vessels to become leaky, permitting the entry of immune cells and causing alterations in fluid levels within the anterior chamber. It is possible that the IOP peaks occurring after the increased levels of kaolin were negated by the altering permeability of vessels caused by LPS. In support of this proposition, the IOP did drop towards the lower end of normal in the LPS only group. The transient IOP peaks were only observed in the LPS+30%kaolin injected eyes, suggesting an acute phase IOP altering effect of kaolin.

The inherent variability of IOP, together with the measurements returning to normal levels, suggested that AqH outflow was not significantly restricted and therefore, fibrosis of the TM had not been established. Indeed, this was supported with qualitative immunohistochemical analysis of the angle. Endogenous total TGF-β, laminin and fibronectin levels showed no differences between eyes injected with LPS and those injected with LPS+30%kaolin. These

two groups also demonstrated similar levels of TGF-β, laminin and fibronectin levels to that seen in the intact eye from the qualitative analysis in the kaolin pilot studies.

The ability of LPS to cause cellular infiltration into the anterior chamber was successfully modelled in this study. The immunoperoxidase staining for total TGF-β showed a uniform cellular/particulate mass embedded within the angle. The staining of this mass yielded a very dense brown/grey stained area that was thought to be an accumulation of mostly kaolin. Further analysis showed densely stained fibronectin uniformly distributed in a circular manner within this accumulation of cells/kaolin particles. Laminin deposition was also observed in a peri-cellular arrangement throughout the mass.

### 3.4.3 Conclusion

In summary, the data from these pilot studies evaluating the use of kaolin alone or in conjunction with LPS to induce TM fibrosis led to the conclusion that kaolin was not suitable as a fibrogenic agent in the anterior chamber. However, there are important considerations to note with regards to the experimental design used in this study. Perhaps longer time course experiments and more frequent intracameral injections would have shown more favourable results. In addition, the IOP monitoring was not continuous and therefore data with regards to IOP levels may have been missed. Continuous pressure monitoring would have overcome this limitation but would have been a more invasive procedure. This model was useful to show the inflammatory effects of LPS and to induce transient increases in IOP when LPS is combined with kaolin, but due to the lack on ECM deposition in both groups, this model was deemed unsuitable to induce TM fibrosis and sustained IOP elevations.

# Chapter 4

# TGF-β induced Trabecular Meshwork Fibrosis, IOP elevations and RGC death

## 4.1 Rationale

POAG is a multifactorial disease featuring fibrosis within the anterior chamber of the eye (Tripathi et al., 1994). The main and only modifiable risk factor is increasing levels of IOP (Quigley et al., 1980; Sommer et al., 1991). Elevations in IOP are thought to occur from fibrosis of the TM preventing drainage of AqH (Junglas et al., 2012). Elevated increases in IOP are correlated with RGC death (Morrison et al., 1998). Although no single experimental paradigm mimics all of the known pathobiology in POAG, *in vivo* rodent models are useful to investigate biological aspects of the disease in isolation. The pathobiology of glaucoma is routinely investigated using rodent models of IOP elevation (reviewed by Johnson & Tomarev, 2010). However, until recently there were few rodent models available to investigate TM fibrosis specifically. The most notable study of TM fibrosis was by Junglas et al., (2012) who successfully demonstrated TM fibrosis in mice through gene mediated up-regulation of TGF-β signalling. New more disease-related means of generating TM fibrosis are needed that create a sustained elevation in IOP and consequent RGC death. Such experimental tools would then enable investigations into the efficacy of potentially therapeutic anti-fibrotic agents.

TGF-β is a potent fibrogenic agent implicated in TM fibrotic diseases (Junglas et al., 2012; Fuchshofer et al., 2014). Over-expression of TGF-β1 increases TM fibrosis and elevates IOP (Junglas et al., 2012). Patients with open angle glaucoma have high levels of TGF-β1 in the AqH, associated with pseudoexfoliation glaucoma (Schlötzer-Schrehardtl et al., 2001), and

TGF-β-2, associated with primary open angle glaucoma (Tripathi et al., 1994) compared to age-matched controls.

The ability of exogenous TGF-β1 and 2 to mimic the disease-related pathology to increase fibrosis of the TM were studied in this thesis to test the hypothesis that increasing levels of TGF-β1/2 in the AqH leads to TM fibrosis, sustained IOP elevations and RGC death.

## 4.2 Experimental design

### 4.2.1 Study 1 - Effects of general *vs* local anaesthetic on IOP

To investigate the effects of general anaesthesia on IOP, IOP recordings studies under both local and general anaesthesia were conducted. On 3 successive days rats were given either 5% Isoflurane by inhalation (n=3) or topical eye drops of Minims Oxybuprocaine Hydrochloride 0.4% w/v (n=3) and IOP measured by tonometry. Rats receiving local anaesthetic were habituated to handling one week before and manually restrained during IOP recordings. IOP data were analysed for normality, followed by testing for significance ($p<0.05$) using the within-subjects repeated measures design.

### 4.2.2 Study 2 - Optimising the TGF-β dosing regimen to sustain elevated IOP

A pilot study comprised control rats (n=3) intracamerally injected with PBS and rats treated with active TGF-β1 (n=3) at 0.5ng/ml on 4d and 11d then 5ng/ml on 18d and 49d and IOP monitored over a 55 day period (Figure 4.1). Baseline IOP readings were taken on 0d. IOP measurements were taken between 9-11am on days 0, 4, 6, 11, 13, 18, 25, 27, 31, 35, 42, 49 and 55. IOP measurements were taken before intracameral injections to avoid immediate post-operative spikes in IOP. IOP data were analysed for normality, followed by testing for significance ($p<0.05$) using the within-subjects repeated measures design.

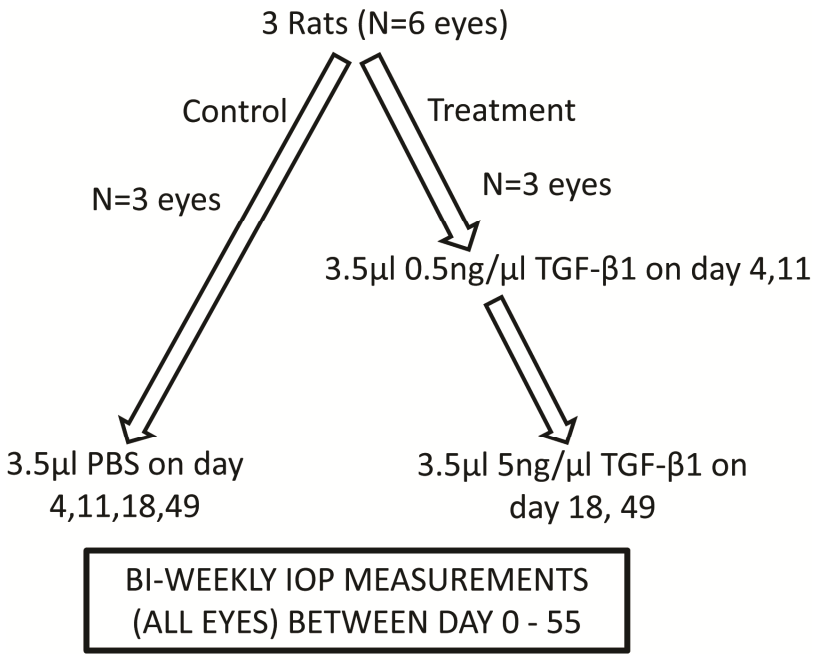


**Figure 4.1 Experimental design for testing TGF-β1 dosing regimen.**

### 4.2.3 Study 3 - Testing the effects of Latanoprost on the TGF-β induced increase in IOP

IOP in rats over a period of 0-45d was elevated by intracameral injections of 5ng/µl of TGF-β1 at 10d, 33d and 35d to investigate if topical administration of latanoprost (Xalatan™), a well-known IOP lowering agent, attenuated the TGF-β induced elevations in IOP (Figure 4.2). The IOP was monitored at 0d, 6d, 10d, 14d, 21d, 30d, 35d, 40d, 42d and 45d. Rats (n=8) received unilateral intracameral injections of PBS (n=8 eyes) or 5ng/µl TGF-β1 (n=8 eyes). Each of the PBS and TGF-β groups were subsequently administered one drop of 0.005% latanoprost (n=4) or PBS eye drops (n=4) once a day from experimental days 35-45. IOP data were analysed for normality, followed by testing for significance ($p<0.05$) using generalised estimated equations.

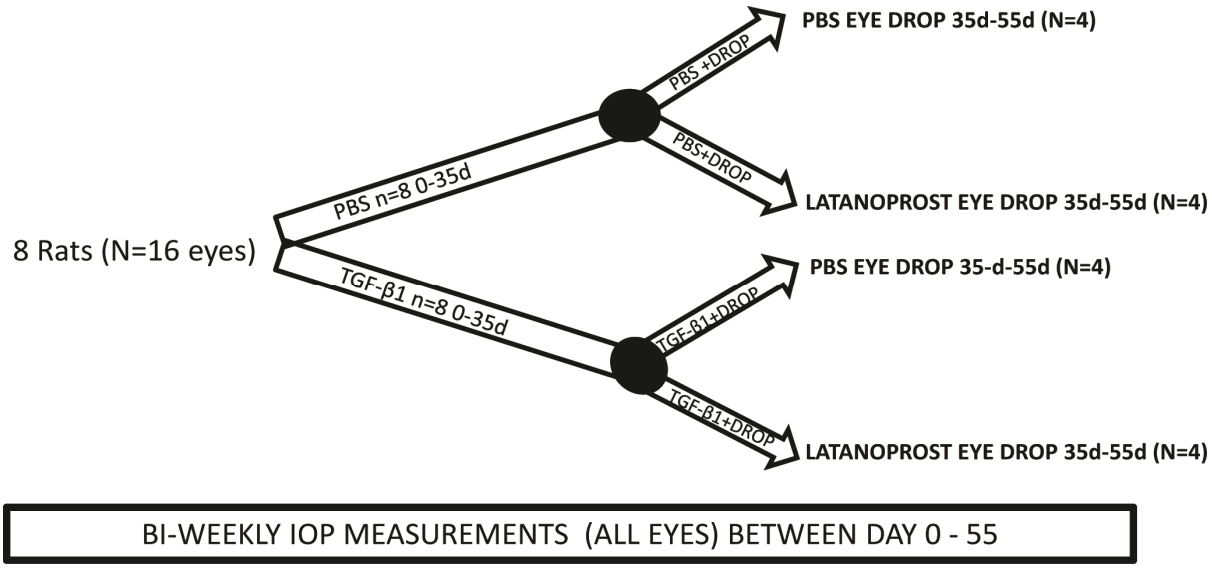


**Figure 4.2 Design of experiment to investigate the effects of an IOP lowering eye drop (latanoprost) to attenuate the IOP rise induced by intracameral injections of TGF-β1.**

### 4.2.4 Study 4 - Sustained increase in IOP, TM fibrosis and RGC death by intracameral injections of TGF-β1

Bi-weekly intracameral injections of TGF-β1 (n=6 eyes), PBS (n=6 eyes) or TGF-β1/PBS (n=6 eyes) were given and IOP measured by tonometry as described in Section 2.2 (Figure 4.3). All rats were killed at 30d. Laminin immunohistochemistry of the TGF-β1 (n=3 eyes), PBS (n=3 eyes) and TGF-β1/PBS (n=6 eyes) injected eyes determined levels of ECM deposition around Schlemm's canal. RGC that were βIII-tubulin$^{+}$ were counted in 250µm linear tracts of the retina from parasagittal sections to assess RGC death. RGC counting from whole mounted retina labelled with 4% FluoroGold was also performed on the TGF-β1 (n=3 eyes) and PBS (n=3 eyes) injected eyes. IOP data were analysed for normality, followed by testing for significance ($p<0.05$) using the within-subjects repeated measures design. The Student's paired *t* test was used for statistical analysis of TM fibrosis and RGC survival.

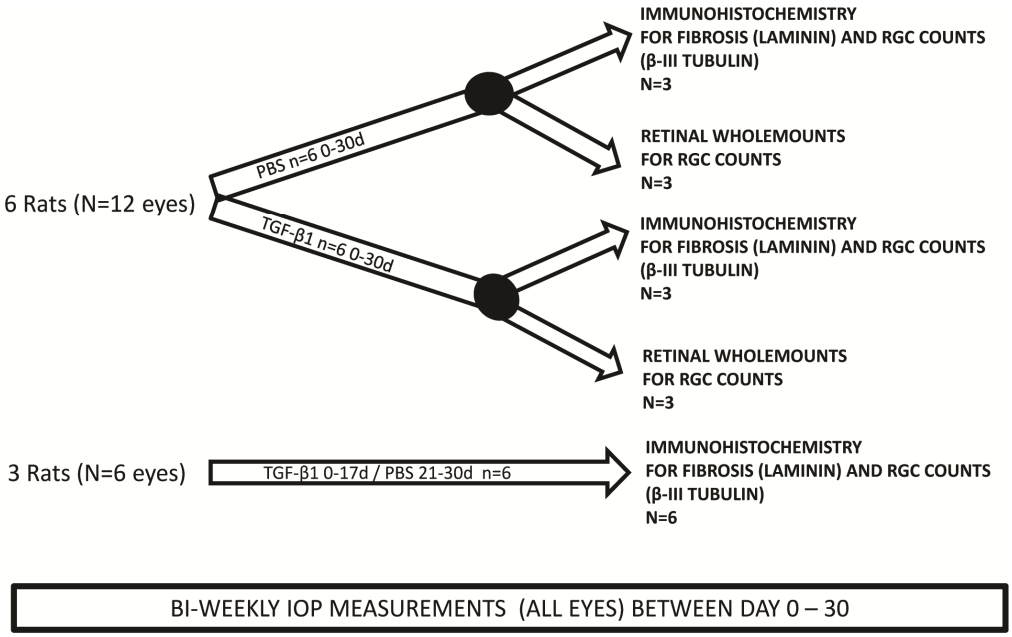


**Figure 4.3 Design of experiment for intracameral injections of TGF-β1 to induce fibrosis, IOP elevation and RGC death.**

### 4.2.5 Study 5 - Sustained increase in IOP, TM fibrosis and RGC death using TGF-β2

Bi-weekly intracameral injections of TGF-β2 (n=12 eyes) or PBS (n=12) were administered as described in Section 2.2 (Figure 4.4). Bi-weekly IOP was measured by tonometry throughout the 30d. Functional analysis of the retina and visual pathway using VEP was performed before rats were killed on 30d. Laminin and fibronectin immunohistochemistry in the TM (n=4) and electron microscopy (n=4) determined induction of TM fibrosis. RGC counting from whole mounted retina labelled with 4% FluoroGold was also performed on the TGF-β2 (n=4 eyes) and PBS (n=4 eyes) injected eyes. IOP data were analysed for normality, followed by testing for significance ($p<0.05$) using the within-subjects repeated measures design. The Students paired *t* test was used for statistical analysis of TM fibrosis and RGC survival.

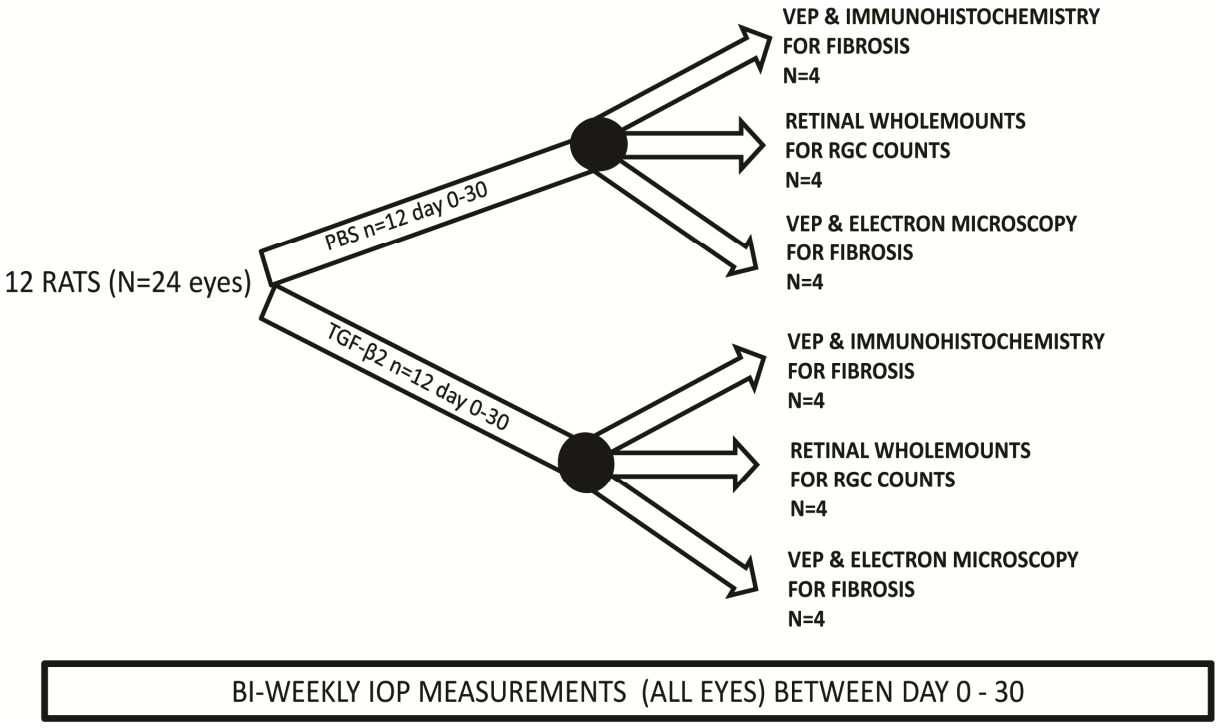


**Figure 4.4 Design of experiment for intracameral injections of TGF-β2 to induce fibrosis, IOP elevation and RGC death.**

## 4.3 Results

### 4.3.1 Study 1 - General compared to local anaesthetic lowered IOP

The administration of a general anaesthetic significantly lowered the overall mean IOP of 11.6±0.5 mmHg from 3 separate recordings at 0d, 9d and 13d compared to local anaesthetic ($p<0.05$), which had a mean IOP of 14.8±0.55mmHg (Figure 4.5). The individual IOP recordings over the 3 separate days under general anaesthetic were 10.9±0.3, 11.3±.4 and 12.6±0.3 mmHg and under local anaesthetic were 15.9±1.6, 14.1±0.3 and 14.3±0.01mmHg. These data demonstrate that general anaesthetic lowers the IOP compared to local anaesthetic which was maintained at each time point throughout the experiment. Manual restraint used under local anaesthesia caused some distress to the rats and was time consuming when compared to general anaesthetic and so IOP was measured under general anaesthesia subsequently.

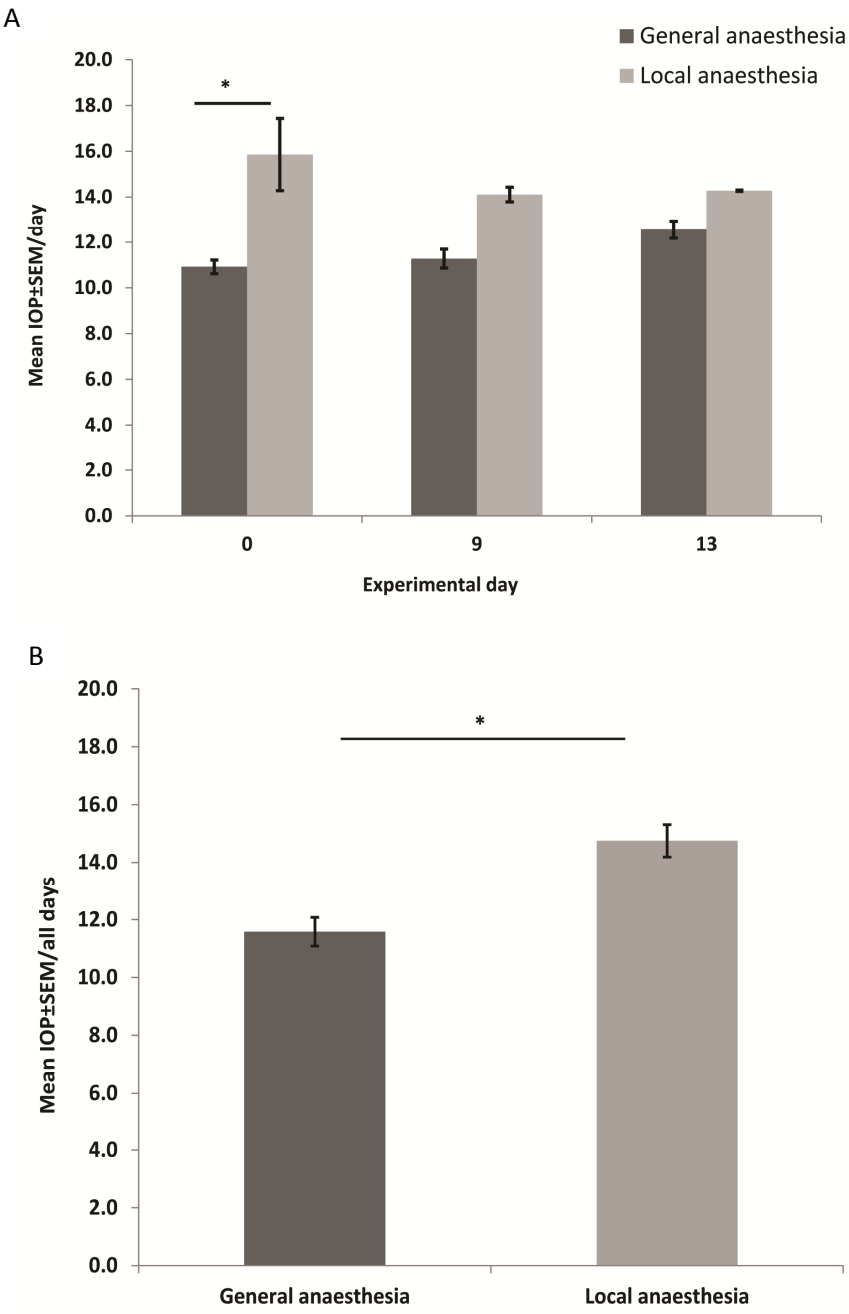


**Figure 4.5 Effects of IOP after local and general anaesthesia. (A)** On 0d, 9d and 13d the IOP measurements were lower after general than after local anaesthesia. However, the difference was only significantly lower on 0d ($p<0.05$); **(B)** the mean IOP of the pooled data from the 3 daily readings were significantly lower after general than local anaesthesia ($p<0.05$).

### 4.3.2 Study 2 - Optimising TGF-β dosing regimen to cause sustained increase in IOP

IOP were recorded after 2 injections of TGF-β1 at 0.5ng/µl between 0-17d and 2 further injections of 5ng/µl between 18-49d to ascertain the optimal dose and injection regime to use in further studies. There was no sustained elevation in IOP with intermittent injections of TGF-β1 at either 0.5ng/µl or 5ng/µl (Figure 4.6). At 0.5ng/µl after injections on 0d and 11d the IOP remained at baselines levels i.e. 9.4±0.1-13.2±2.5mmHg, a range which was not significantly different from control IOP of 9.1±0.6 and 11.9±0.9mmHg. Interestingly, between 18-31d and 49-55d the higher dose of 5ng/µl TGF-β trended towards higher IOP values of up to 15.5±1.3mmHg but this difference did not reach statistical significance when compared to PBS. These data suggest: (1) a dose of 0.5ng/µl was not sufficient to increase IOP above baseline and PBS controls; and (2) the marginal efficacy of the higher dose of 5ng/µl over a period of 9 days suggesting that it could be given more frequently to sustain the raised IOP.

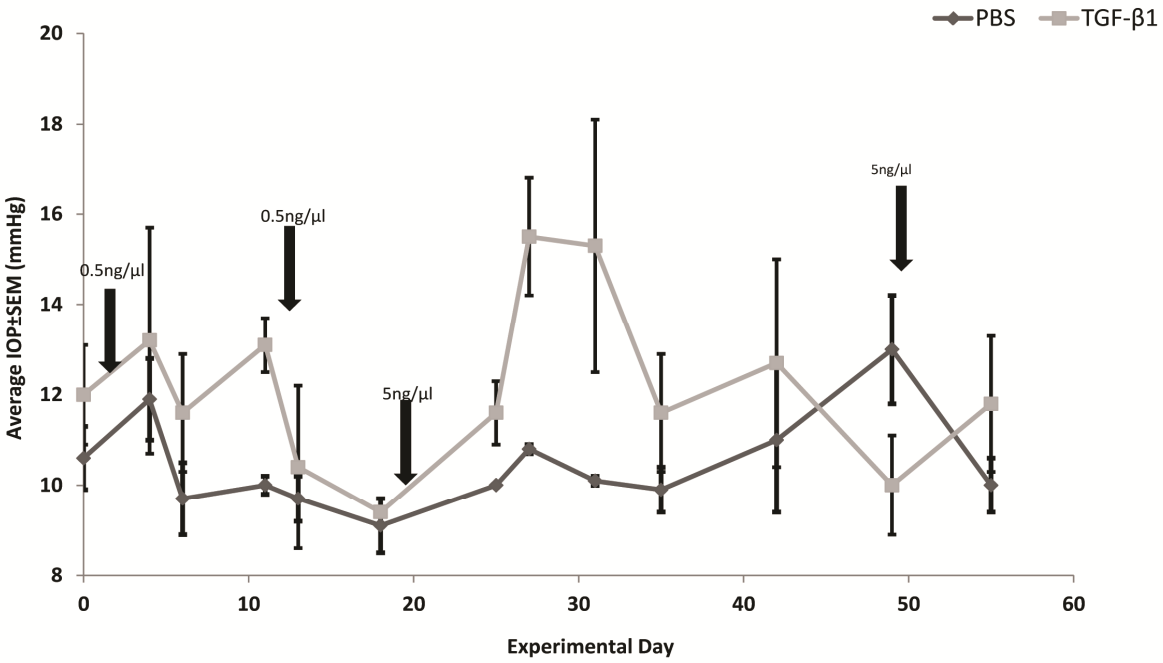


**Figure 4.6 IOP measurements after specific concentrations of TGF-β1 injections.** The mean±SEM IOP is displayed here as a single point on the graph. The arrows represent the dose and day of injections. No sustained elevations in IOP were observed at either concentrations of TGF-β1 or in the PBS controls. IOP in the higher dose TGF-β did spike after injections between 25-35d but significantly higher than control PBS injected eyes.

### 4.3.3 Study 3 – Repeated TGF-β injections induced a sustained increase in IOP which could be attenuated by latanoprost

The aim of this experiment was to investigate IOP after injections of TGF-β1 at 5ng/µl on 10d, 30d and 35d with and without the IOP lowering eye drop, latanoprost, from 30-45d. In both PBS and TGF-β groups, IOP levels remained at normal levels of 9 and 13mmHg between 0-21d showing that the single injection of TGF-β on day 10 did not cause IOP to increase (Figure 4.7). Decreasing the interval between TGF-β injections, by administering on 30d and 35d led to a significant ($p<0.05$), and sustained, increase in IOP from 13.4±1mmHg at 30d to 17±1.6mmHg at 45d, compared to PBS which was at 13.9±1.7 at 30d and at 11.2±0.9 at 45d. The elevated IOP shown in the TGF-β group after 30d was significantly ($p<0.05$) lowered by the topical administration of latanoprost from 30-45d, so that the IOP in TGF-β1+latanorpost group remained within the normal range of 11-12mmHg.

This data suggests that more frequent injections of TGF-β led to a sustained increase in IOP compared to PBS and that this raised IOP is lowered through the use of a commonly prescribed IOP lowering agent to increase AqH outflow through the uveoscleral tract.

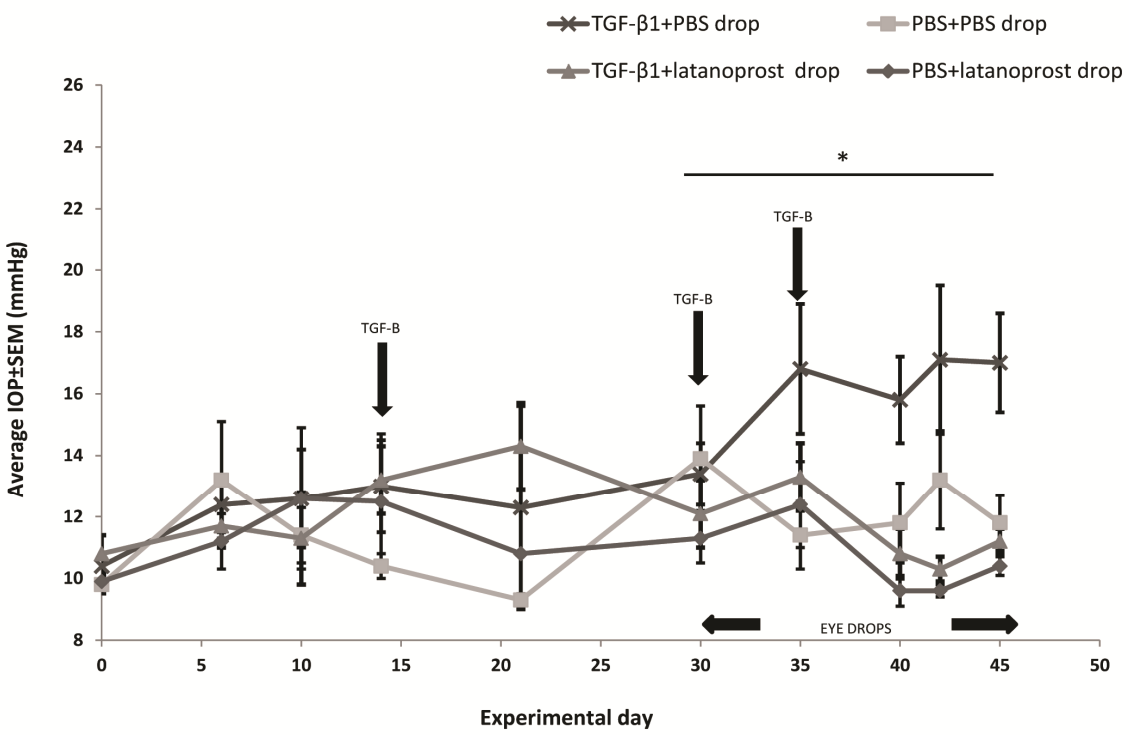


**Figure 4.7 IOP measurements after TGF-β1 injections and latanoprost eye drops.** Three IOP measurements were taken to provide an average reading/eye. The average IOP is displayed here as a single point on the graph±SEM. The arrows represent the day of injections and eye drop administration. A single injection of TGF-β did not lead to a sustained increase in IOP compared to controls between days 10-30. A biweekly injection regime of TGF-β caused a sustained increase in IOP between days 30-45 compared to controls. This TGF-β induced IOP increase was significantly reduced by the topical application of latanoprost reducing IOP to those in the control groups ($p<0.05$).

### 4.3.4 Study 4 - TM fibrosis, sustained IOP elevation and RGC death after intracameral TGF-β1 injections

#### *4.3.4.1 Bi-weekly intracameral injection of TGF-β1 led to sustained elevations in IOP*

Compared to PBS, bi-weekly injections of 5ng/µl TGF-β1 increased IOP (Figure 4.8) although, the difference did not reach statistical significance until 10d, where IOP remained within normal range of 9.7±0.4mmHg-11.1±0.6mmHg in the PBS injected eyes and 10.4±0.4mmHg - 12.6±0.77mmHg in the TGF-β1 injected eyes. Between 10-30d the difference in IOP increased so that after TGF-β1 injections a sustained level of 14.6±0.9mmHg was achieved becoming statically ($p<0.05$) elevated above the normal range of 10.6±0.7mmHg-11.8±0.6MmHg. The sustained increased in IOP (Figure 4.8) demonstrated that TGF-β1 had caused sustained higher level of IOP probably attributable to AqH outflow impairment.

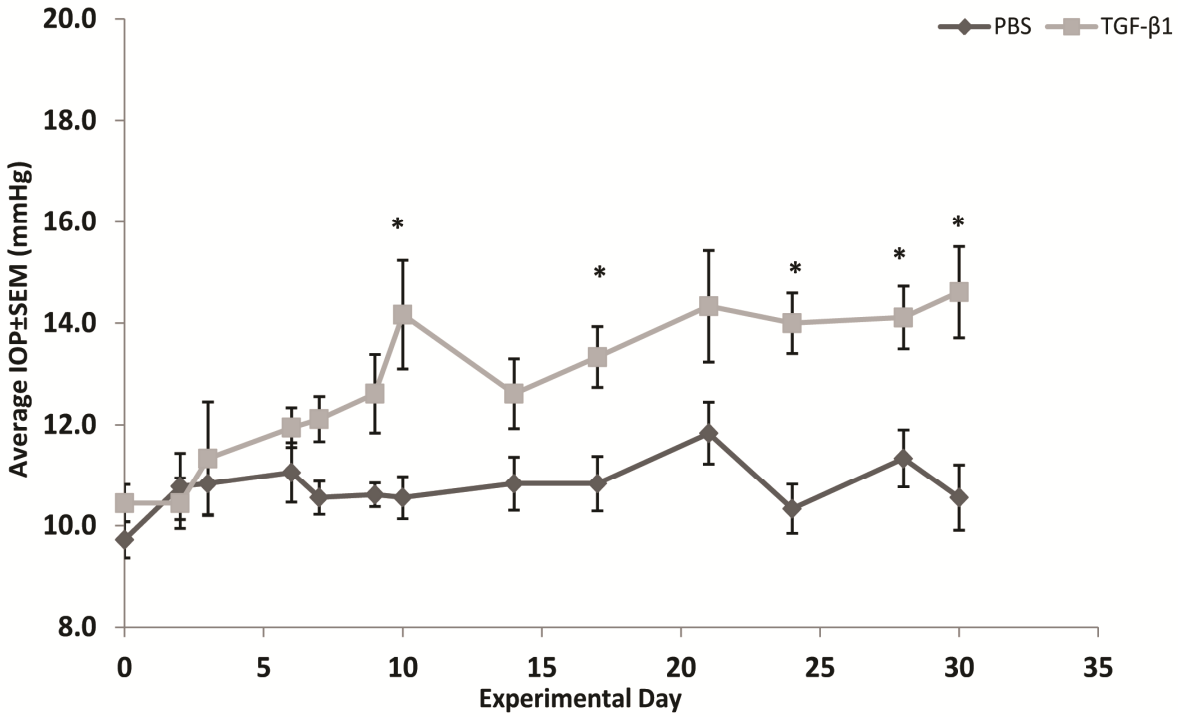


**Figure 4.8 IOP measurements after TGF-β1 injections.** The average IOP±SEM is displayed here as a single point on the graph. There was a sustained increase in IOP observed after injections of TGF-β compared to PBS from 10d to the end of the experiment at 30d ($p<0.05$).

Another group of rats received TGF-β1 injections for 17 days when the IOP plateaued at 13.9±1.38mmHg, thereafter, received intracameral injections of PBS only (TGF-$\beta1_{0\text{-}17d}$/$PBS_{21\text{-}30d}$) where the IOP continued to rise to a measurement of 16.7±1.3mmHg by 30d. TGF-$\beta1_{0\text{-}17d}$/$PBS_{21\text{-}30d}$ study was designed to confirm that it was not just continual injections of exogenous TGF-β that was maintaining the higher level IOP but that the earlier injections of TGF-β were sufficient to cause fibrosis in the TM and hence a sustained resistance to AqH outflow. Indeed, the data (Figure 4.9) demonstrated that the TGF-β1 induced rise in IOP was maintained until the end of the experiment at 30d, despite cessation of TGF-β1 injections 17d.

IOP after TGF-$\beta1_{0\text{-}17d}$/$PBS_{21\text{-}30d}$ injections were significantly higher than the PBS control group on 24d, 28d and 30d ($p<0.05$) suggesting that the induced rise in IOP was not from the continued repeated injections of TGF-β1 and that the sustained increase was induced successfully within the first 17 days, probably from inducing a permanent restriction to AqH outflow.

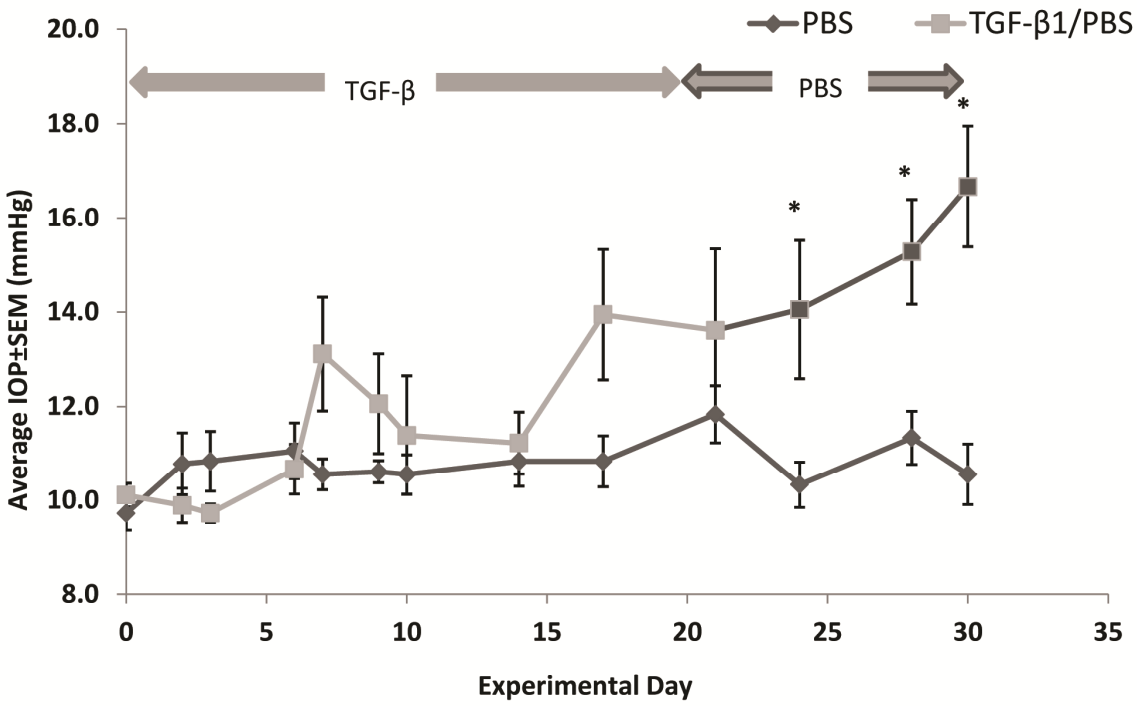


**Figure 4.9 IOP measurements after TGF-β1$_{0\text{-}17d}$/PBS$_{21\text{-}30d}$ injections.** The mean IOP±SEM is displayed here as a single point on the graph. There was a sustained higher level of IOP observed from 17d until 30d despite cessation of TGF-β1 injections on 17d. The IOP were significantly higher than PBS from 24d until 30d ($P<0.05$).

#### *4.3.4.2 Repeated intracameral administration of TGF-β1 increased laminin deposition in inner wall of Schlemm's canal*

Laminin deposition staining was especially prominent around in the basement membrane surrounding Schlemm's canal in the TGF-β-injected eyes compared to the PBS-injected eyes (Figure 4.10). In the PBS groups, the laminin staining was observed as a discontinuous pattern localised mainly to the outer wall of Schlemm's canal (towards the sclera) whereas, the inner wall of Schlemm's canal (towards the TM) had very little laminin deposition (Figure 4.10a). In the TGF-β group, laminin was deposited in a continuous band around Schlemm's canal of equal thickness in the outer and inner walls (Figure 4.10b). Quantitation of this observation using pixel counts demonstrated that TGF-$\beta_{0\text{-}30d}$ and TGF-$\beta_{0\text{-}17d}$/$PBS_{21\text{-}30d}$ injected eyes had significantly ($p<0.001$) more laminin staining around Schlemm's canal compared to the $PBS_{0\text{-}30d}$ injected eyes. These data show that by 30d, TGF-β1 increased laminin deposition around Schlemm's canal, both when injected bi-weekly from 0-30d and importantly, when injections were stopped at 17d suggesting that increase ECM deposition had contributed to increased "stiffness" or "resistance" leading to the sustained IOP elevation shown in these eyes.

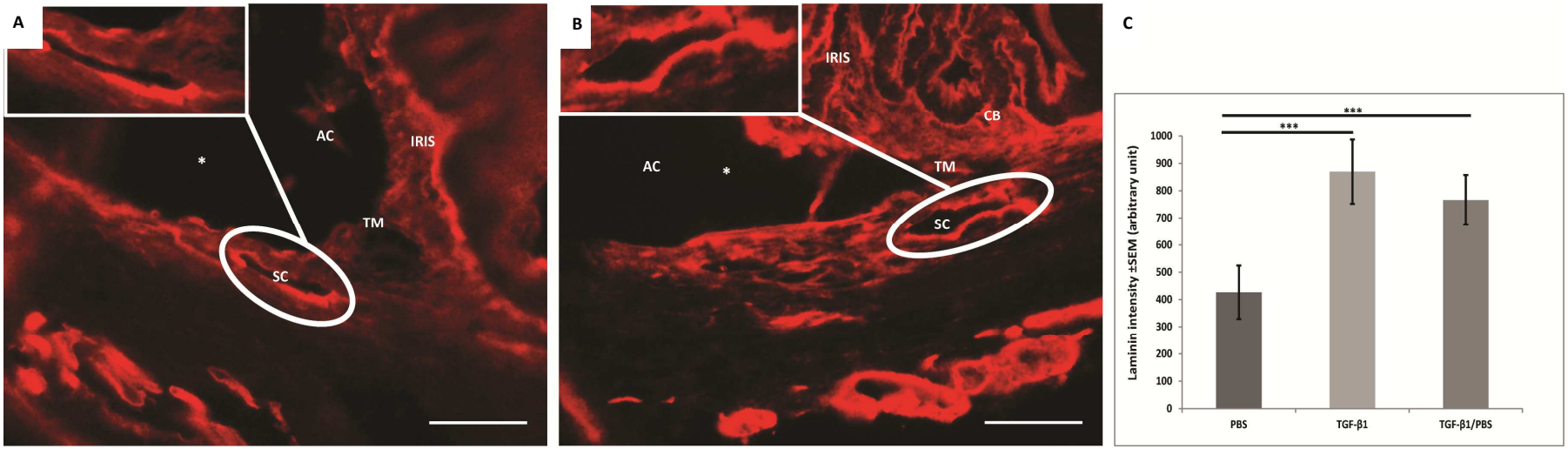


**Figure 4.10 Distribution of laminin around Schlemm's canal.** Parasagittal eye sections illustrating laminin staining in the iridiocorneal angle (*) and inset image of Schlemm's canal. Laminin deposition was found around Schlemm's canal in both **(A)** PBS and **(B)** TGF-β1 injected eyes. **(C)** Bi-weekly injections of TGF-β from 0-30d (n=3) and 0-17d (n=6) led to significant ($p<0.001$) increase laminin deposition within the outer and inner walls of Schlemm's canal, which were at minimal levels in the PBS group (n=6). Scale bar – 100µm; CB – Ciliary body; SC – Schlemm's canal; TM – trabecular meshwork; AC – anterior chamber.

#### *4.3.4.3 Repeated intracameral injections of TGF-β1 and RGC death*

B-III tubulin$^{+}$ RGC counts from retinal sections showed and 8% loss of RGC at the optic nerve head (i.e. 92±2% compared to PBS counts of 100±5%) compared to the peripheral retina but was not significantly lower (Figure 4.11 A). The peripheral RGC counts demonstrated no statistical difference in numbers between the PBS or the TGF-β1 group at 91±7% and 91±3%, respectively. These data showed that RGC death trended towards a preferential loss at the optic nerve head compared to the peripheral retina. In the TGF-$\beta_{0\text{-}17d}$/$PBS_{21\text{-}30d}$ group there was 13% loss of RGC compared to the PBS group which was not significant (Figure 4.11 B). Interestingly, $FG^{+}$RGC counts from whole mounted retina demonstrated a significant (n=3, $p<0.01$) 27% loss in RGC in the TGF-β1 injected eyes compared to PBS group (Figure 4.12). These data suggest that RGC death occurred, although there was a discrepancy in the level of RGC death measure from retinal sections *vs* retinal whole mounts.

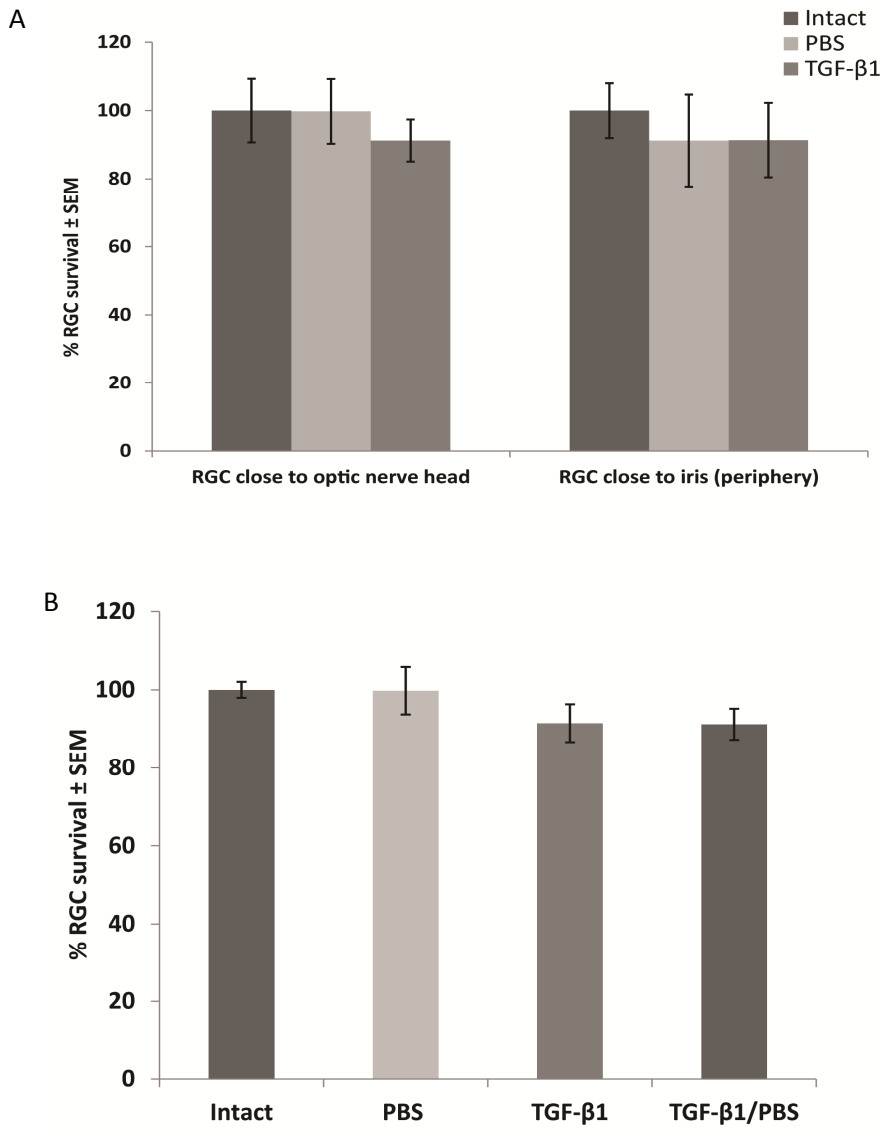


**Figure 4.11 RGC counts from retinal sections.** Data points are the mean %RGC±SEM from intact retinal counts. **(A)** The preferential loss of RGC at the optic disc compared to the retina close to the iris (periphery) after injections of TGF-β was not significant. **(B)** RGC counts from the retina close to the optic nerve head showed that TGF-β1 and TGF-$\beta_{0\text{-}17d}$/$PBS_{21\text{-}30d}$ groups had less RGC compared to intact and PBS injected eyes by 30d but this did not reach significance.

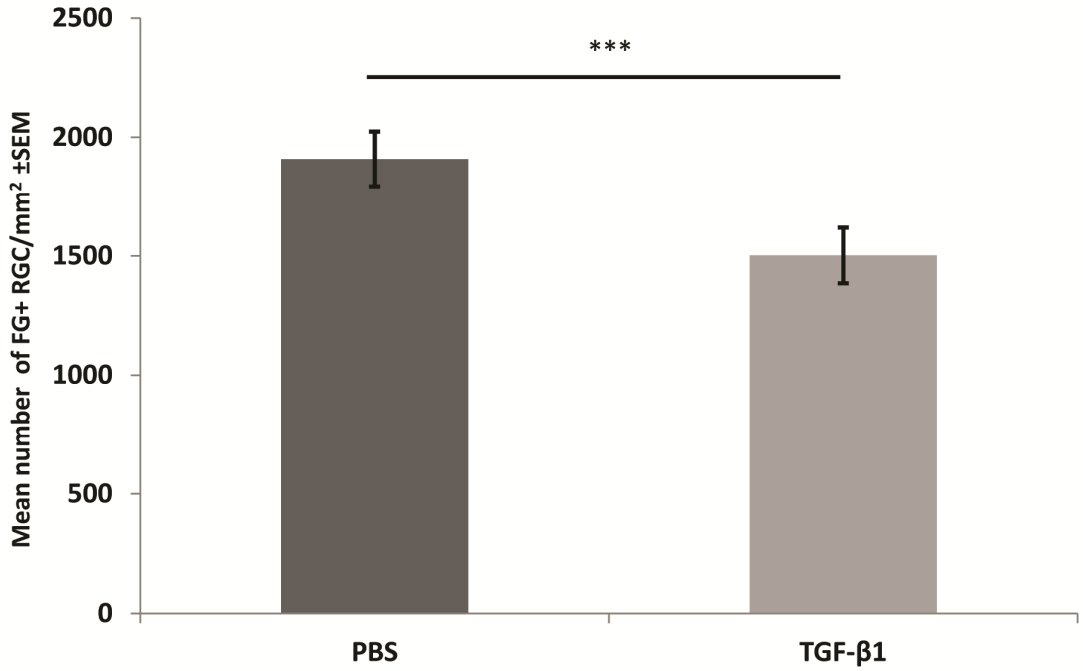


**Figure 4.12 RGC counts from whole mounted retinae**. Mean number of RGC±SEM from the TGF-β1 and PBS groups. By 30d there was 27% loss of RGC in the TGF-β1 group compared to PBS (n=3, ***p<0.01).

In summary, these data showed that the increasing levels of TGF-β1 in the AqH increased the deposition of laminin, increased and maintained an elevated IOP (that was not dependent on continued administration of exogenous TGF-β) and resulted in 27% RGC death (from retinal whole mount data only).

### 4.3.5 Study 5 - TM fibrosis, sustained IOP elevation and RGC death after intracameral injections of TGF-β2

#### *4.3.5.1 Bi-weekly intracameral injection of TGF-β2 led to a sustained elevation in IOP*

Compared to PBS and as with injections of TGF-β1, bi-weekly injections of 5ng/µl TGF-β2 increased IOP (Figure 4.13) although, the difference did not reach statistical significance until 7d before which, the IOP remained within a normal range of 10.4±0.3mmHg -12.4±0.7mmHg in the TGF-β2 injected eyes. From 7d until 30d IOP increased and was maintained at a higher level after TGF-β2 injections to 14±0.3mmHg. IOP in the TGF-β2 injected eyes was significantly higher ($p<0.05$ between 9d and 14d; $p<0.001$ between 16d and 30d) than in the PBS injected eyes, which remained within normal range of 10.5±0.4mmHg-11.7±0.3MmHg. The sustained increased in IOP (Figure 4.13) demonstrated that TGF-β2 is a suitable agent to cause a restriction in AqH outflow as represented by a sustained higher level of IOP. Interestingly, the IOP levels for TGF-β2 were consistent with those recorded after similar injections of TGF-β1.

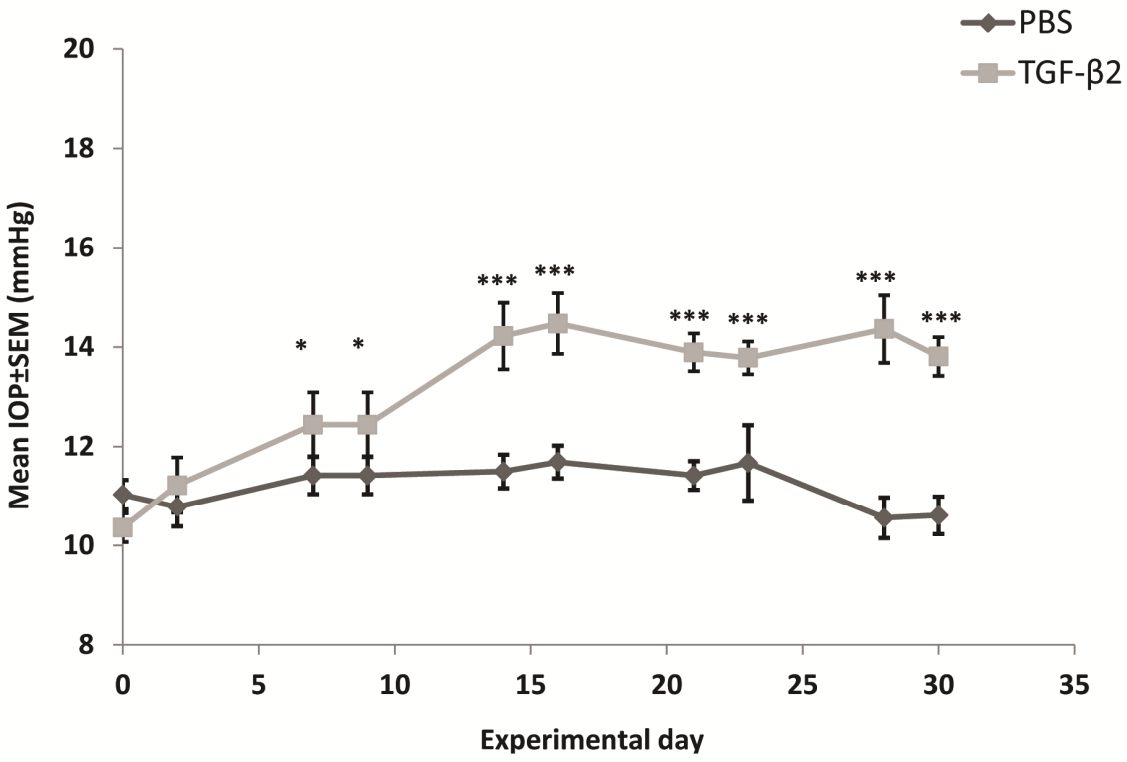


**Figure 4.13 IOP measurements after intracameral injection of TGF-β2.** The average IOP is displayed here as a single point on the graph±SEM. There was a significant and sustained higher level of IOP observed after injections of TGF-β2 compared to PBS (*$p<0.05$; *** $p<0.001$).

#### *4.3.5.2 Bi-weekly intracameral injections of TGF-β2 causes TM fibrosis*

Intracameral injection of TGF-β2 led to fibrosis in the TM (Figure 4.14). In the intact and PBS injected eyes, immunostaining for laminin was observed in the ciliary body, iris and in vascular basement membranes and was dense around Schlemm's Canal in the outer wall but thinner in the inner wall. Laminin staining was also present at very low levels within the TM, but when present, was observed as thin linear strands throughout the meshwork. By 30d, after bi-weekly injections of TGF-β2, laminin levels had significantly increased throughout the TM ($p<0.001$), being especially prominent in the JCT region of the TM and in the inner wall of Schlemm's Canal, compared to intact and PBS injected eyes. By 30d, the TM was also densely packed with fibronectin deposits compared to intact and PBS injected eyes ($P<0.001$).

TEM of parasagittal sections of the eyes revealed increased ECM deposition (Figure 4.15). In the JCT region of PBS eyes there was an irregular organisation of trabecular cells. Intra-trabecular spaces could be identified along with thin strands of basement membrane and electron dense elastic fibres with collagen and surrounded by ECM. The inner wall of Schlemm's Canal was comprised of a monolayer of flat endothelial cells on a basement membrane. After TGF-β2 injections, the organisation of the TM became disorganised with fewer trabecular cells found in an irregular array with disrupted connections with other trabecular cells. Homogenous granular ECM was found in the sub-endothelial region and the endothelium of the inner wall of Schlemm's Canal appeared thicker (data not shown). With the increase by laminin and fibronectin shown on immunohistochemistry together with the

ECM deposition by TEM confirm that injections of TGF-β2 caused fibrosis of the TM and Schlemm's Canal.

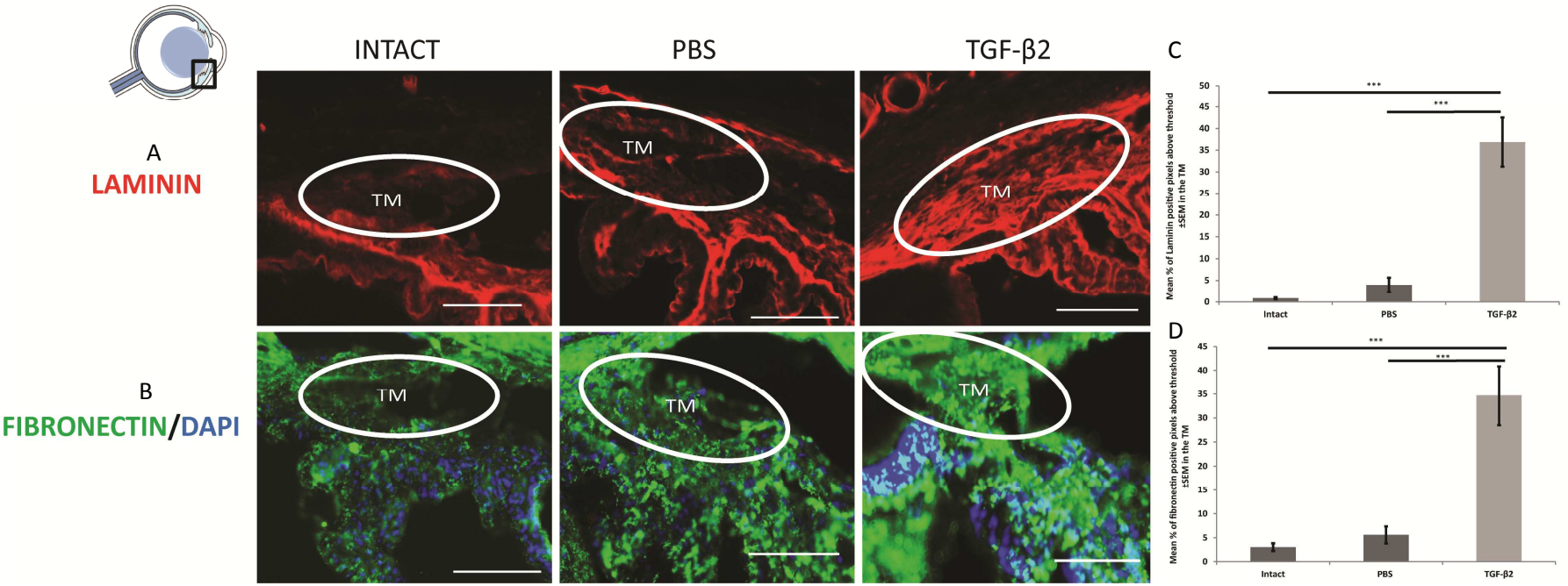


**Figure 4.14 TM fibrosis in the iridiocorneal angle.** Parasagittal eye sections illustrating areas of fibrosis by immunostaining of **(A)** laminin (red) in the upper row and **(B)** fibronectin (green) with DAPI stained cell nuclei (blue) in the lower row. The circled area contains the TM. Immunostaining for **(C)** laminin and **(D)** fibronectin was increased in the TM after TGF-β2 injections compared to intact and PBS eyes ($p<0.001$). Scale bar – 100µm; TM – trabecular meshwork.

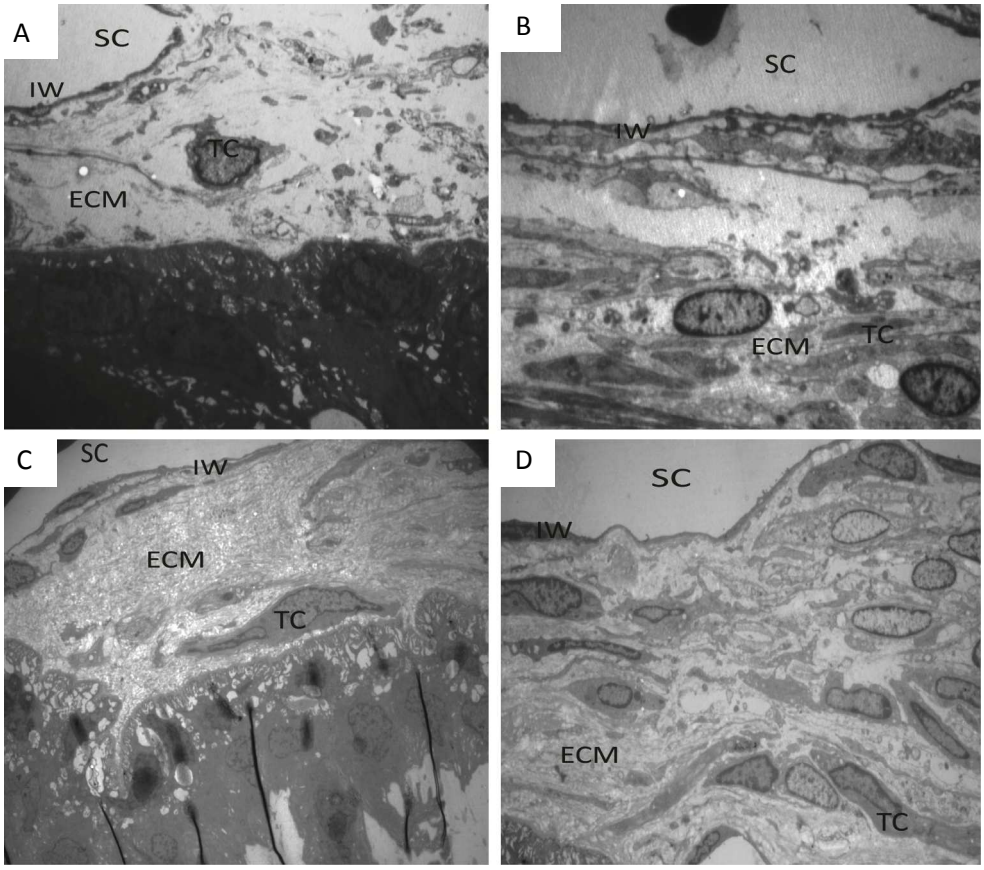


**Figure 4.15 Electron micrograph of the trabecular meshwork (X2500). (A,B)** In the PBS group, the TM showed expanded beam-like structures running in parallel and interconnecting with each other. In between the trabecular cells (TC), there were inter-trabecular spaces in which there were low levels of ECM deposition. There was a varying thickness of a mono-layer of endothelium on the inner wall (IW) of Schlemm's canal (SC). **(C, D)** In the TGF-β2 injected eyes the TM was more irregular, with disruption between TC. There was fewer TC and the ECM was markedly increased in the JCT region and the endothelium of the inner wall of SC appeared thicker after TGF-β2 compared to PBS.

#### *4.3.5.3 Bi-weekly intracameral injection of TGF-β2 decreased retinal function and RGC death*

Deficits in retinal function assessment of the retina and visual pathway using flash VEP, occurred after bi-weekly intracameral injections of TGF-β2 on 30d (Figure 4.16). There was a significant decrease in theP1/N2 amplitude in the VEP recorded from TGF-β2 compared to PBS injected eyes ($n=8$; $p<0.01$) but there were no change in latency at P1/N2 ($p>0.05$). There were no statistical significance observed in latency or amplitude from baseline to N1 or from N1 to P1 (data not shown). Compared to PBS, TGF-β2 injections also decreased RGC numbers 30d (Figure 4.17) in retinal whole mounts by 30% with counts of 1888±100 RGC/mm$^2$ and 1316±107 RGC/mm$^2$ ($p<0.001$), respectively. The decrease in amplitude on VEP suggested that the number of axons in the visual projections was reduced which correlated with fewer numbers of RGC after intracameral TGF-β2 compared to PBS injections. Latency was unaffected, suggesting that the speed of conduction through the visual pathway was unaffected.

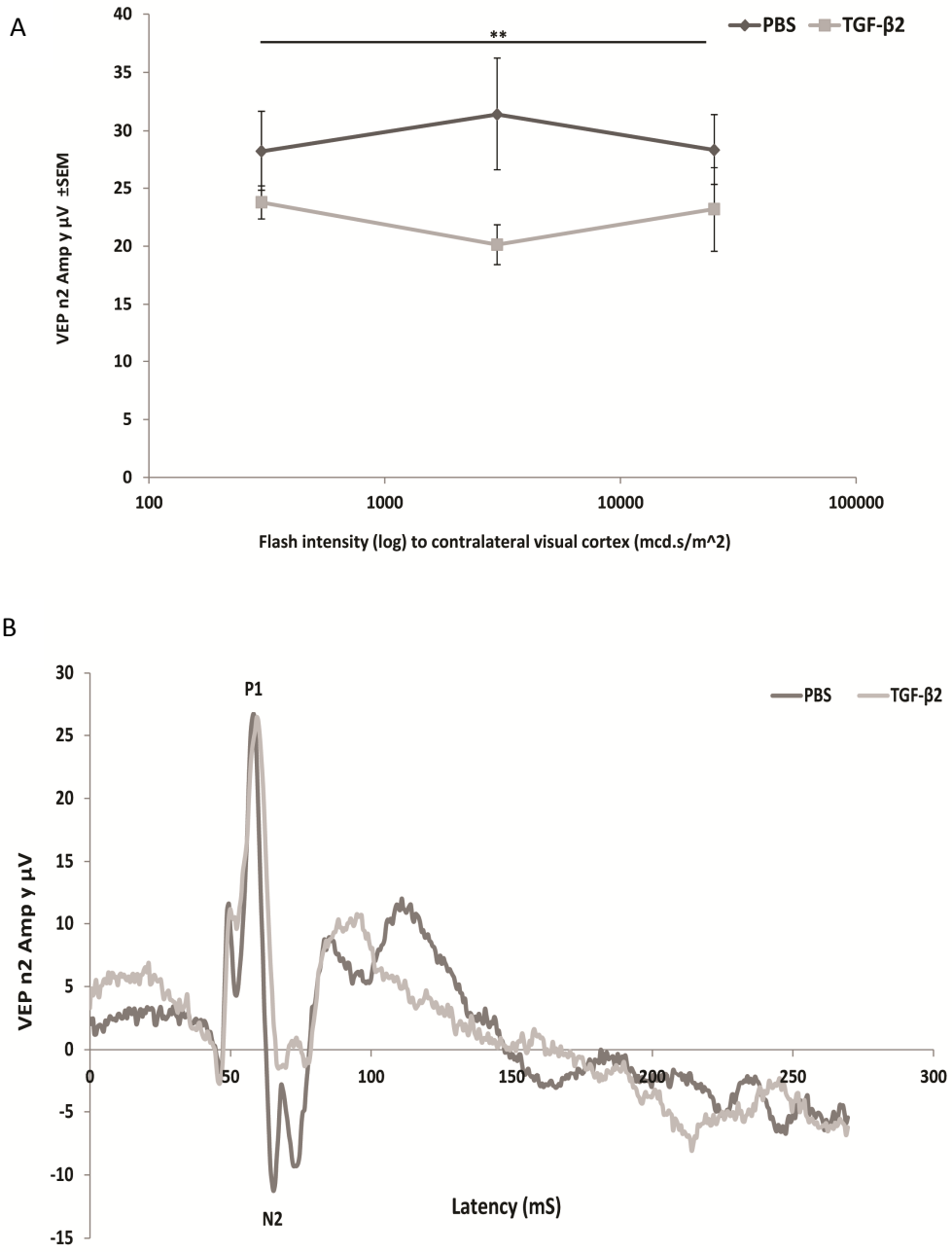


**Figure 4.16 Functional assessment of the visual pathway using flash VEP.**

**(A)** Average amplitude VEP at P1/N2 after PBS and TGF-β2 injections. There was a significant reduction in amplitude at P1/N2 in the TGF-β2 group compared to the PBS group (n=8 eyes/group **P<0.01). **(B)** Representative VEP traces at flash intensity of 3000mcd.s/$m^2$ showing a decrease in amplitude after TGF-β2 compared to PBS injections.

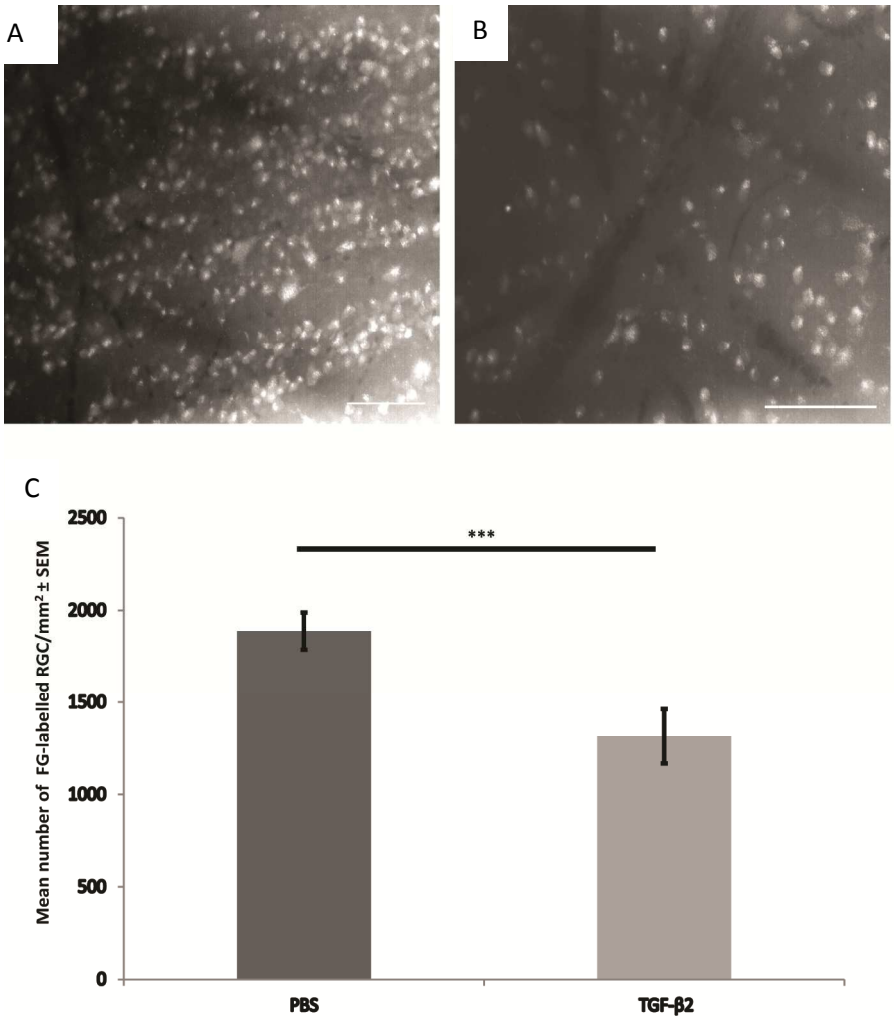


**Figure 4.17 Representative micrographs of FG$^+$ RGC. (A)** FG$^+$ RGC in retinal whole mounts at 30d after bi-weekly injections of PBS **(B)** FG$^+$ RGC at 30d after bi-weekly injections of TGF-β2. There were fewer RGC present after injections of TGF-β2 injections. **(C)** Quantification of FG$^+$RGC survival in PBS and TGF-β2 injected eyes. Injections of TGF-β2 led to significant RGC death compared to PBS (n=4 eyes/group **P<0.001). Scale bar 100µm.

## 4.4 Discussion

This study demonstrated that bi-weekly intracameral injections of both TGF-β1 and TGF-β2 led to TM fibrosis, sustained elevations of IOP and RGC death; all pathological features of open angle glaucoma. Increasing levels of TGF-β1/2 in the AqH induced high levels of laminin and fibronectin around the TM and IOP increases, suggesting impaired AqH outflow and was associated with RGC loss and consequent functional deficits.

### 4.4.1 The effect of general compared to local anaesthetic on IOP

It is well documented that compared to local anaesthesia IOP is lowered under inhalation anaesthesia in both humans and rodents (Ausinsch et al., 1975; Jia et al., 2007; Ding et al., 2011). In study 1 reported here, IOP in rats decreased by 22% under general anaesthesia compared to local anaesthesia. IOP is the main risk factor in the development of POAG, thus reliable rodent models should utilise reliable and reproducible methods of recording IOP. For administration of local anaesthetic behavioural training was required but this proved to be unsuccessful and repeated handing contributed to stress the rats, resulting in more variable IOP readings. Other studies have successfully trained mice (Cohan et al., 2001; Jia et al., 2011) and rats (Wang et al., 2005) to tolerate IOP measurements while awake whereas, varying IOP measurements have been recorded from strains making interpretation of the data more difficult and have recommended that IOP be recorded under general anaesthetia with Isoflurane (Robertson et al., 2013). Although Isoflurane lowers IOP, IOP tends to remain stable for up to 3 minutes after the induction of anaesthesia (thus providing a

temporal window in which to take accurate measurements) (Ding et al., 2011; Cone et al., 2012), at which point IOP can decrease up to 20%, corresponding to the decrease in IOP using general anaesthesia shown in the present study. From the results presented in this study (4.3.1) it was concluded that use of general anaesthesia is preferable to local anaesthesia to minimise distress of the rats during IOP measurements, which should be recorded within 3 min of induction. Thus, rats in all treatment groups were administered general anaesthesia.

### 4.4.2 Development of a sustained elevation in IOP was attained from increasing AqH levels of TGF-β

A sustained IOP elevation to 4-5mmHg above control (40%) was achieved for up to 3 weeks by administering TGF-β1 or 2 bi-weekly at a concentration of 5ng/µl. In human studies IOP elevations of 1mmHg can significantly increase the risk of developing POAG (Coleman & Miglior, 2008). Thus, the modest elevation shown in this experimental model of glaucoma would be sufficient to replicate the modest increases in IOP recorded in patients with POAG.

Consistent with other fibrotic models of raised IOP (Fleenor et al., 2006; Robertson, 2010; Shepard et al., 2010; Han et al., 2013; Robertson, 2013), the intracameral TGF-β delivery regime used here generated a sustained and significant increase in IOP by 14d compared to controls. Fleenor et al., (2006) in human anterior segment perfusion studies, showed that TGF-β2 (at 5ng/ml) generates a steady increase in IOP (up to 13-14mmHg from control IOP of 8-10mmHg) to levels similar to those seen in this study. The level of control IOP reported

in the Wistar rat by Robertson et al (2010) was similar of that of seen in this study (12mmHg), but in contrast to the results here, they demonstrated using TGF-β1 adenovirus, that IOP was elevated and sustained at 20mmHg from 14 - 29d after injection. However, the higher elevated IOP levels by increasing TGF-β1 levels, using gene-expression (Robertson et al., 2010), could probably be explained by the constitutive production TGF-β compared to the interrupted bolus regime of bi-weekly intracameral injections used in this study. What hasn't been described previously, and was shown in these studies, was that elevated IOP levels were maintained until the end of the experiment at 30d despite cessation of TGF-β injection after 16d. This demonstrates that the raised IOP in this study was not attributable to the continued injections of exogenous TGF-β and that the IOP elevation was a consequence of established outflow resistance.

### 4.4.3 TM fibrosis resulted from increasing AqH levels of TGF-β1/2

Using established (Botfield et al., 2014) semi-quantitative analysis these studies demonstrated that TGF-β1 and TGF-β2 increased ECM deposition in the TM. TM cells together with ECM components are required to maintain AqH outflow. Several electron microscopic and immunohistologic studies of glaucomatous eyes have noted excessive accumulation of ECM in the TM (Weinreb et al., 1996) and it is widely accepted that increased levels of TGF-β in the AqH in patients and rodents is associated with TM fibrosis. Since AqH constantly flows through the TM, its protein content, including TGF-β, directly alters ECM dynamics. Concentrations of TGF-β lower than those used in these studies induce ECM production from fibroblasts (Kottler et al., 2005). Kottler et al., (2005) observed increased ECM production of fibronectin and collagen induced by 0.1-5ng/ml of both TGF-β1 and TGF-β2 in isolated human tenon's fibroblasts.

A high density of TGF-β receptors is expressed in TM cells making the TM particularly sensitive to the effects of raised TGF-β levels in the AqH from TM cells, the lens and ciliary body (Tripathi et al., 1994). TGF-β receptor binding and subsequent intracellular SMAD signalling in the TM causes local fibrogenesis by increasing ECM protein translation (including fibronectin and laminin) and modulating ECM protease activity by down-regulating MMPs and also up-regulating TIMPs (Weinreb et al., 1996), resulting in the accumulation of matrix around the TM and increased resistance to AqH outflow (Tripathi et al., 1994).

The ECM not only provides a scaffold for cells but also alters the dynamics cell-ECM interactions. Laminin and fibronectin are glycoproteins that bind multiple growth factors and substrates and play a role in cell attachment, motility and wound healing. Laminin is present within the TM basement membrane and increasing levels have been noted in steroid induced glaucomatous cultured human TM cells (Dickerson et al., 1998). The present study mirrors this finding. Similarly, fibronectin, is normally localised to the trabecular beams and basement membranes (Weinreb et al., 1996) which is present in the TM as an insoluble form. The discontinuous appearance of laminin in the control eyes in this study has also been observed in electron microscopic studies by Gong et al. (2002). Experimental steroid-induced glaucoma (Steely et al., 1992) and whole-eye and trabeculectomy samples (Floyd et al., 1985) show increased fibronectin levels in those with POAG (Babizhayev & Brodskaya, 1989). In addition, the electron microscopic evaluation carried out in these studies also illustrate the effects of excess ECM deposition in the TM as shown by the granular plaque appearance in and around the JCT and Schlemm's Canal. Kottler et al., (2005) showed a similar granular appearance of large aggregates of activated tenon's fibroblasts after TGF-β1 and 2 treatment (although they stated it was more apparent after TGF-β1 compared to TGF-β2). Within the JCT region, cells that have adjacent basement-membrane components fill the spaces between ECM (Fuchshofer et al., 2006; Keller & Acott, 2013). There is also an array of elastic fibers which run along the endothelial inner wall of Schlemm's Canal which fluctuate by mechanical stress from changes in IOP. Studies have described the loss of TM elasticity in POAG and a stiffening of the JCT region, through the accumulation of cross-linking ECM molecules (Last et al. 2011). Giant vacuoles in the inner wall of Schlemm's Canal

in POAG observed by Gong et al., (1996), were not seen in the present electron microscopic analysis.

Interestingly, the electron microscopic analysis of the TM after TGF-β2 injections did show ECM accumulation in the JCT region. The JCT region is the least porous part of the TM containing sub-micron flow channels for AqH (Johnson, 2006) compared to the uveal and corneoscleral regions, which contain pore sizes of 25-75µm and 2-15µm respectively, and contains ECM and fibroblasts (Johnson, 2006). It is thought that the ECM in the JCT provides resistance to outflow (Johnson, 2006), which would support the hypothesis that IOP elevation is a response to the accumulation of ECM induced by exogenous TGF-β.

### 4.4.4 RGC death resulted from increasing AqH levels of TGF-β

Elevations in IOP cause structural and functional damage to the optic nerve head leading to apoptotic death of RGC through many biochemical and mechanical alterations (Guo et al., 2005; Robertson et al., 2010). In the present study significant RGC death of 30% was induced by exogenous administration of TGF-β1 and TGF-β2 and these data support those from other TGF-β induced TM fibrotic models (Robertson et al., 2010) in which a substantial loss (raw data or % loss not stated) of RGC by apoptosis was reported after increasing TGF-β expression in the anterior chamber. Robertson et al., (2006) showed levels of TGF-β in the retina after 14d TGF-β treatment (to rule out any direct effects of TGF-β) were not increased compared to controls concluding that the RGC death observed was an indirect result of IOP elevation and not by directly attributable to RGC death from TGF-β toxicity. Although there

is no precise explanation of why high IOP causes RGC death, a multitude of factors caused by IOP increases compression of the optic nerve head (Tsai, 2012) may contribute, including compromised RGC axonal transport of neurotrophic factors, activation of apoptosis and mitochondrial dysfunction of RGC from both biomechanical and ischemic insults.

The results from this study also demonstrated differences in RGC counts related to the counting method used. Counts taken from a linear 250um parasagittal section of the retina of RGC stained with β-III tubulin and DAPI did not show any differences between TGF-β and control groups. However, the same treatments yielded significant results when $FG^{+}$RGC were counted from whole mounted retinae. The whole retinal counts were considered more suitable and reliable as the 250um linear counts may not have included the areas of cell death. It is well documented that the RGC are most vulnerable to death close to the optic nerve head (Johnson et al., 2000; Nickells et al., 2012) and the linear counts may have missed these areas completely.

To assess the functional integrity of the visual pathway flash VEP were recorded at 30d. Flash VEP has been used in other rat models of ocular hypertension to assess functional damage (Belforte et al., 2010). Reduced amplitudes and increased latency occur in other experimental glaucoma models (Towle et al., 1983) but only a reduction in amplitude was observed in the present study. A model of ocular hypertension from intracameral injections of chondroitin sulphate yielded differences in N2 amplitude, but not latency (Belforte et al., 2010), as mirrored in this present study. VEP amplitudes decrease in monkey's with experimental glaucoma (Johnson et al., 1989). The VEP represents activity of all the retinal

and visual cortex cells and their axons so the actual location of reduced function is not easily identified.

### 4.4.5 Conclusion

Taken together, these results show that raised intracameral TGF-β levels induce TM fibrosis and increase IOP, leading to RGC death and reduced visual function as assessed by VEP, and indicated that the rat TGF-β model is useful for translational studies of experimental POAG. Unlike the most popular experimental glaucoma models, which use artificial means (such as epi-scleral vein ligation or injecting micro-beads) to increase IOP, the TGF-β model is based on increasing IOP by inducing fibrosis of the TM as occurs in the human pathology, and is, therefore, suitable to assess anti-fibrotic agents as potential treatments for patients.

# Chapter 5

# Decorin attenuates trabecular meshwork fibrosis, elevated IOP and RGC death

## 5.1 Rationale

Current treatments for the management of POAG are based either on the chemical or surgical lowering of IOP with the aim of preserving retinal function (McKee et al., 2005). The heterogeneous and multifactorial nature of POAG poses difficulties for providing adequate treatments. The current treatments for IOP lowering include the use of β blockers (e.g. Timolol) to reduce AqH production from the ciliary body and latanoprost (e.g. Xalatan), which increases flow through the uveoscleral drainage pathways (Alm et al., 1995). Surgical options, including trabeculectomy, serve to increase AqH drainage through by-passing the TM. Although helpful, these treatments do not combat the underlying fibrotic pathology that characterises POAG. Alternative treatment strategies that better control IOP and ameliorate POAG by preventing and/or reversing the fibrogenic effects of cytokines in the TM are needed.

In this regard, the naturally occurring TGF-β antagonist Decorin, a small leucine rich proteoglycan that acts as a matrikine to directly interfere with collagen fibril assembly and also activate ECM-degrading proteases, thereby inhibiting fibrogenesis and inducing dissolution of established scar tissue (Logan et al., 1999; Davies et al., 2004; Järvinen & Ruoslahti, 2010; Mohan et al., 2011; Ahmed et al., 2013; Botfield et al., 2013), holds therapeutic promise.

However, the effectiveness of Decorin for the treatment of TM fibrosis has not yet been elucidated. Using the developed experimental TGF-β model of TM fibrosis (Chapter 4), the anti-fibrogenic/fibrolytic actions of human recombinant Decorin on the TM were

investigated to evaluation its candidature as a therapeutic agent that attenuates established TM fibrosis, reduces IOP, and protects RGC from death.

## 5.2 Experimental design

### 5.2.1 Decorin attenuates TGF-β1 induced TM fibrosis, IOP elevation and RGC death

Intracameral injections were given bi-weekly using TGF-$\beta1_{0\text{-}17d}$ then $Decorin_{21\text{-}30d}$ (n=3 eyes), regimens and tonometric IOP measurements were taken as described in Section 2.2 (Figure 5.1). Decorin-related data were compared to that obtained in the TGF-$\beta1_{0\text{-}17d}$ then $PBS_{21\text{-}30d}$ (n=6) treated rats as described in Chapter 4. All rats were killed on 30d and immunohistochemical analysis determined levels of laminin deposition around Schlemm's canal. RGC that were βIII-tubulin$^{+}$ were counted over a 250μm sampling line of the ganglion cell layer from parasagittal sections of the retina to assess RGC death. IOP data were analysed for normality, followed by testing for significance ($p<0.05$) using generalised estimated equations. The Students paired *t* test was used for statistical analysis of TM fibrosis and RGC survival.

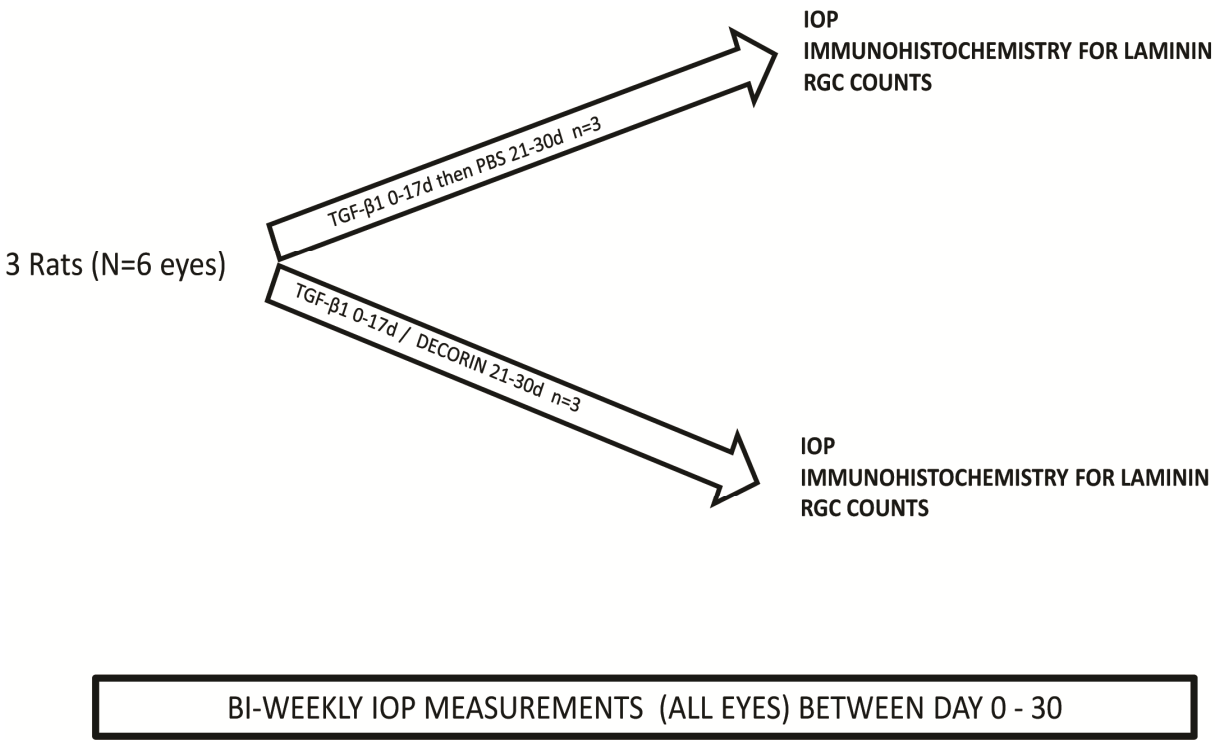


**Figure 5.1 Design of experiment to assess the effects of Decorin on TM fibrosis, IOP and RGC survival in the TGF-β1 model of induced TM fibrosis.**

### 5.2.2 Effects of Decorin on TGF-β2-induced TM fibrosis, raised IOP and RGC death

Bi-weekly unilateral TGF-$\beta2_{0\text{-}17d}$ then $Decorin_{21\text{-}30d}$ (n=12 eyes) intracameral injections were given and tonometric IOP measurements were taken as described in Section 2.2 (Figure 5.2). Decorin-related data were compared to that obtained in the TGF-$\beta2_{0\text{-}30d}$ (n=12) and $PBS_{0\text{-}30d}$ (n=12) treated rats described in Chapter 4 (all *in-vivo* TGF-β2 studies in Chapter 4 were performed simultaneously to these studies). All rats were killed on 30d and electron microscopy and immunohistochemical analysis of laminin and fibronectin determined levels of ECM deposition in the angle and around the TM and Schlemm's Canal. RGC function and survival were assessed using VEP and whole mounted retina retrogradely labelled with FluoroGold, respectively. IOP data were analysed for normality, followed by testing for

significance ($p<0.05$) using generalised estimated equations. The Student's paired *t* test was used for statistical analysis of TM fibrosis and RGC survival. Generalised estimated equations was used for VEP analysis and One-Way ANOVA for TM fibrosis.

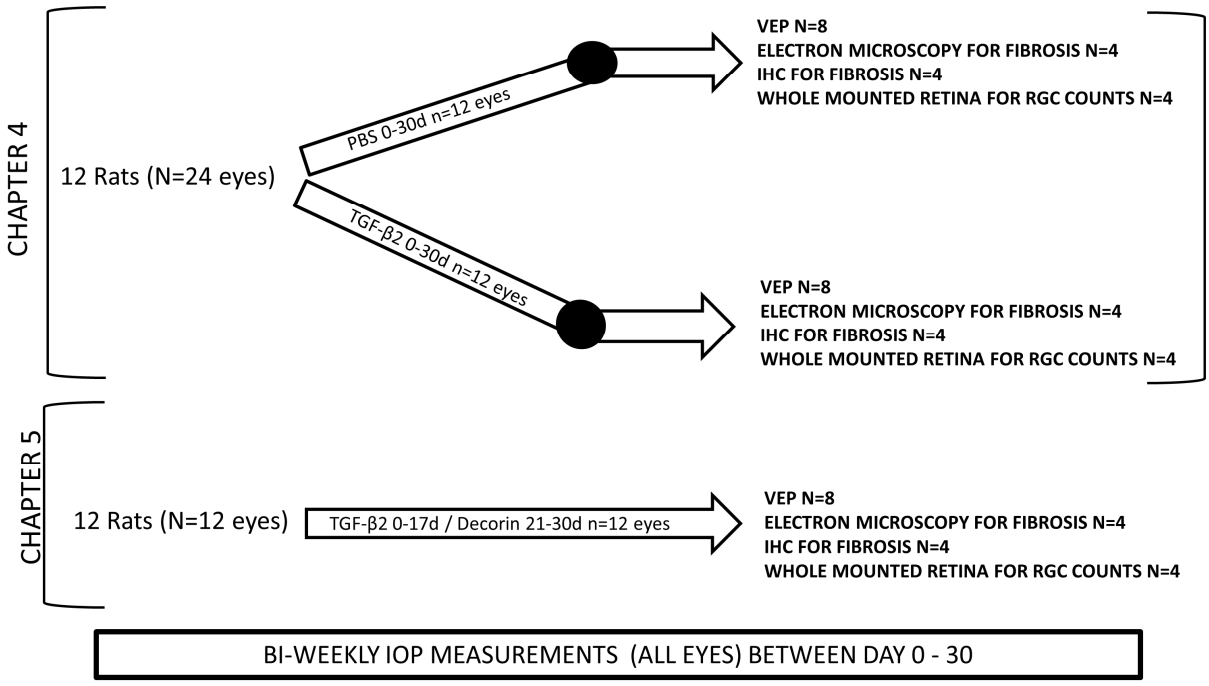


**Figure 5.2 Experimental design to assess the effects of Decorin on TM fibrosis, raised IOP and RGC survival in the TGF-β2 model of induced TM fibrosis.**

## 5.3 Results

### 5.3.1 Decorin attenuated the TGF-β induced elevation in IOP

After establishing a sustained elevation in IOP using repeated intracameral TGF-β1 injections, the administration of Decorin, from 21-30d, led to a significant decrease in IOP compared to eyes injected with PBS ($p<0.001$) (Figure 5.3). At day 21d, the IOP in the TGF-$\beta1_{0\text{-}17d}$ then $PBS_{21\text{-}30d}$ injected group was 14±2mmHg, which was indistinguishable from that in the TGF-$\beta1_{0\text{-}17d}$/$Decorin_{21\text{-}30d}$ group that had an IOP of 15±2mmHg. However, by 30d the IOPs were significantly different, so that between 21d until the end of the experiment at 30d the IOP in the TGF-$\beta1_{0\text{-}17d}$/$Decorin_{21\text{-}30d}$ group reduced from 15±2mmHg to 10±0.6mmHg, whereas in the TGF-$\beta1_{0\text{-}17d}$/$PBS_{21\text{-}30d}$ group the IOP remained elevated to 16±1mmHg.

Decorin similarly attenuated the elevations in IOP induced by intracameral injections of TGF-β2 (Figure 5.4). After 21d, TGF-β2 injections had led to a sustained elevation in IOP to 14±0.2mmHg. When Decorin was administered between 21d to 30d (TGF-$\beta2_{0\text{-}17d}$/$Decorin_{21\text{-}30d}$ group), the IOP decreased back to 10±0.3mmHg. This was significantly lower than the IOP of 14±0.3mmHg measured at 30d in the TGF-β2 group ($p<0.001$).

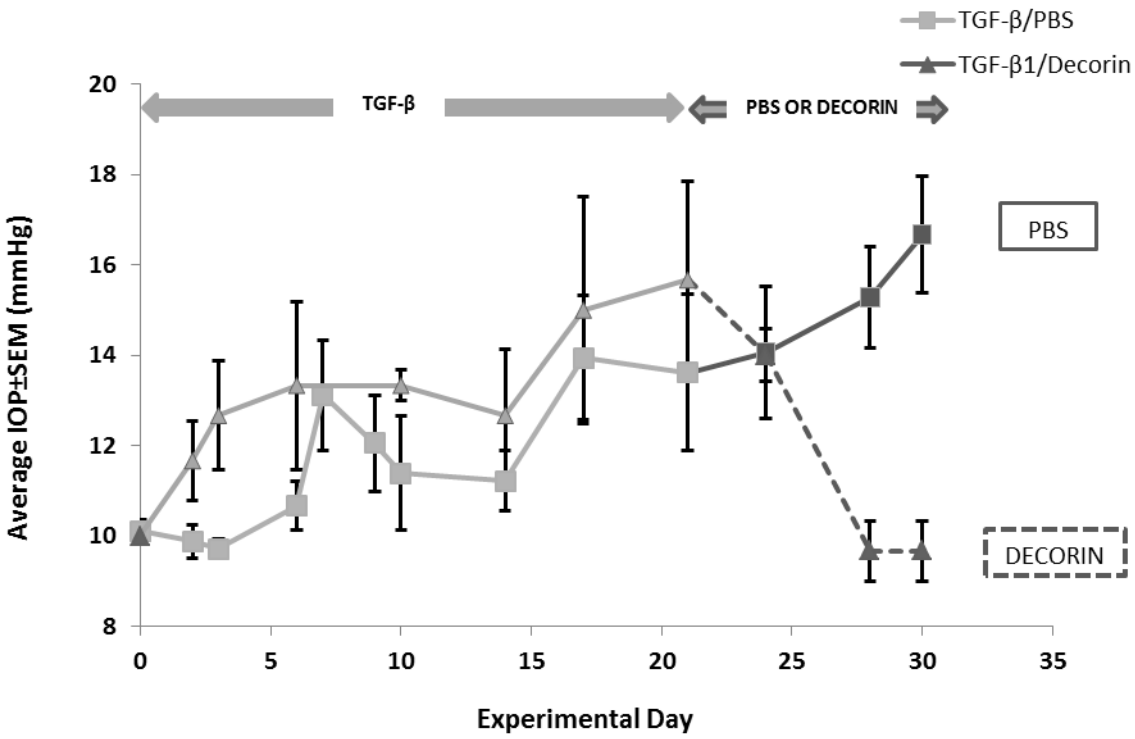


**Figure 5.3 Mean IOP±SEM measurements after intracameral injections of TGF-β1±Decorin.**

The TGF-β1-induced sustained elevation in IOP was attenuated by intracameral injections of Decorin (TGF-$\beta1_{0\text{-}17d}$/$Decorin_{21\text{-}30d}$), to levels that were significantly lower to those in the control group (TGF-$\beta1_{0\text{-}17d}$/$PBS_{21\text{-}30d}$) ($p<0.001$).

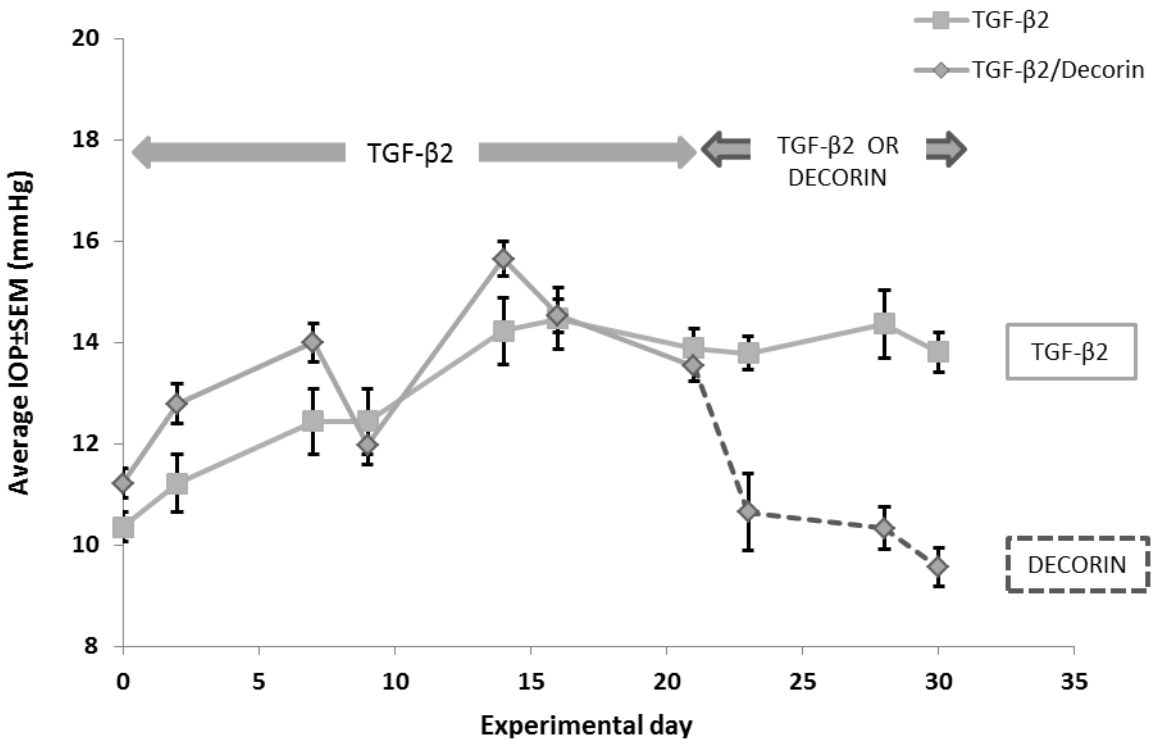


**Figure 5.4 Mean IOP±SEM measurements after intracameral injections of TGF-β2±Decorin.**

The TGF-β2-induced sustained elevation in IOP was attenuated by intracameral injections of Decorin (TGF-$\beta2_{0\text{-}17d}$/$Decorin_{21\text{-}30d}$), to levels that were significantly lower to those in the TGF-β2 group ($p<0.001$).

### 5.3.2 Decorin reversed established TM fibrosis

Intracameral injections of Decorin significantly ($p<0.05$) reduced fibrosis (to similar levels observed in the $PBS_{0\text{-}30d}$ eyes), evidenced by more intense staining for laminin and fibronectin deposition around Schlemm's Canal and throughout the TM after TGF-$\beta1_{0\text{-}17d}$/$Decorin_{21\text{-}30d}$ (Figure 5.5) or TGF-$\beta2_{0\text{-}17d}$/$Decorin_{21\text{-}30d}$ (Figure 5.6) compared to TGF-$\beta1_{0\text{-}17d}$/$PBS_{21\text{-}30d}$ and TGF-β2, respectively. Laminin deposition after TGF-$\beta1_{0\text{-}17d}$/$PBS_{21\text{-}30d}$ injections was most prominent throughout the inner wall of Schlemm's Canal and the JCT region of the TM. Collections of fibronectin deposits throughout the TM were observed after TGF-$\beta1_{0\text{-}17d}$/$PBS_{21\text{-}30d}$ and TGF-β2 injections, however, TGF-$\beta1_{0\text{-}17d}$/$Decorin_{21\text{-}30d}$ and TGF-$\beta2_{0\text{-}17d}$/$Decorin_{21\text{-}30d}$ were able to significantly ($p<0.001$) reduce these deposits, demonstrating lower levels of fibronectin staining to that observed in the TGF-$\beta1_{0\text{-}17d}$/$PBS_{21\text{-}30d}$ and the TGF-β2 injected eyes.

TEM of parasagittal sections of the eyes revealed decreased ECM deposition in the angle of the TGF-$\beta2_{0\text{-}17d}$/$Decorin_{21\text{-}30d}$ injected eyes compared to that in the TGF-β2 injected eyes (Figure 5.7). In the JCT region of the TGF-$\beta2_{0\text{-}17d}$/$Decorin_{21\text{-}30d}$ eyes, ECM was absent from the intra-trabecular spaces and the TM was more organised than observed in the TGF-β2 injected eyes. The decrease in laminin and fibronectin revealed in the angle by immunohistochemistry, together with the appearance of less ECM deposition shown with electron microscopy, suggest that injections of Decorin reversed the established fibrosis induced by intracameral TGF-β2 injections.

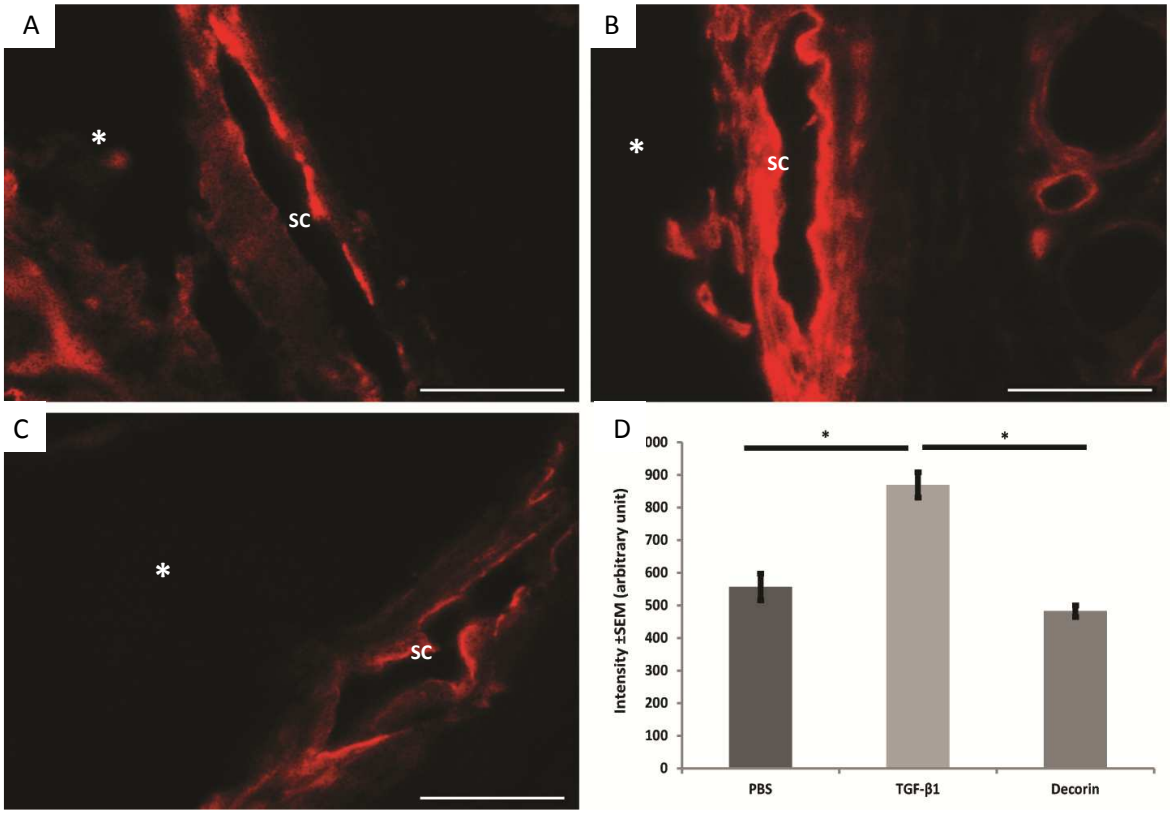


**Figure 5.5 Distribution of laminin around Schlemm's Canal.** Photomicrographs of parasagittal eye sections illustrating laminin staining (red) in the iridiocorneal angle (*) and Schlemm's Canal. Laminin deposition was found around Schlemm's Canal in **(A)** $PBS_{0\text{-}30d}$, **(B)** TGF-$\beta1_{0\text{-}17d}$/$PBS_{21\text{-}30d}$ and **(C)** TGF-$\beta1_{0\text{-}17d}$/$Decorin_{21\text{-}30d}$ injected eyes. Bi-weekly injections of Decorin between 21d and 30d (n=3) led to a significant ($p<0.05$) reduction in laminin deposition within the inner wall of Schlemm's Canal, compared to TGF-$\beta1_{0\text{-}17d}$/$PBS_{21\text{-}30d}$ injected eyes. **(D)** Decorin reversed laminin deposition back to levels seen in the $PBS_{0\text{-}30d}$ group. Scale bar – 50µm; SC – Schlemm's Canal.

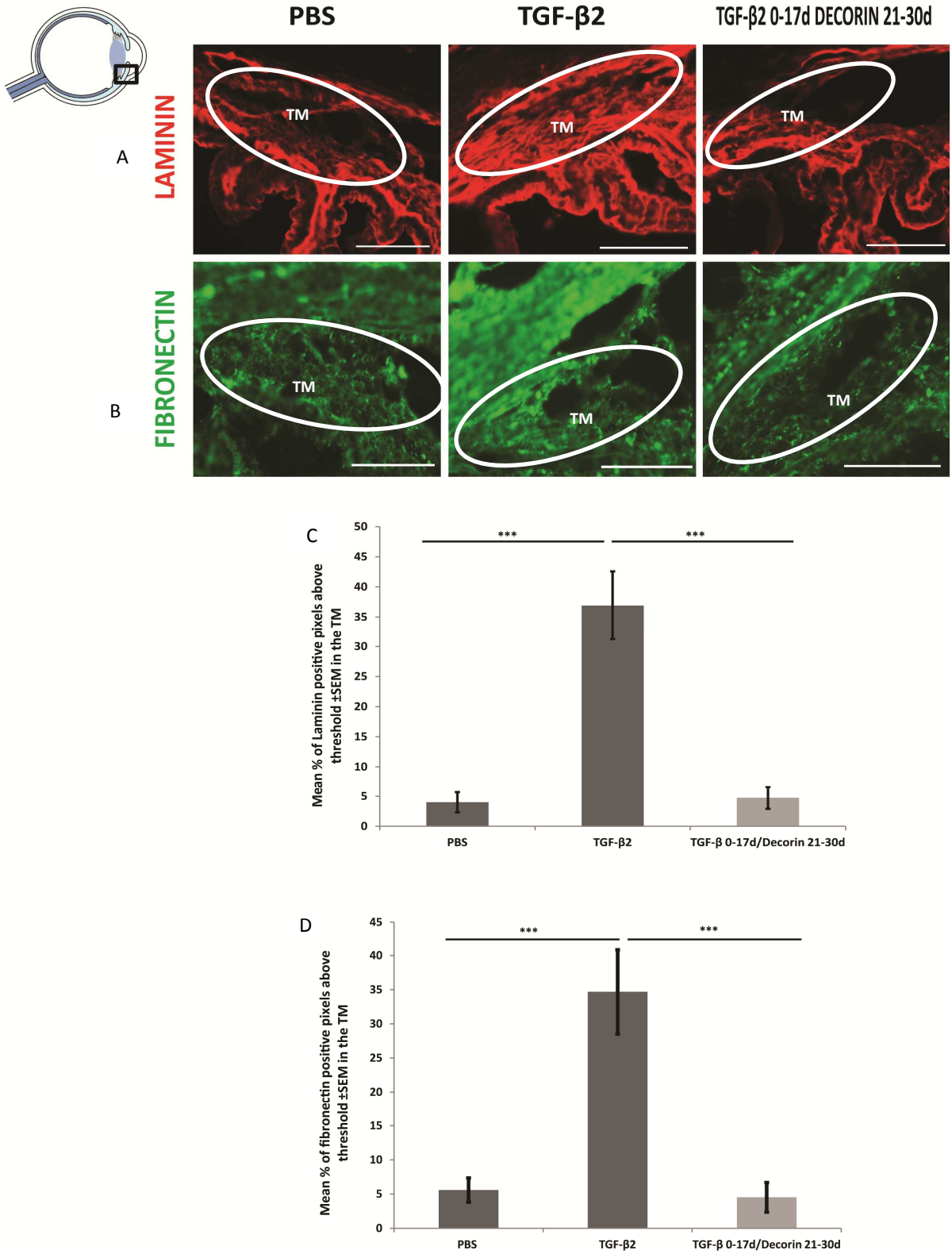


*(Figure 5.6 legend on next page)*

**Figure 5.6 Fibrosis in the TM.** Parasagittal eye sections illustrating areas of fibrosis revealed by immunostaining of **(A)** laminin (red) and **(B)** fibronectin (green). The area circled in white defines the TM. Quantification of the immunostaining for **(C)** laminin and **(D)** fibronectin about the TM shows that both ECM molecules were increased after TGF-β2 injections and this ECM deposition was reversed in the TGF-$\beta2_{0\text{-}17d}$/$Decorin_{21\text{-}30d}$ injected group to similar levels observed in the PBS injected eyes ($p<0.001$). Scale bar – 100µm; TM – trabecular meshwork.

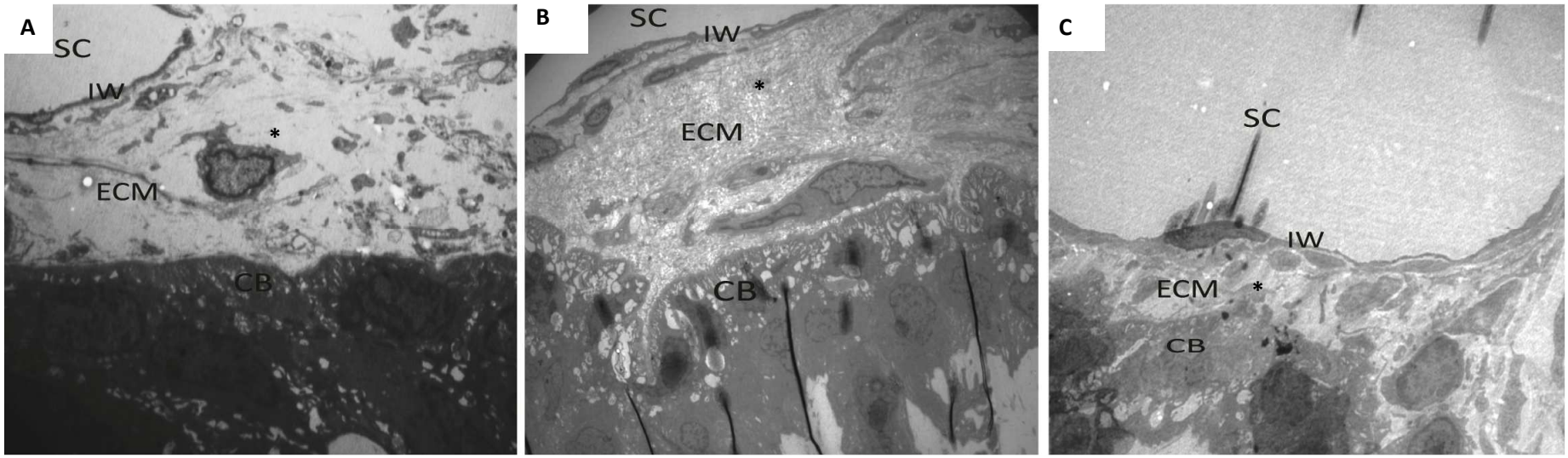




**Figure 5.7 TEM of the trabecular meshwork at 30d (X2500). (A)** In the PBS group the TM showed expanded 'beam-like' ECM structures running in parallel and interconnecting with each other. In between the trabecular cells, the intra-trabecular spaces had low levels of ECM deposition (*). There was varying thickness of a mono-layer of endothelium on the inner wall (IW) of Schlemm's Canal (SC). **(B)** In the TM of the TGF-β2 injected eyes the trabecular spaces were disorganised, there were fewer trabecular cells and the ECM was markedly increased in the JCT region and also around outer wall of SC. In addition, the endothelium of the inner wall of SC appeared thicker in the TGF-β2 compared to the PBS injected eyes. **(C)** In the TGF-$\beta2_{0\text{-}17d}$/$Decorin_{21\text{-}30d}$ group, Decorin had attenuated the level of ECM deposition in the TM compared to the TGF-β2 injected eyes, to levels seen in the PBS group. SC – Schlemm's Canal, IW – Inner Wall, ECM – Extracellular Matrix, CB – Ciliary Body.

### 5.3.3 Decorin altered protease activity in the TM

Immunostaining was undertaken to observe the localisation of injected Decorin in the TM at 30d (Figure 5.8A). After TGF-$\beta2_{0\text{-}17d}$/$Decorin_{21\text{-}30d}$ injections significant levels of immunoreactive human Decorin were apparent in the tissues about the TM. Figure 5.8E shows quantitation of the immunostaining for human Decorin and confirms the higher levels of human Decorin in the TGF-$\beta2_{0\text{-}17d}$/$Decorin_{21\text{-}30d}$ treated eyes when compared to the PBS and TGF-β2 injected eyes ($p<0.05$).

MMP2 staining was increased after TGF-$\beta2_{0\text{-}17d}$/$Decorin_{21\text{-}30d}$ injections to similar levels seen in the PBS injected eyes. There was little immunoreactive active MMP2 apparent after TGF-β2 injections. Similarly, the TGF-β2 injected eyes had lower levels of immunoreactive active MMP9 than did TGF-$\beta2_{0\text{-}17d}$/$Decorin_{21\text{-}30d}$ and PBS injected eyes. Conversely, TIMP2 immunoreactivity was highest in the TGF-β2 injected eyes and was lowest in the Decorin treated eyes, compared to TGF-β2 and PBS treated eyes. Quantitation of the immunoreactivity confirmed that TGF-$\beta2_{0\text{-}17d}$/$Decorin_{21\text{-}30d}$ treatment led to significant ($p<0.05$) increases in active MMP2 and MMP9, and a significant ($p<0.001$) decrease in active TIMP2 (Figure 5.8E) about the TM. These results indicate that TGF-β2 down-regulated both MMP2 and MMP9 bioactivity in the TM and that Decorin antagonised this effect, suggesting a mechanism for Decorin's fibrolytic actions to reverse fibrosis in the TM.

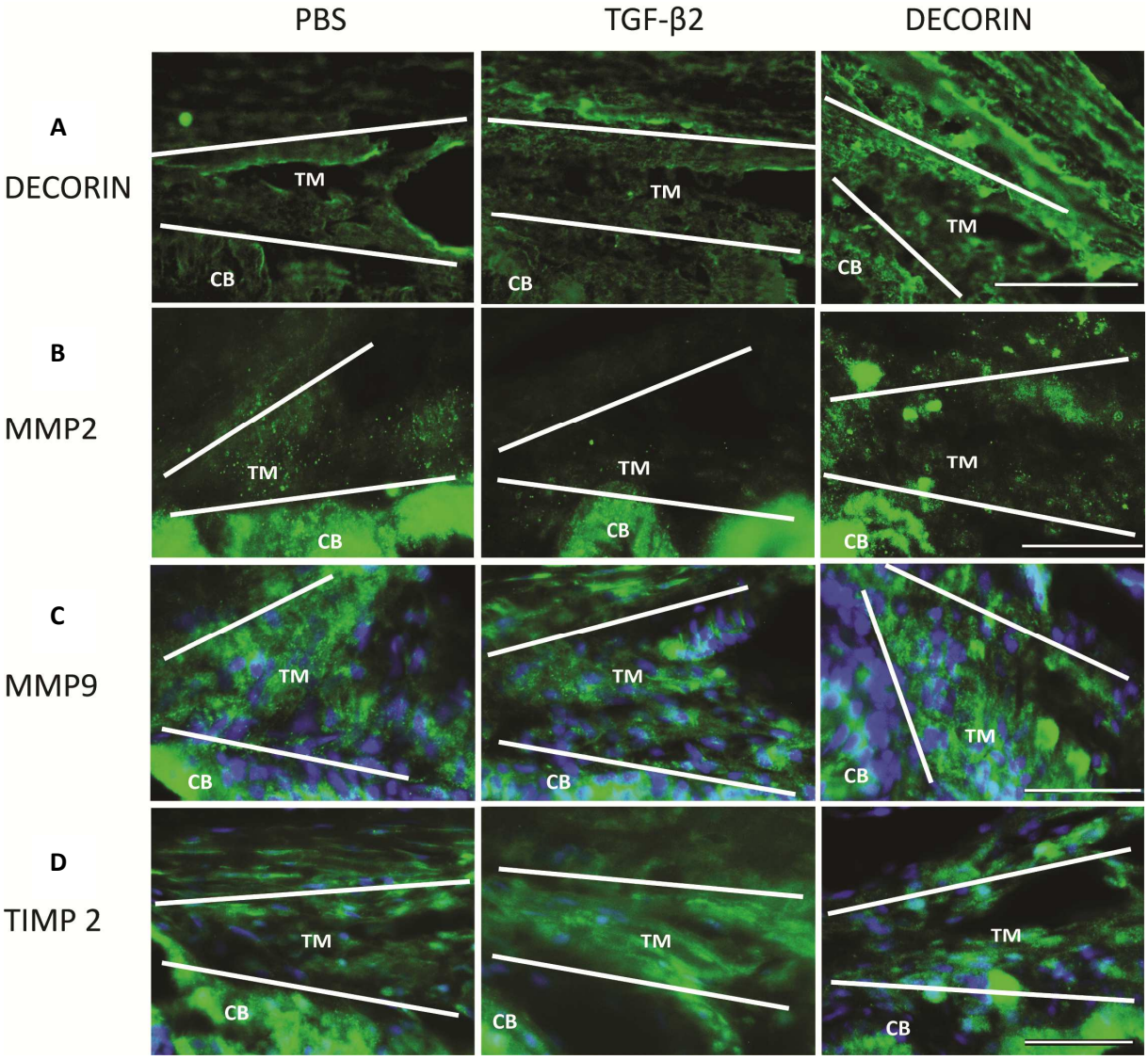


*(Figure 5.8 legend on next page)*

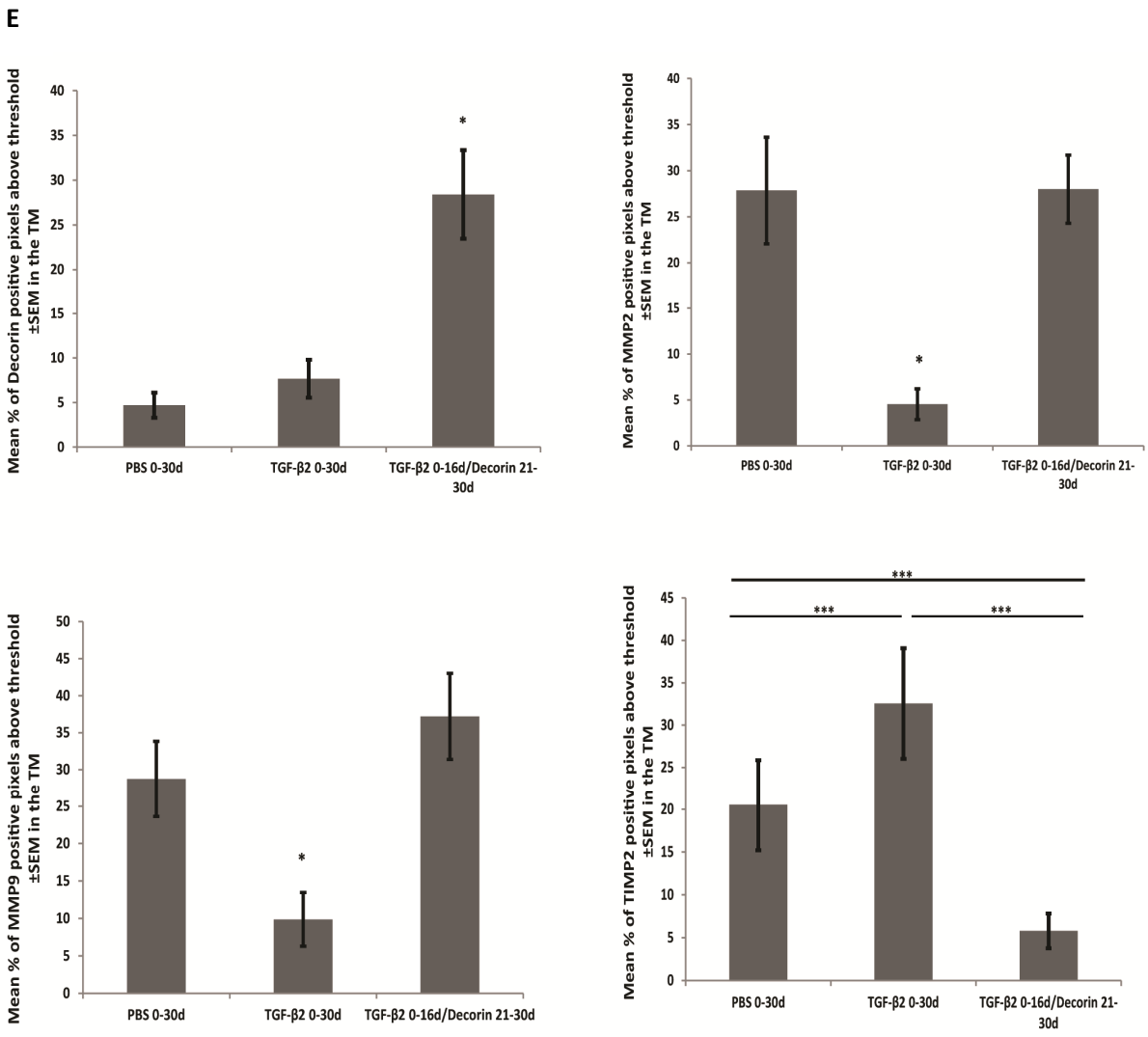


**Figure 5.8 Human Decorin and protease activity in the TM at 30d.** Representative images of immunoreactive (green) **(A)** Human Decorin**, (B)** MMP2, **(C)** MMP9 and **(D)** TIMP2 in the PBS, TGF-β2 and TGF-$\beta2_{0\text{-}17d}$/$Decorin_{21\text{-}30d}$ injected eyes with (E) quantification of pixel intensities above a set threshold (* $p<0.05$; *** $p<0.001$). DAPI (blue) was used to mark cell nuclei. Scale bar – 50µm; TM – trabecular meshwork; CB ciliary body. White lines demarcate the TM in A-D.

### 5.3.4 Decorin treatment protected RGC from death but did not from functional compromise

Between-subject analysis showed no functional recovery of the retina or visual pathway after TGF-$\beta2_{0\text{-}17d}$/$Decorin_{21\text{-}30d}$ treatment using Flash VEP compared to TGF-β2 treatment at P1/N2 (Figure 5.9). Overall, there were no significant differences between the treatment groups across all three flash intensities at the P1/N2 amplitude or latency (p=0.571). Eyes injected with TGF-$\beta2_{0\text{-}17d}$/$Decorin_{21\text{-}30d}$ had a significantly higher number of surviving RGC at 30d compared to TGF-β2 injections, with 1794±107 RGC/$mm^2$ and 1316±146 RGC/$mm^2$ respectively (p<0.001). Decorin treated eyes had similar RGC counts to the PBS injected eyes 1888±100 RGC/$mm^2$ (Figure 5.10). These data suggested that Decorin was able to prevent further loss of RGC but was not able to restore or prevent functional deficits.

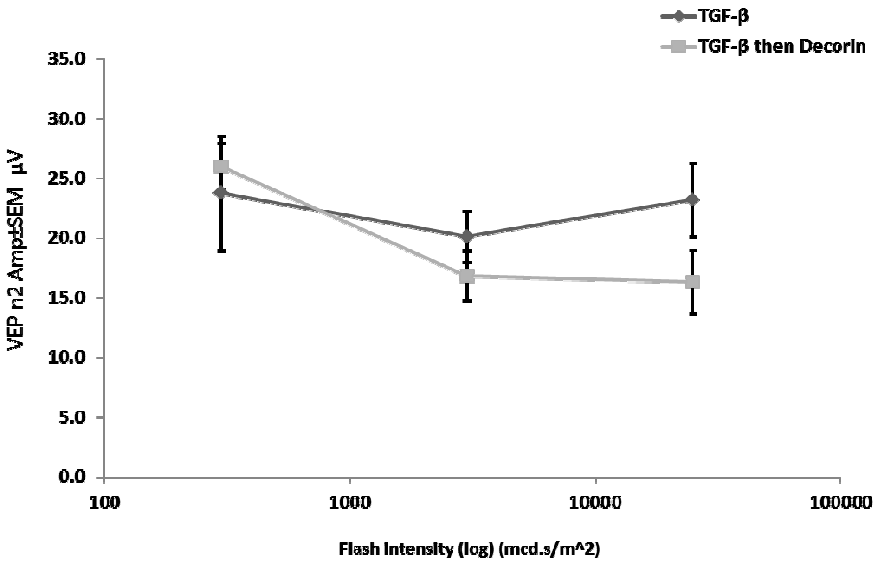


**Figure 5.9 Flash VEP summary of P1/N2 amplitude at 30d.** Decorin from day 21 to 30 did not have any effects on visual pathway function compared to TGF-β2 injected eyes (n=8; p=0.571).

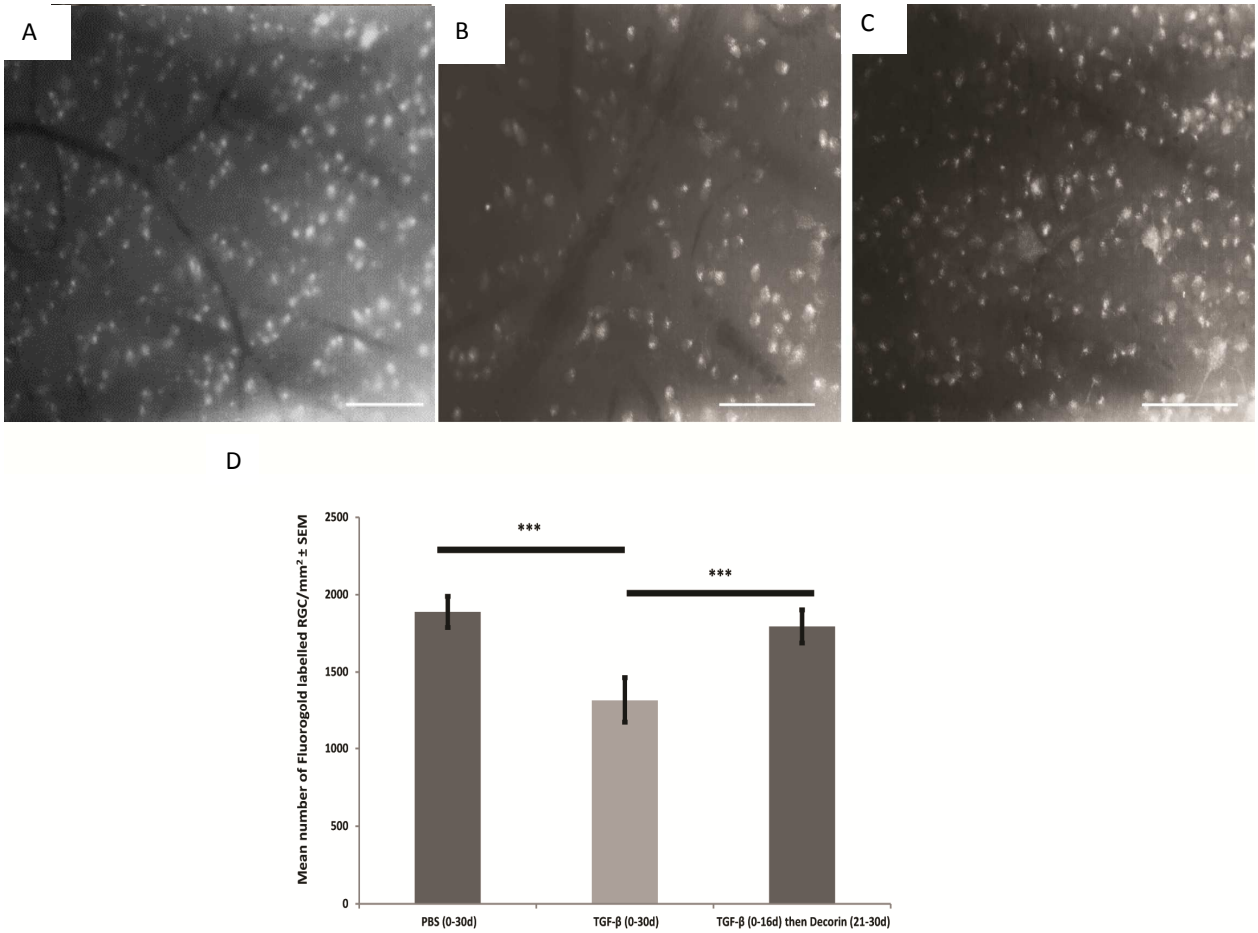


**Figure 5.10 Representative photomicrographs and quantitation of FG-labelled RGC for assessment of RGC survival.** **(A)** FG-labelled RGC at experimental day 30 after PBS injections; **(B)** FG-labelled RGC at experimental day 30 after TGF-β2injections; **(C)** FG-labelled RGC at experimental day 30 after TGF-$\beta2_{0\text{-}17d}$/$Decorin_{21\text{-}30d}$ injections. **(D)** Quantification of RGC survival in all three groups. $Decorin_{21\text{-}30d}$ treatment significantly reduced the amount of RGC death compared to TGF-β2 injections (n=4 eyes/group **P<0.001) and yielded similar counts to those in the PBS injected eyes. Scale bar = 100µm.

## 5.4 Discussion

This study showed that intracameral Decorin treatment led to MMP-induced dissolution of established TM fibrosis with associated lowering of raised IOP and indirect protection from progressive RGC death.

### 5.4.1 Decorin reduced elevations in IOP through attenuating TM fibrosis

In this study the sustained elevation of IOP, induced by TGF-β, was attenuated by Decorin. Sequential staging of the injections of TGF-β and Decorin excluded the possibility of direct interference by Decorin in the binding of exogenously delivered TGF-β to the TGF-β receptor, implying that the IOP reduction observed resulted from lysis of the established TM fibrosis, probably by activation of locally produced fibrolytic MMP. In this study, Decorin had significantly reduced IOP within 72 hours suggesting a fibrolytic response had occurred within this timeframe and therefore reduced the IOP compared to PBS controls, which remained significantly higher. Similar acute fibrolytic actions of Decorin have been previously reported by Botfield et al. (2014) who demonstrated a reduction in fibrosis and inflammation within the brain after 3 days of Decorin treatment. Decorin has also been reported to lower IOP by 3 days in a rabbit model of glaucoma filtration surgery (Grisanti et al, 2005), supporting our attribution of fibrolytic properties to Decorin in the TM. The observation that Decorin promoted the dissolution of established ECM protein deposits in and around the TM by activating the MMP axis is supported by observations in multiple rodent CNS injury models that demonstrate Decorin's anti-fibrogenic and fibrolytic actions in

both acute and chronic scarring situations (Logan, 1999; Davies, 2004; Ahmed et al., 2013; Botfield et al., 2013).

The fibrolytic actions of Decorin were evidenced by monitoring the levels of laminin and fibronectin in the TM. Data presented in Chapter 4 showed that TGF-β induced laminin and fibronectin deposition in the angle and that the levels of these ECM molecules were attenuated by Decorin after TGF-β injections were stopped and any exogenous TGF-β would have cleared from the anterior chamber by this time and only endogenously released TGF-β would be present. Decorin's anti-fibrotic actions, through direct inhibition of endogenous TGF-β, have been documented in the rat brain (Logan et al., 1999; Botfield et al., 2013) and other fibrotic diseases including cirrhosis (Baghy et al., 2012), lung fibrosis (Kolb et al., 2001), cardiac fibrosis (Yan et al., 2009) and renal fibrosis (Isaka et al., 1996). It is unclear if Decorin's actions in the eye are the result of inhibiting endogenous TGF-β or achieved solely through TGF-β independent mechanisms. This would need to be tested in future studies, for example, by administering Decorin in combination with TGF-β antibodies (to neutralize endogenous TGF-β) to measure the TGF-β independent effects of Decorin on TM fibrosis.

Notwithstanding, Decorin increased levels of MMP2 and MM9 and decreased TIMP2 in the TM compared to eyes that were treated with TGF-β alone. This data supports findings from Ahmed et al., (2013) who demonstrated the Decorin treatment after spinal cord injury increased MMP2 and MMP9. The rebalancing of the MMP:TIMP ratio to favour protease activity by Decorin shown in this study mirrors the pathological process shown from patients with POAG where MMP, released from TM cells, have a role in controlling IOP

through regulation of ECM degradation in the TM (Schlötzer-Schrehardt et al., 2003). Eye perfusion studies have shown that the stretching of TM cells that occurs with increased IOP upregulates levels of MMP2 and downregulates levels of TIMP2 favouring ECM degradation in an attempt to reduce outflow resistance and lowering IOP (Bradley et al., 2003). It is becoming more widely accepted that dysfunctional ECM remodelling leads to TM fibrosis in open angle glaucoma (Maatta et al., 2002; Yang et al., 2003; Rönkkö et al., 2007). This study has shown that Decorin was able to reverse established TM fibrosis and to restore proteolytic activity in the TM, probably in part through by modulating MMP bioactivity, making it ideal drug for further investigation as a therapeutic agent in POAG.

### 5.4.2 Decorin indirectly protected against progressive RGC Death

The increased MMP activity, the reduction in TM ECM immunostaining and the lowering of IOP seen after Decorin treatment of established TM fibrosis was correlated with increased RGC survival compared to controls. However, the RGC survival was not correlated with evidence of functional preservation after Decorin treatment as measured by VEP.

*In vitro* studies from our laboratory have demonstrated that Decorin is not directly neuroprotective to RGC (Peter Morgan-Warren, unpublished work), providing evidence that the Decorin-related neuroprotection seen in this study was attributable to its IOP lowering effects from MMP-induced dissolution of TM fibrosis. Although there is no precise explanation of why high IOP causes RGC death, a multitude of factors may contribute, including compromised axonal transport of neurotrophic factors, activation of apoptosis and

mitochondrial dysfunction of RGC from both biomechanical and ischemic insults caused by compression of the optic nerve head (reviewed in Almasieh et al., 2012).

Given the high level of RGC survival after treatment with Decorin, it was surprising that there was no functional preservation measured by VEP. This result could have been attributed to the between, rather than within, subjects experimental design in comparing TGF-β with Decorin, thereby confounding the VEP data. These results could have been further confounded by the incomplete occlusion of the contralateral eye during recording. In future studies, a within subjects design for VEP studies would be more suitable as variability between animals will be minimised.

### 5.4.3 Conclusion

Intracameral Decorin treatment effectively reversed established TM fibrosis and lowered IOP, and thereby indirectly protected RGC from progressive IOP-related death. Thus, intracameral Decorin has the potential to be developed into an effective therapy for patients with POAG.

# Chapter 6

# Transcorneal delivery of Decorin

## 6.1 Rationale

The previous chapter showed that intracameral injections of Decorin that increase Decorin titres within the AqH were efficacious in attenuating chronic TM fibrosis. Although bi-weekly intracameral injections proved to be an effective means of achieving proof of principle data in an experimental model of raised IOP that supported Decorin's therapeutic potential to treat POAG, this delivery method would not be an ideal treatment regime for patients in clinic. Therefore, a more suitable method of drug delivery would be better suited in order to advance these studies towards pre-clinical testing.

Most patients are given drugs in the form of eye drops to manage their IOP. Therefore, developing a similar method to deliver Decorin would prove valuable. Decorin is a 70kDa (Brandan et al., 1992) negatively charged glycoprotein, and due to its large size and charge is likely to be unable to penetrate and traverse epithelial barriers unaided. We hypothesised that formulation of Decorin with a nanosome (NS) based carrier molecule would enable Decorin to successfully cross the cornea. In collaboration with Dr. de Cogan (University of Birmingham), an arginine rich polypeptide (NS) that can be electrostatically or covalently bound with Decorin was developed to assess if NS-Decorin-complexes could penetrate the cornea and deliver pharmacologically relevant titres of the drug into the AqH of rodents.

## 6.2 Experimental design

Adult rats (n=4) had 3 drops of 60µl of the 2 NS-Decorin formulations (± electrostatic or covalently bound Decorin) given to each eye. All left eyes were given Nanosome-PBS drops and all right eyes given NS-Decorin eye drops. Four further control groups were Intact eyes (n=4), eyes given PBS eye drops (n=4), eyes given NS in PBS eye drops (n=4) and eyes given Decorin in PBS eye drops (n=4). Two minutes after the eye drops were administered, rats were killed using increasing concentrations of $CO_2$ over 8 minutes to enable a 10 min timed experiment. Thereafter, 10µl of AqH was removed from the anterior segment of each of the 4 eyes/group that was pooled together to give a final volume of 40µl AqH. The AqH samples were analysed to measure the Decorin concentrations achieved 10 min after application using the commercially available human Decorin ELISA kit (R&D Systems, Cat: DY143). The ELISA protocol was performed as directed in the kit instructions.

## 6.3 Results

No human Decorin was detected in the pooled AqH samples following NS+PBS eye drops. Following application of the NS-Decorin covalent eye drops and the NS-Decorin electrostatic eye drops, 17.6ng/ml and 16.9ng/ml of human Decorin was detected in the AqH, respectively. This data demonstrates that Decorin successfully traversed the cornea into the AqH and that the covalent and electrostatic eye drops were equally effective.

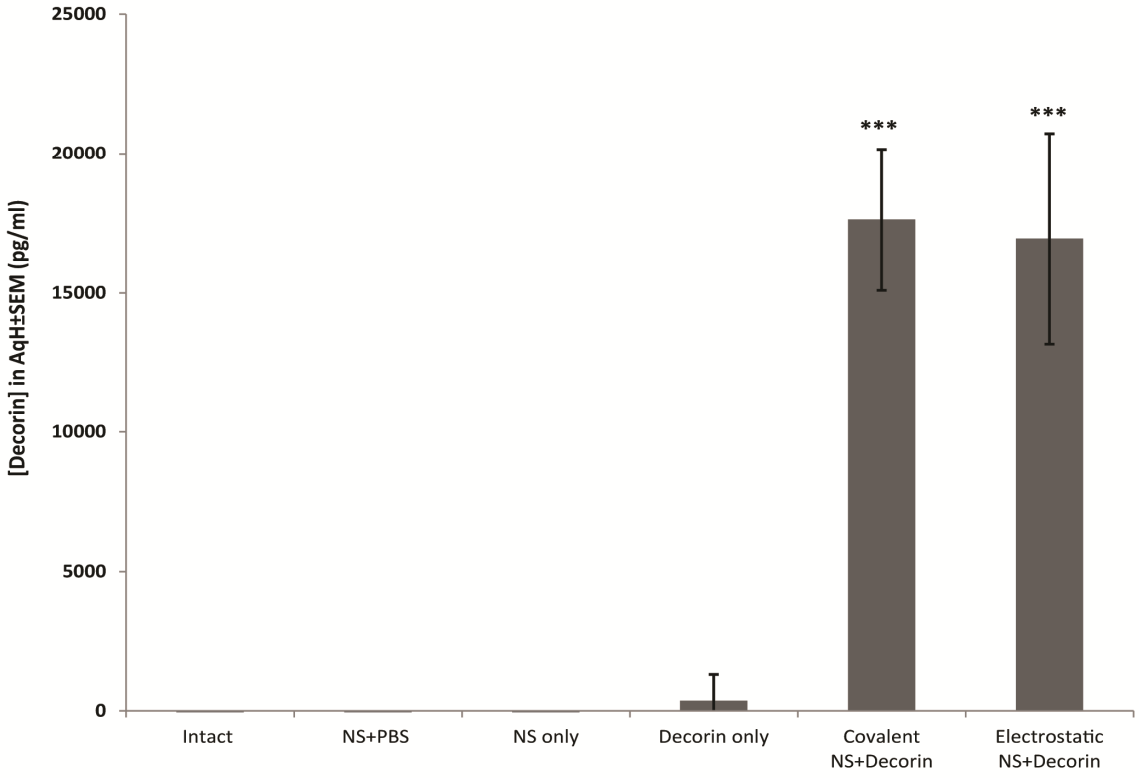


**Figure 6.1 Levels of human Decorin±SEM in AqH after NS eye drops.** Human Decorin was detected by ELISA in the AqH 10 minutes after covalent and electrostatic NS-Decorin eye drops were applied to the cornea.

Movement into the anterior chamber of the NS-Decorin eye drop was captured using OCT anterior segment imaging, whereby fluorescently labelled NS-Decorin complexes were as bright dots (Figure 6.2). Immediately after the eye drops were applied they formed a droplet that covered the cornea (Figure 6.2 A), then at 6 minutes the labelled NS-Decorin complexes were seen to have penetrated through the cornea into the anterior chamber (Figure 6.2 B). These observations suggest that the NS-Decorin complexes had aggregated permitting them to be visualised (this aggregation of the complexes was later confirmed by Dr De Cogan using dynamic light scattering).

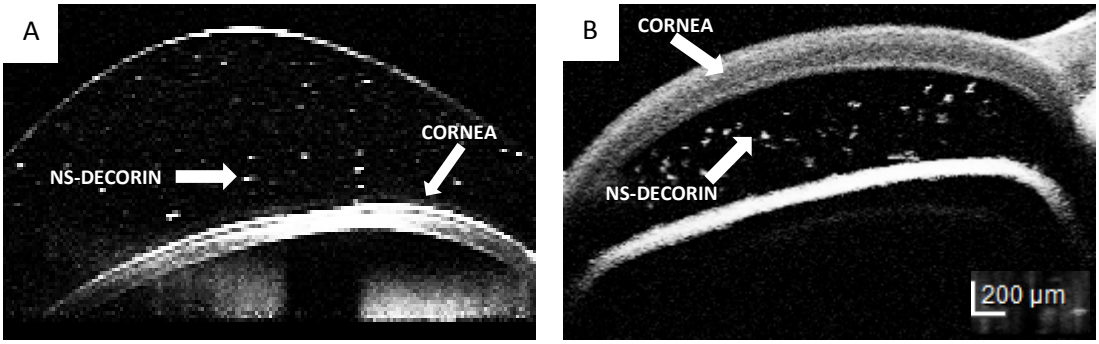


**Figure 6.2 OCT imaging of NS-Decorin complexes crossing into the anterior chamber using Fluorescein angiography (blue light, 465-490nm). (A)** Eye drops containing fluorescently labelled NS-Decorin complexes were placed onto the cornea. **(B)** After 6 minutes the fluorescently labelled NS-Decorin complexes had traversed the cornea into the anterior chamber.

## 6.4 Discussion

This study showed that electrostatically and covalently bound NS-Decorin complexes when given in an eye drop formulation were able to traverse the cornea into the anterior chamber, and be detected in the AqH using OCT. As both NS-Decorin formulations were equally able to penetrate the cornea, the ionic formulation was chosen as more favourable as the peptide synthesis required less harmful chemicals that would be less likely to cause any ocular surface irritation.

The cornea presents a significant barrier to drug permeability, especially for large molecules like Decorin, as its multiple layers include a lipophilic endothelium, a hydrophilic stromal layer, an ECM layer and an epithelial layer. In addition, there are multiple phases where the delivered drug will be diluted before reaching its intraocular target (the TM), including the pre-corneal tear film and the AqH itself. The previous studies (Chapter 5) showed efficacy of Decorin at a dose 3µl of 5mg/ml directly injected into the anterior chamber of 15µl which is a much higher dose that the 2ng/ml detected in the AqH after the eye drop delivery. Hence, the therapeutic efficacy of the NS-Decorin eye drop formulation will have to be tested in further studies as it is still unclear if the final concentration achieved in the AqH will be sufficient to reverse TM fibrosis in experimental glaucoma.

The use of arginine polypeptides have been previously reported as useful carrier moieties to deliver drugs across biological barriers due to their cell penetrating properties, with

particular emphasis in previous studies on delivering insulin across gut epithelium (Morishita et al., 2007). Of direct relevance, a recent study by Liu et al., (2014) demonstrated the use of polyarginines for intraocular drug delivery and the study reported herein was able to provide confirmatory evidence that polyarginine NS are suitable carriers for drug delivery into the eye.

In summary, this data has given proof of principle that Decorin is able to traverse the cornea into the anterior chamber when joined with a known cell penetrating compound consisting of polyarginines. With further development, this may provide a basis for delivering Decorin at therapeutic titres into the anterior chamber as a treatment for experimental glaucoma. It also provides a translational arm that holds potential for advancing these studies with Decorin towards the clinic.

# Chapter 7

# General Discussion

## 7.1 General conclusions

The first aim of these studies was to develop a rodent model to mirror certain pathological aspects of POAG, namely fibrosis of the TM, elevations in IOP and RGC death. The second aim was to assess the potential value of intracamerally injected Decorin as a therapeutic agent that attenuated chronic TM fibrosis, thereby reducing IOP and limiting progressive RGC death. Finally, the third aim was to pilot an eye drop method of Decorin delivery to the anterior chamber, which could be easily adopted in a clinical setting.

Two *in vivo* models were developed; the kaolin and the TGF-β models. Intracamerally injected kaolin did not induce fibrosis in the TM in these experiments, nor did it raise IOP (Chapter 3). Although transient peaks in IOP were observed acutely, they were not sustained, even though kaolin remained present within the angle in some rats. In addition, there was no evidence of induced TM fibrosis, although the addition of LPS did induce an inflammatory response in the anterior chamber with a noticeable increase in the numbers of ED1+ macrophages present. Therefore, the kaolin model was deemed unsuitable to model chronic TM fibrosis and IOP elevation although, when given in combination with LPS, it might be a useful model for anterior segment inflammation.

TGF-β was predicted to be a more appropriate agent to induce chronic TM fibrosis since it is widely accepted that active TGF-β levels are higher in the AqH of patients that develop POAG. Initially a dosing regimen was piloted along with investigation of IOP variability using local or general anaesthetic for the surgical procedures. Other research groups differ in their

preference for anaesthesia of rodents in their experimental models. The most notable reason for using local anaesthetic is to avoid the associated lowering of IOP, however, the results of these studies and others (Robertson et al., 2013) deemed the use of general anaesthetic in rodents as providing a more reliable measure of IOP. General anaesthetics minimise having to train rodents and avoids any compromising distress of the animals. Any confounding lowering of IOP between treatments was avoided experimentally, as both treatment and controls injections were administered under general anaesthesia would receive the general anaesthesia, thus reducing any bias in results due to variable anaesthesia. The other reason to choose general anaesthetic over local, was the unfeasibility of performing intraocular injections on awake rats. In addition, IOP were generally taken just before rats were given intracameral injections, which was required by our home office license to be carried out under general anaesthetic. Thus, using a general anaesthetic helped to streamline the surgical procedures, thus making it less stressful for the animals and providing a more controlled experiment.

The initial TGF-β studies were conducted using TGF-β1. However, two weeks of bi-weekly intracameral injections of either active TGF-β1 or TGF-β2, achieved similar sustained elevations in IOP of 30-40%, associated with significant TM fibrosis and 30% RGC death by 30 days. It is generally accepted that TGF-β2 levels are higher in patients with POAG (Inatani et al., 2001), whereas higher levels of TGF-β1 are mostly associated with the development of PXG. Experimental models using Tenon's capsule fibroblasts from patients to assess fibrogenic effects of both TGF-β1 and 2 also noted non-significant differences between the

levels of TGF-β isoforms in terms of the type and morphology of ECM deposition and fibrosis with higher TGF-β2 levels being associated with enhanced fibrosis (Kottler et al., 2005).

Accordingly, although the differences between TGF-β1 and TGF-β2 were not thoroughly investigated in this thesis (EM nor VEP were assessed after TGF-β1 injections, but were after TGF-β2), it was decided after the initial TGF-β1 studies that TGF-β2 would be the more appropriate isoform to use for subsequent studies.

The studies reported here highlighted several technical issues that were addressed by modified experimental design. For example, levels of ECM deposition were measured using changes in pixel intensities; this is a subjective semi-quantitative method. Using western blot or ELISA to objectively measure ECM deposition from protein levels would be preferable in future studies. Another issue was related to the method of counting RGC. There was a difference between the RGC counts obtained from β-III tubulin stained parasagittal sections and those from whole mounted retinae after retrograde FluoroGold labelling so that, after raised IOP, RGC death was recorded at 8% and 30% respectively. The retinal whole mount method was used in subsequent studies as it was felt to be more representative, with FluoroGold-labelled RGC counts being sampled across the whole retina. FluoroGold is a more specific marker of RGC than β-III tubulin, which relies heavily on the experimenter to identify immunopositive RGC within retinal sections based on location and morphology. Another technical issue of note was the observation that in the TGF-β2 model of raised IOP, it was possible to demonstrate a functional deficit on VEP with lower amplitudes, which provided evidence of the visual pathway being disrupted. This feature was reminiscent of

observations in patients with POAG although, unlike in POAG patients, there were no alterations in latency (Parisi, 2001).

The TGF-β2 model was thus employed to investigate the potential use of recombinant human Decorin to target and reduce established TM fibrosis (Chapter 5). Decorin had already shown much potential to reverse fibrosis in other rodent models (Botfield et al., 2013, Ahmed et al., 2013), therefore it was ideally suited to be tested in this new experimental model of POAG, which is based around the induction of chronic TM fibrosis. A GCP grade of Decorin was used in these studies, which is helpful as the same molecule can be carried through from pre-clinical to clinical studies in patients.

The studies described showed that Decorin was able to reverse established fibrosis in the TM, leading to lowering of IOP, thereby indirectly protecting RGC from progressive death. Through analysis of MMP and TIMP immunostaining it was determined that Decorin (Chapter 5) was able to reverse established TM fibrosis through altering ECM turnover, providing a fibrolytic microenvironment rather than the pro-fibrogenic microenvironment induced through exogenous administration of TGF-β2 (Chapter 4). Although treatment with Decorin was able to reverse established TM fibrosis, lower IOP and indirectly protect RGC, it did not provide any functional benefit according to the VEP data. It is thought that the between, rather than within, subjects design had confounded the data recorded here so the experimental design would need to be altered to record a within subjects VEP, as was carried out in the TGF-β2 alone studies. Another limitation presented in these studies was not recording ERG during the functional testing experiments. It was thought that VEP was

the most suited method to validate the TGF-β model as there were functional deficits shown on VEP demonstrating a reduced visual pathway function to the brain. However, ERG would have been more sensitive to pick up death of cells within the retina and may have been more suited to highlight any functional alterations from cell survival within the retina after Decorin treatment.

Finally, after showing promise as a fibrolytic agent that attenuated established TM fibrosis, a novel method of transcorneal Decorin delivery was developed and tested *in vivo*. The use of a polypeptide arginine conjugated with Decorin showed that the proteoglycan could cross the cornea and penetrate the anterior chamber suggesting that this drug formulation could be further developed as a non-invasive method of drug delivery that could be carried forward for next phase pre-clinical and clinical studies.

## 7.2 Limitations and future studies

### 7.2.1 Alternative method for IOP monitoring

All the IOP monitoring carried out in these studies was intermittent and could, therefore, only provide snapshot IOP values. Although all experiments were designed to take the IOP at the same time of day and at the same frequency for both controls and treatment groups, it may be more useful to conduct continuous IOP monitoring using a contact lens sensor as has been trialled in patients (Mansouri et al., 2012) or pressure sensors as used in rabbits (McLaren et al., 1996). Continuous monitoring of IOP would provide valuable data on IOP

variations throughout a 24 hour time period, permitting any spikes or dips in IOP to be observed, which were not apparent in these studies.

### 7.2.2 Use of contralateral eye for controls

One limitation of this study was the use of the contralateral eye for control PBS injections. Rodent studies have demonstrated that raised IOP in one eye caused microglial activation in the untreated, normotensive, contralateral eye (Rojas et al., 2014). Systemic absorption of agents into the anterior chamber may also alter the IOP in contralateral eyes (Urtti & Salminen, 1993). However, the control data presented here were significantly different to that in the treatment data sets obtained from the same rat using contralateral eyes for controls. This demonstrated that any IOP altering effects to control eyes contralateral to treatment eyes were negligible. Had the control (PBS) group IOP data been similar to the test (TGF-β / Decorin) groups, the systemic effects of TGF-β and Decorin would have been investigated further.

The use of the contralateral eye for a control is a well-established method in other ocular hypertensive models (Ueda et al., 1998; Moreno et al., 2005; Urcola et al., 2006) and this experimental design was therefore deemed appropriate for the IOP models presented here. In addition, the use of a contralateral eye as a control enables a reduction in the number of animals used.

### 7.2.3 Longer experimental time points

Longer term studies would be useful to ascertain if the TGF-β2-induced rise in IOP was sustained over many weeks or months as shown in other experimental glaucoma models. In these studies, the main experiments were all conducted over a 30 day time period. This was decided based on the time taken to induce a sustained elevation in IOP in pilot studies (2 weeks) and the time that it took for IOP to be brought back to baseline after Decorin pilot studies (4 weeks). It is not clear from these studies what would have happened after 4 weeks. Chapter 5 has shown evidence of Decorin reversing established fibrosis, so future studies should involve longer time course experiments which cease Decorin treatment after weeks 2-4 and monitor IOP for a further few weeks to see if it remains at normal levels, as would be expected to happen if TM fibrosis had been reversed.

### 7.2.4 The TGF-β model *versus* alternative models of TM fibrosis to assess the effects of Decorin

Decorin is a direct antagonist for TGF-β, therefore inducing TM fibrosis using exogenous TGF-β could be considered to be a confounded factor in this experimental model. However, the experiments were designed with sequential staging and temporal spacing of the injections of TGF-β and Decorin to overcome any direct interference by Decorin in the binding of exogenously delivered TGF-β. Hence, this implied that the IOP reduction observed with Decorin treatment resulted from lysis of the established TM fibrosis probably by activation of locally produced fibrolytic MMP. Ideally, Decorin will need to be tested in another model

of TM fibrosis which is induced in a TGF-β independent manner. It is possible that TM fibrosis could be induced through administration of steroids, which are known to increase the risk of developing POAG in a subset of patients through increasing myocilin expression in the TM, thus reducing outflow and increasing IOP (Jacobson et al., 2001). Accordingly, Decorin could be tested in a steroid-induced model of TM fibrosis in future work.

Another fruitful avenue of investigation would be to assess the levels of fibrosis attained after 2 weeks, the point at which raised IOP was deemed to be sustained, so that TGF-β2 injections ceased before administering Decorin. However, we tried to address this through the switching of TGF-β to PBS (Chapter 4) injections in control groups, where IOP continued to remain elevated compared to controls. In addition, confirming the baseline level of TGF-β in the normotensive rat eye may have been useful data to gather before commencing TGF-β injections. This would provide further information for dose/response studies with regards how much TGF-β would be required to more closely model in the rat what level of TGF-β changes occur in patients with POAG.

### 7.2.5 Decorin studies

The Decorin studies (Chapter 5) were successful in demonstrating a fibrolytic effect in the TM, with lowering of IOP and subsequent protection of RGC from progressive death. However, the dose of Decorin used in these experiments of 5mg/ml (which would have been further diluted in AqH after injection) was based on previous experiments with Decorin in our laboratory (Botfield et al., 2013; Ahmed et al., 2013) and no dose response studies were

performed to ascertain the lowest concentration to show efficacy. In addition, the effects of intracameral injections of Decorin on normal IOP would need to be assessed as it is unknown from these studies if Decorin would lower IOP in normal, healthy eyes. These will need to be addressed in future studies.

### 7.2.6 Mechanisms of RGC death

Another area which was not addressed in this thesis was the mechanism of RGC death that occurred in the TGF-β model. Some early experimental concerns that were addressed were the possible direct effect of TGF-β on RGC. However, others have shown that TGF-β is neuroprotective for cultured RGC (Walsh et al., 2011), therefore it seems most likely that the RGC death shown *in vivo* in the present studies when TGF-β2 was administered was indeed a result of the TM fibrosis and IOP elevation.

### 7.2.7 Overcoming the translational barriers in glaucoma treatment

IOP lowering agents have been a success story in effective translation from animal models to humans, for example, the trials of Timolol in rabbit (Vareilles et al., 1977). However, most neuroprotective drugs that have worked well in animal models have failed to translate to the clinic, mostly because of fundamental differences in ocular anatomy and relevant experimental designs (reviewed in Ergorul & Levin, 2013). In order to translate Decorin into the clinic as a routine treatment to combat TM fibrosis it would need to be shown to be efficacious in a number of distinct animal models (from mouse to non-human primates) and

future animal model studies for experimental glaucoma should be designed as close to human studies as possible with regards to experimental methods, measured end points and disease relevant time points. The most important barrier to translating new treatments for POAG into the clinic is that no single animal model can replicate the complex pathobiology involved in the development and progression of POAG in patients. However, animals can be useful in mirroring certain aspects of the disease, such as TM fibrosis, to assess the potential of newer treatments, including Decorin.

### 7.3 Final conclusions

Increasing TGF-β levels in AqH induced TM fibrosis, IOP elevations and RGC death, all characteristics of POAG. Decorin was successfully able to reduce established fibrosis, lower IOP and thereby, protect RGC from death. Having established Decorin's promise as a fibrolytic agent to reduce established TM fibrosis, a patented method of transcorneal Decorin delivery was developed and, demonstrated successfully that Decorin could traverse the cornea and penetrate into the anterior chamber. Transcorneal Decorin delivery will be further developed as a non-invasive drug delivery system that could be carried forward for next phase pre-clinical and clinical studies.

## REFERENCES


A Bouhenni, R., J. Dunmire, et al. (2012). "Animal models of glaucoma." Journal of Biomedicine and Biotechnology **2012**.

Acott, T. S. and M. J. Kelley (2008). "Extracellular matrix in the trabecular meshwork." Experimental Eye Research **86**(4): 543-561.

Ahmed, Z., D. Bansal, et al. (2013). "Decorin blocks scarring and cystic cavitation in acute and induces scar dissolution in chronic spinal cord wounds." Neurobiology of Disease.

Alexander, R. and I. Grierson (1989). "Morphological effects of argon laser trabeculoplasty upon the glaucomatous human meshwork." Eye **3**(6): 719-726.

Allen, J. B., M. G. Davidson, et al. (1998). "The lens influences aqueous humor levels of transforming growth factor-β2." Graefe's Archive for Clinical and Experimental Ophthalmology **236**(4): 305-311.

Alm, A., I. Widengård, et al. (1995). "Latanoprost administered once daily caused a maintained reduction of intraocular pressure in glaucoma patients treated concomitantly with timolol." British Journal of Ophthalmology **79**(1): 12-16.

Almasieh, M., A. M. Wilson, et al. (2012). "The molecular basis of retinal ganglion cell death in glaucoma." Progress in Retinal and Eye Research **31**(2): 152-181.

Alvarado, J., C. Murphy, et al. (1984). "Trabecular meshwork cellularity in primary open angle glaucoma and nonglaucomatous normals." Ophthalmology **91**(6): 564-579.

Alvarado, J., C. Murphy, et al. (1981). "Age-related changes in trabecular meshwork cellularity." Investigative Ophthalmology & Visual Science **21**(5): 714-727.

Annes, J. P., Y. Chen, et al. (2004). "Integrin αvβ6-mediated activation of latent TGF-β requires the latent TGF-β binding protein-1." J Cell Biol **165**(5): 723-734.

Asejczyk-Widlicka, M. and B. K. Pierscionek (2007). "Fluctuations in intraocular pressure and the potential effect on aberrations of the eye." Br J Ophthalmol **91**(8): 1054-1058.

Ausinsch, B., S. A. Graves, et al. (1975). "Intraocular pressures in children during isoflurane and halothane anesthesia." Anesthesiology **42**(2): 167-172.

Babizhayev, M. A. and M. W. Brodskaya (1989). "Fibronectin detection in drainage outflow system of human eyes in ageing and progression of open-angle glaucoma." Mechanisms of Ageing and Development **47**(2): 145-157.

Baghy, K., R. V. Iozzo, et al. (2012). "Decorin–TGFβ Axis in Hepatic Fibrosis and Cirrhosis." Journal of Histochemistry & Cytochemistry **60**(4): 262-268.

Barcellos-Hoff, M. and T. A. Dix (1996). "Redox-mediated activation of latent transforming growth factor-beta 1." Molecular Endocrinology **10**(9): 1077-1083.

Becquet, F., M. Goldschild, et al. (1998). "Histopathological effects of topical ophthalmic preservatives on rat corneoconjunctival surface." Curr Eye Res **17**(4): 419-425.

Belforte, N., P. Sande, et al. (2010). "Effect of Chondroitin Sulfate on Intraocular Pressure in Rats." Investigative Ophthalmology & Visual Science **51**(11): 5768-5775.

Benozzi, J., L. P. Nahum, et al. (2002). "Effect of Hyaluronic Acid on Intraocular Pressure in Rats." Investigative Ophthalmology & Visual Science **43**(7): 2196-2200.

Bhan, A., A. C. Browning, et al. (2002). "Effect of Corneal Thickness on Intraocular Pressure Measurements with the Pneumotonometer, Goldmann Applanation Tonometer, and Tono-Pen." Investigative Ophthalmology & Visual Science **43**(5): 1389-1392.

Blobe, G. C., X. Liu, et al. (2001). "A Novel Mechanism for Regulating Transforming Growth Factor β (TGF-β) Signaling FUNCTIONAL MODULATION OF TYPE III TGF-β RECEPTOR EXPRESSION THROUGH INTERACTION WITH THE PDZ DOMAIN PROTEIN, GIPC." Journal of Biological Chemistry **276**(43): 39608-39617.

Borisuth, N., B. Tripathi, et al. (1992). "Identification and partial characterization of TGF-beta 1 receptors on trabecular cells." Investigative Ophthalmology & Visual Science **33**(3): 596-603.
Botfield, H., A. M. Gonzalez, et al. (2013). "Decorin prevents the development of juvenile communicating hydrocephalus." Brain **136**(9): 2842-2858.
Bradley, J. M., M. J. Kelley, et al. (2003). "Signaling pathways used in trabecular matrix metalloproteinase response to mechanical stretch." Investigative Ophthalmology & Visual Science **44**(12): 5174-5181.
Brandan, E., M. E. Fuentes, et al. (1992). "Decorin, a chondroitin/dermatan sulfate proteoglycan is under neural control in rat skeletal muscle." Journal of Neuroscience Research **32**(1): 51-59.
Brubaker, R. F. (1991). "Flow of aqueous humor in humans [The Friedenwald Lecture]." Investigative Ophthalmology & Visual Science **32**(13): 3145-3166.
Brubaker, R. F. (1997). Chapter 9 Clinical Measurements of Aqueous Dynamics: lmplications for Addressing Glaucoma. Current Topics in Membranes. M. C. Mortlmer, Academic Press. **Volume 45:** 233-284.
Buller, C., D. H. Johnson, et al. (1990). "Human trabecular meshwork phagocytosis. Observations in an organ culture system." Investigative Ophthalmology & Visual Science **31**(10): 2156-2163.
Calthorpe, C. M. and I. Grierson (1990). "Fibronectin induces migration of bovine trabecular meshwork cells in vitro." Experimental Eye Research **51**(1): 39-48.
Cantor, L. B. (2006). "Brimonidine in the treatment of glaucoma and ocular hypertension." Therapeutics and clinical risk management **2**(4): 337.
Cao, Y., H. Wei, et al. (2003). "[Effect of transforming growth factor beta 2 on phagocytosis in cultured bovine trabecular meshwork cells]." Der Ophthalmologe: Zeitschrift der Deutschen Ophthalmologischen Gesellschaft **100**(7): 535-538.
Chang, L. and M. Karin (2001). "Mammalian MAP kinase signalling cascades." Nature **410**(6824): 37-40.
Chen, W., K. C. Kirkbride, et al. (2003). "ß-Arrestin 2 mediates endocytosis of type III TGF-ß receptor and down-regulation of its signaling." Science **301**(5638): 1394-1397.
Chi, Z.-L., F. Yasumoto, et al. (2010). "Mutant WDR36 directly affects axon growth of retinal ganglion cells leading to progressive retinal degeneration in mice." Human Molecular Genetics: ddq299.
Chiquet, M., A. S. Renedo, et al. (2003). "How do fibroblasts translate mechanical signals into changes in extracellular matrix production?" Matrix Biology **22**(1): 73-80.
Chiu, K., W. M. Lau, et al. (2008). "Retrograde labeling of retinal ganglion cells by application of fluoro-gold on the surface of superior colliculus." J Vis Exp(16).
Clark, A. F., K. Wilson, et al. (1994). "Glucocorticoid-induced formation of cross-linked actin networks in cultured human trabecular meshwork cells." Investigative Ophthalmology & Visual Science **35**(1): 281-294.
Cohan, B. E. and D. F. Bohr (2001). "Measurement of intraocular pressure in awake mice." Investigative Ophthalmology & Visual Science **42**(11): 2560-2562.
Cone, F. E., M. R. Steinhart, et al. (2012). "The effects of anesthesia, mouse strain and age on intraocular pressure and an improved murine model of experimental glaucoma." Experimental Eye Research **99**(0): 27-35.
Congdon, N., F. Wang, et al. (1992). "Issues in the epidemiology and population-based screening of primary angle-closure glaucoma." Survey of Ophthalmology **36**(6): 411-423.
Cousins, S., M. McCabe, et al. (1991). "Identification of transforming growth factor-beta as an immunosuppressive factor in aqueous humor." Investigative Ophthalmology & Visual Science **32**(8): 2201-2211.
Cousins, S. W., W. B. Trattler, et al. (1991). "Immune privilege and suppression of immunogenic inflammation in the anterior chamber of the eye." Curr Eye Res **10**(4): 287-297.
Cox, D. A. (1995). "Transforming growth factor-beta 3." Cell biology international **19**(5): 357-372.

Crawford, S. E., V. Stellmach, et al. (1998). "Thrombospondin-1 Is a Major Activator of TGF-β1 In Vivo." Cell **93**(7): 1159-1170.
Crouch, E. (1990). "Pathobiology of pulmonary fibrosis." American Journal of Physiology - Lung Cellular and Molecular Physiology **259**(4): L159-L184.
Dai, C., P. T. Khaw, et al. (2012). "Structural basis of glaucoma: the fortified astrocytes of the optic nerve head are the target of raised intraocular pressure." Glia **60**(1): 13-28.
Danielson, K. G., H. Baribault, et al. (1997). "Targeted Disruption of Decorin Leads to Abnormal Collagen Fibril Morphology and Skin Fragility." J Cell Biol **136**(3): 729-743.
Danielson, K. G., A. Fazzio, et al. (1993). "The Human Decorin Gene: Intron-Exon Organization, Discovery of Two Alternatively Spliced Exons in the 5' Untranslated Region, and Mapping of the Gene to Chromosome 12q23." Genomics **15**(1): 146-160.
Davies, J. E., X. Tang, et al. (2004). "Decorin suppresses neurocan, brevican, phosphacan and NG2 expression and promotes axon growth across adult rat spinal cord injuries." European Journal of Neuroscience **19**(5): 1226-1242.
Dickerson, J. J. E., J. H. T. Steely, et al. (1998). "The Effect of Dexamethasone on Integrin and Laminin Expression in Cultured Human Trabecular Meshwork Cells." Experimental Eye Research **66**(6): 731-738.
Diegelmann, R. F. and M. C. Evans (2004). "Wound healing: an overview of acute, fibrotic and delayed healing." Front Biosci **9**(1): 283-289.
Ding, C., P. Wang, et al. (2011). "Effect of general anesthetics on IOP in elevated IOP mouse model." Experimental Eye Research **92**(6): 512-520.
Dong, K., A. K. Ahmed, et al. (1996). "Retrograde fluorescent double-labeling study of bilaterally projecting retinal ganglion cells in albino rats at different stages of development." Brain Res Dev Brain Res **95**(1): 55-62.
Ergorul, C. and L. A. Levin (2013). "Solving the lost in translation problem: Improving the effectiveness of translational research." Current Opinion in Pharmacology **13**(1): 108-114.
Fingert, J. (2011). "Primary open-angle glaucoma genes." Eye **25**(5): 587-595.
Fingert, J. H., A. F. Clark, et al. (2001). "Evaluation of the Myocilin (MYOC) Glaucoma Gene in Monkey and Human Steroid-Induced Ocular Hypertension." Investigative Ophthalmology & Visual Science **42**(1): 145-152.
Fleenor, D. L., A. R. Shepard, et al. (2006). "TGFβ2-Induced Changes in Human Trabecular Meshwork: Implications for Intraocular Pressure." Investigative Ophthalmology & Visual Science **47**(1): 226-234.
Floyd, B. B., P. H. Cleveland, et al. (1985). "Fibronectin in human trabecular drainage channels." Investigative Ophthalmology & Visual Science **26**(6): 797-804.
Flügel-Koch, C., A. Ohlmann, et al. (2004). "Thrombospondin-1 in the trabecular meshwork: localization in normal and glaucomatous eyes, and induction by TGF-β1 and dexamethasone in vitro." Experimental Eye Research **79**(5): 649-663.
Foster, P. J. (2002). The epidemiology of primary angle closure and associated glaucomatous optic neuropathy. Seminars in ophthalmology, Informa UK Ltd UK.
Fuchshofer, R., S. Kuespert, et al. (2014). "The Prostaglandin F2α Analog Fluprostenol Attenuates the Fibrotic Effects of Connective Tissue Growth Factor on Human Trabecular Meshwork Cells." Journal of Ocular Pharmacology and Therapeutics.
Fuchshofer, R. and E. R. Tamm (2009). "Modulation of extracellular matrix turnover in the trabecular meshwork." Experimental Eye Research **88**(4): 683-688.
Fuchshofer, R., U. Welge-Lussen, et al. (2003). "The effect of TGF-β2 on human trabecular meshwork extracellular proteolytic system." Experimental Eye Research **77**(6): 757-765.
Fuchshofer, R., U. Welge-Lüssen, et al. (2006). "Biochemical and morphological analysis of basement membrane component expression in corneoscleral and cribriform human trabecular meshwork cells." Investigative Ophthalmology & Visual Science **47**(3): 794-801.

Gallenberger, M., D. M. Meinel, et al. (2011). "Lack of WDR36 leads to preimplantation embryonic lethality in mice and delays the formation of small subunit ribosomal RNA in human cells in vitro." Human Molecular Genetics **20**(3): 422-435.
Garcia-Valenzuela, E., S. Shareef, et al. (1995). "Programmed cell death of retinal ganglion cells during experimental glaucoma." Experimental Eye Research **61**(1): 33-44.
Giri, S. N., D. M. Hyde, et al. (1997). "Antifibrotic effect of decorin in a bleomycin hamster model of lung fibrosis." Biochemical pharmacology **54**(11): 1205-1216.
Goel, M., R. G. Picciani, et al. (2010). "Aqueous humor dynamics: a review." The open ophthalmology journal **4**: 52.
Goldblum, D., A. Kontiola, et al. (2002). "Non-invasive determination of intraocular pressure in the rat eye. Comparison of an electronic tonometer (TonoPen), and a rebound (impact probe) tonometer." Graefe's Archive for Clinical and Experimental Ophthalmology **240**(11): 942-946.
Goldblum, D. and T. Mittag (2002). "Prospects for relevant glaucoma models with retinal ganglion cell damage in the rodent eye." Vision Research **42**(4): 471-478.
Gonzalez, P., D. L. Epstein, et al. (2000). "Characterization of Gene Expression in Human Trabecular Meshwork Using Single-Pass Sequencing of 1060 Clones." Investigative Ophthalmology & Visual Science **41**(12): 3678-3693.
Gordon, M. O., J. A. Beiser, et al. (2002). "The Ocular Hypertension Treatment Study: baseline factors that predict the onset of primary open-angle glaucoma." Archives of Ophthalmology **120**(6): 714.
Gottanka, J., D. Chan, et al. (2004). "Effects of TGF-β2 in Perfused Human Eyes." Investigative Ophthalmology & Visual Science **45**(1): 153-158.
Gould, D. B., L. Miceli-Libby, et al. (2004). "Genetically increasing Myoc expression supports a necessary pathologic role of abnormal proteins in glaucoma." Molecular and cellular biology **24**(20): 9019-9025.
Grant, W. (1951). "CLinical measurements of aqueous outflow." A.M.A. Archives of Ophthalmology **46**(2): 113-131.
Grierson, I. and R. C. Howes (1987). "Age-related depletion of the cell population in the human trabecular meshwork." Eye **1**(2): 204-210.
Grisanti, S., P. Szurman, et al. (2005). "Decorin Modulates Wound Healing in Experimental Glaucoma Filtration Surgery: A Pilot Study." Investigative Ophthalmology & Visual Science **46**(1): 191-196.
Grover, J., X.-N. Chen, et al. (1995). "The Human Lumican Gene: ORGANIZATION, CHROMOSOMAL LOCATION, AND EXPRESSION IN ARTICULAR CARTILAGE." Journal of Biological Chemistry **270**(37): 21942-21949.
Guo, L., S. E. Moss, et al. (2005). "Retinal Ganglion Cell Apoptosis in Glaucoma Is Related to Intraocular Pressure and IOP-Induced Effects on Extracellular Matrix." Investigative Ophthalmology & Visual Science **46**(1): 175-182.
Haines, D. E. (2013). Fundamental Neuroscience for Basic and Clinical Applications, Elsevier.
Hamanaka, T. and A. Bill (1994). "Platelet Aggregation on the Endothelium of Schlemm's Canal." Experimental Eye Research **59**(3): 249-256.
Hann, C. R., M. J. Springett, et al. (2001). "Ultrastructural localization of collagen IV, fibronectin, and laminin in the trabecular meshwork of normal and glaucomatous eyes." Ophthalmic Research **33**(6): 314-324.
Heiduschka, P., S. Schnichels, et al. (2010). "Electrophysiological and Histologic Assessment of Retinal Ganglion Cell Fate in a Mouse Model for OPA1-Associated Autosomal Dominant Optic Atrophy." Investigative Ophthalmology & Visual Science **51**(3): 1424-1431.
Heijl, A., M. C. Leske, et al. (2002). "Reduction of intraocular pressure and glaucoma progression: results from the Early Manifest Glaucoma Trial." Archives of Ophthalmology **120**(10): 1268.

HENKIND, P., M. LEITMAN, et al. (1973). "The Diurnal Curve in Man: New Observations." Investigative Ophthalmology & Visual Science **12**(9): 705-707.
Hennis, A., S.-Y. Wu, et al. (2003). "Hypertension, diabetes, and longitudinal changes in intraocular pressure." Ophthalmology **110**(5): 908-914.
Hocking, A. M., T. Shinomura, et al. (1998). "Leucine-rich repeat glycoproteins of the extracellular matrix." Matrix Biology **17**(1): 1-19.
Holder, G. (2004). "Electrophysiological assessment of optic nerve disease." Eye (London, England) **18**(11): 1133.
Iester, M., A. Mermoud, et al. (2001). "New Tonopen XL: comparison with the Goldmann tonometer." Eye **15**(1): 52-58.
Inatani, M., H. Tanihara, et al. (2001). "Transforming growth factor-β2 levels in aqueous humor of glaucomatous eyes." Graefe's Archive for Clinical and Experimental Ophthalmology **239**(2): 109-113.
Isaka, Y., D. K. Brees, et al. (1996). "Gene therapy by skeletal muscle expression of decorin prevents fibrotic disease in rat kidney." Nature Medicine **2**(4): 418-423.
Jacobson, N., M. Andrews, et al. (2001). "Non-secretion of mutant proteins of the glaucoma gene myocilin in cultured trabecular meshwork cells and in aqueous humor." Human Molecular Genetics **10**(2): 117-125.
Jampel, H. D., N. Roche, et al. (1990). "Transforming growth factor-β in human aqueous humor." Curr Eye Res **9**(10): 963-969.
Järvinen, T. A. and E. Ruoslahti (2010). "Target-seeking antifibrotic compound enhances wound healing and suppresses scar formation in mice." Proceedings of the National Academy of Sciences **107**(50): 21671-21676.
Jia, L., W. O. Cepurna, et al. (2000). "Effect of General Anesthetics on IOP in Rats with Experimental Aqueous Outflow Obstruction." Investigative Ophthalmology & Visual Science **41**(11): 3415-3419.
Jia, L., W. O. Cepurna, et al. (2000). "Effect of general anesthetics on IOP in rats with experimental aqueous outflow obstruction." Invest Ophthalmol Vis Sci **41**(11): 3415-3419.
Johnson, D. H. (2007). "Histologic findings after argon laser trabeculoplasty in glaucomatous eyes." Experimental Eye Research **85**(4): 557-562.
Johnson, E. C., L. M. H. Deppmeier, et al. (2000). "Chronology of Optic Nerve Head and Retinal Responses to Elevated Intraocular Pressure." Investigative Ophthalmology & Visual Science **41**(2): 431-442.
JOHNSON, E. C., J. C. MORRISON, et al. (1996). "The effect of chronically elevated intraocular pressure on the rat optic nerve head extracellular matrix." Experimental Eye Research **62**(6): 663-674.
Johnson, M. (2006). "'What controls aqueous humour outflow resistance?'." Experimental Eye Research **82**(4): 545-557.
Johnson, M. A., B. A. Drum, et al. (1989). "Pattern-evoked potentials and optic nerve fiber loss in monocular laser-induced glaucoma." Investigative Ophthalmology & Visual Science **30**(5): 897-907.
Johnson, M. C. and R. D. Kamm (1983). "The role of Schlemm's canal in aqueous outflow from the human eye." Investigative Ophthalmology & Visual Science **24**(3): 320-325.
Johnson, T. V., S. Fan, et al. (2010). "Efficacy and mechanisms of intraocular pressure reduction with latanoprost and timolol in participants with ocular hypertension: a comparison of 1 and 6 weeks of treatment." Journal of Glaucoma **19**(6): 356-364.
Johnson, T. V. and S. I. Tomarev (2010). "Rodent models of glaucoma." Brain Research Bulletin **81**(2): 349-358.

Junglas, B., S. Kuespert, et al. (2012). "Connective Tissue Growth Factor Causes Glaucoma by Modifying the Actin Cytoskeleton of the Trabecular Meshwork." The American Journal of Pathology **180**(6): 2386-2403.
Kass, M. A., W. M. Hart, et al. (1980). "Risk factors favoring the development of glaucomatous visual field loss in ocular hypertension." Survey of Ophthalmology **25**(3): 155-162.
Keller, K. E. and T. S. Acott (2013). "The Juxtacanalicular Region of Ocular Trabecular Meshwork: A Tissue with a Unique Extracellular Matrix and Specialized Function." Journal of ocular biology **1**(1): 3.
Khalil, N. (1999). "TGF-β: from latent to active." Microbes and Infection **1**(15): 1255-1263.
Kim, D. H., H. S. Kim, et al. (2004). "Ganglion cell death in rat retina by persistent intraocular pressure elevation." Korean Journal of Ophthalmology **18**(1): 15-22.
Klein, B. E., R. Klein, et al. (1992). "Intraocular pressure in an American community. The Beaver Dam Eye Study." Investigative Ophthalmology & Visual Science **33**(7): 2224-2228.
Klein, B. E. K., R. Klein, et al. (2005). "Intraocular pressure and systemic blood pressure: longitudinal perspective: the Beaver Dam Eye Study." British Journal of Ophthalmology **89**(3): 284-287.
Kolb, M., P. J. Margetts, et al. (2001). "Transient transgene expression of decorin in the lung reduces the fibrotic response to bleomycin." American journal of respiratory and critical care medicine **163**(3): 770-777.
Koliakos, G., U. Schlötzer-Schrehardt, et al. (2001). "Transforming and insulin-like growth factors in the aqueous humour of patients with exfoliation syndrome." Graefe's Archive for Clinical and Experimental Ophthalmology **239**(7): 482-487.
Kontiola, A. I., D. Goldblum, et al. (2001). "The Induction/Impact Tonometer: a New Instrument to Measure Intraocular Pressure in the Rat." Experimental Eye Research **73**(6): 781-785.
Kottler, U. B., A. G. M. Jünemann, et al. (2005). "Comparative effects of TGF-β1 and TGF-β2 on extracellular matrix production, proliferation, migration, and collagen contraction of human Tenon's capsule fibroblasts in pseudoexfoliation and primary open-angle glaucoma." Experimental Eye Research **80**(1): 121-134.
Krishna, R., A. Mermoud, et al. (1995). "Circadian Rhythm of Intraocular Pressure: A Rat Model." Ophthalmic Research **27**(3): 163-167.
Kroese, M. and H. Burton (2003). "Primary open angle glaucoma. The need for a consensus case definition." Journal of epidemiology and community health **57**(9): 752-754.
Kwon, Y. H., J. H. Fingert, et al. (2009). "Primary open-angle glaucoma." New England Journal of Medicine **360**(11): 1113-1124.
Last, J. A., T. Pan, et al. (2011). "Elastic Modulus Determination of Normal and Glaucomatous Human Trabecular Meshwork." Investigative Ophthalmology & Visual Science **52**(5): 2147-2152.
LEASK, A. and D. J. ABRAHAM (2004). "TGF-β signaling and the fibrotic response." The FASEB Journal **18**(7): 816-827.
Leivonen, S.-K., K. Lazaridis, et al. (2013). "TGF-β-Elicited Induction of Tissue Inhibitor of Metalloproteinases (TIMP)-3 Expression in Fibroblasts Involves Complex Interplay between Smad3, p38α, and ERK1/2." PloS one **8**(2): e57474.
Leske, M., A. S. Connell, et al. (1995). "Risk factors for open-angle glaucoma: The barbados eye study." Archives of Ophthalmology **113**(7): 918-924.
Leung, E. W., F. A. Medeiros, et al. (2008). "Prevalence of Ocular Surface Disease in Glaucoma Patients." Journal of Glaucoma **17**(5): 350-355 310.1097/IJG.1090b1013e31815c31815f31814f.
Levkovitch-Verbin, H., H. A. Quigley, et al. (2002). "Translimbal laser photocoagulation to the trabecular meshwork as a model of glaucoma in rats." Investigative Ophthalmology & Visual Science **43**(2): 402-410.

Li, J., B. J. Tripathi, et al. (1996). "Transforming growth factor-beta 1 and -beta 2 positively regulate TGF-beta 1 mRNA expression in trabecular cells." Investigative Ophthalmology & Visual Science **37**(13): 2778-2782.
Lijnen, P., V. Petrov, et al. (2000). "Induction of Cardiac Fibrosis by Transforming Growth Factor-β< sub> 1</sub>." Molecular genetics and metabolism **71**(1): 418-435.
Lippa, E. A., L. Carlson, et al. (1992). "DOse response and duration of action of dorzolamide, a topical carbonic anhydrase inhibitor." Archives of Ophthalmology **110**(4): 495-499.
Liton, P. B., G. Li, et al. (2009). "Cross-talk between TGF-β1 and IL-6 in human trabecular meshwork cells." Molecular vision **15**: 326.
Liton, P. B., X. Liu, et al. (2005). "Induction of TGF-β1 in the trabecular meshwork under cyclic mechanical stress." Journal of Cellular Physiology **205**(3): 364-371.
Liu, C., L. Tai, et al. (2014). "Penetratin, a Potentially Powerful Absorption Enhancer for Noninvasive Intraocular Drug Delivery." Molecular Pharmaceutics.
Liu, J. H., D. F. Kripke, et al. (1998). "Nocturnal elevation of intraocular pressure in young adults." Investigative Ophthalmology & Visual Science **39**(13): 2707-2712.
Liu, X., Z. Wu, et al. (2003). "Low dose latrunculin-A inhibits dexamethasone-induced changes in the actin cytoskeleton and alters extracellular matrix protein expression in cultured human trabecular meshwork cells." Experimental Eye Research **77**(2): 181-188.
Liu, Y. (2006). "Renal fibrosis: new insights into the pathogenesis and therapeutics." Kidney international **69**(2): 213-217.
Llobet, A., X. Gasull, et al. (2003). "Understanding Trabecular Meshwork Physiology: A Key to the Control of Intraocular Pressure?" Physiology **18**(5): 205-209.
Logan, A., A. Baird, et al. (1999). "Decorin attenuates gliotic scar formation in the rat cerebral hemisphere." Experimental Neurology **159**(2): 504-510.
Lütjen-Drecoll, E. (1999). "Functional morphology of the trabecular meshwork in primate eyes." Progress in Retinal and Eye Research **18**(1): 91-119.
Maatta, M., H. Autio-Harmainen, et al. (2002). "Altered aqueous humor levels of MMP-2 and TIMP-2 in glaucoma." Invest. Ophthalmol. Vis. Sci. **43**(12): 2458-.
Maier, P. C., J. Funk, et al. (2005). "Treatment of ocular hypertension and open angle glaucoma: meta-analysis of randomised controlled trials." BMJ **331**(7509): 134.
Mansouri, K., F. A. Medeiros, et al. (2012). "Continuous 24-hour monitoring of intraocular pressure patterns with a contact lens sensor: safety, tolerability, and reproducibility in patients with glaucoma." Archives of Ophthalmology **130**(12): 1534-1539.
Marquardt, H., M. N. Lioubin, et al. (1987). "Complete amino acid sequence of human transforming growth factor type beta 2." Journal of Biological Chemistry **262**(25): 12127-12131.
Matsumoto, Y. and D. H. Johnson (1997). "Dexamethasone decreases phagocytosis by human trabecular meshwork cells in situ." Investigative Ophthalmology & Visual Science **38**(9): 1902-1907.
McAnulty, R. J. (2007). "Fibroblasts and myofibroblasts: their source, function and role in disease." The international journal of biochemistry & cell biology **39**(4): 666-671.
McKee, H., M. Gupta, et al. (2004). "First-choice treatment preferences for primary open-angle glaucoma in the United Kingdom." Eye **19**(8): 923-924.
McLaren, J. W., R. F. Brubaker, et al. (1996). "Continuous measurement of intraocular pressure in rabbits by telemetry." Investigative Ophthalmology & Visual Science **37**(6): 966-975.
Mead, A. L., T. T. L. Wong, et al. (2003). "Evaluation of Anti-TGF-β2 Antibody as a New Postoperative Anti-scarring Agent in Glaucoma Surgery." Investigative Ophthalmology & Visual Science **44**(8): 3394-3401.
Mendoza-Reinoso, V., T. S. Patil, et al. (2012). "Novel and known MYOC exon 3 mutations in an admixed Peruvian primary open-angle glaucoma population." Molecular vision **18**: 2067.

Mermoud, A., G. Baerveldt, et al. (1996). "Aqueous humor dynamics in rats." Graefe's Archive for Clinical and Experimental Ophthalmology **234**(1): S198-S203.
Millard, C. B., B. J. Tripathi, et al. (1987). "Age-related changes in protein profiles of the normal human trabecular meshwork." Experimental Eye Research **45**(4): 623-631.
Mirakhur, R. K., P. Elliott, et al. (1990). "Comparison of the effects of isoflurane and halothane on intraocular pressure." Acta Anaesthesiologica Scandinavica **34**(4): 282-285.
Mitchell, P., W. Smith, et al. (1996). "Prevalence of open-angle glaucoma in Australia. The Blue Mountains Eye Study." Ophthalmology **103**(10): 1661-1669.
Mittag, T. W., J. Danias, et al. (2000). "Retinal damage after 3 to 4 months of elevated intraocular pressure in a rat glaucoma model." Investigative Ophthalmology & Visual Science **41**(11): 3451-3459.
Miyara, N., M. Shinzato, et al. (2008). "Proteomic analysis of rat retina in a steroid-induced ocular hypertension model: potential vulnerability to oxidative stress." Japanese Journal of Ophthalmology **52**(2): 84-90.
Mohan, R. R., A. Tandon, et al. (2011). "Significant inhibition of corneal scarring in vivo with tissue-selective, targeted AAV5 decorin gene therapy." Investigative Ophthalmology & Visual Science **52**(7): 4833-4841.
Moore, C. G., E. C. Johnson, et al. (1996). "Circadian rhythm of intraocular pressure in the rat." Curr Eye Res **15**(2): 185-191.
Moreno-Montañes, J., I. Gosende, et al. (2011). "Comparation of the new rebound tonometer IOPen and the Goldmann tonometer, and their relationship to corneal properties." Eye **25**(1): 50-56.
Moreno, M. C., H. J. A. Marcos, et al. (2005). "A new experimental model of glaucoma in rats through intracameral injections of hyaluronic acid." Experimental Eye Research **81**(1): 71-80.
Morishita, M., N. Kamei, et al. (2007). "A novel approach using functional peptides for efficient intestinal absorption of insulin." Journal of Controlled Release **118**(2): 177-184.
Morrison, J. C., F. W. Fraunfelder, et al. (1995). "Limbal microvasculature of the rat eye." Investigative Ophthalmology & Visual Science **36**(3): 751-756.
Morrison, J. C., L. Jia, et al. (2009). "Reliability and Sensitivity of the TonoLab Rebound Tonometer in Awake Brown Norway Rats." Investigative Ophthalmology & Visual Science **50**(6): 2802-2808.
Morrison, J. C., E. C. Johnson, et al. (2005). "Understanding mechanisms of pressure-induced optic nerve damage." Progress in Retinal and Eye Research **24**(2): 217-240.
Morrison, J. C., K. B. Nylander, et al. (1998). "Glaucoma drops control intraocular pressure and protect optic nerves in a rat model of glaucoma." Investigative Ophthalmology & Visual Science **39**(3): 526-531.
Morton, S., L. Hesson, et al. (2008). "Enhanced binding of TBK1 by an optineurin mutant that causes a familial form of primary open angle glaucoma." FEBS Letters **582**(6): 997-1002.
Munger, J. S., J. G. Harpel, et al. (1997). "Latent transforming growth factor-beta: structural features and mechanisms of activation." Kidney international **51**(5): 1376-1382.
Murgatroyd, H. and J. Bembridge (2008). "Intraocular pressure." Continuing Education in Anaesthesia, Critical Care & Pain **8**(3): 100-103.
Mutsaers, S. E., J. E. Bishop, et al. (1997). "Mechanisms of tissue repair: from wound healing to fibrosis." The international journal of biochemistry & cell biology **29**(1): 5-17.
Nakajima, E., T. Nakajima, et al. (2005). "Contribution of ROCK in contraction of trabecular meshwork: proposed mechanism for regulating aqueous outflow in monkey and human eyes." Journal of pharmaceutical sciences **94**(4): 701-708.
Nassar, K., J. Lüke, et al. (2011). "The novel use of decorin in prevention of the development of proliferative vitreoretinopathy (PVR)." Graefe's Archive for Clinical and Experimental Ophthalmology **249**(11): 1649-1660.
Nathan, C. (2002). "Points of control in inflammation." Nature **420**(6917): 846-852.

Nickells, R. W. (2007). "From ocular hypertension to ganglion cell death: a theoretical sequence of events leading to glaucoma." Canadian Journal of Ophthalmology / Journal Canadien d'Ophtalmologie **42**(2): 278-287.
Nickells, R. W., G. R. Howell, et al. (2012). "Under Pressure: Cellular and Molecular Responses During Glaucoma, a Common Neurodegeneration with Axonopathy." Annual Review of Neuroscience **35**(1): 153-179.
Noecker, R. (2001). "Effects of common ophthalmic preservatives on ocular health." Advances in Therapy **18**(5): 205-215.
Ochiai, Y. and H. Ochiai (2002). "Higher concentration of transforming growth factor-β in aqueous humor of glaucomatous eyes and diabetic eyes." Japanese Journal of Ophthalmology **46**(3): 249-253.
Ozcan, A. A., N. Ozdemir, et al. (2004). "The aqueous levels of TGF-β2 in patients with glaucoma." International Ophthalmology **25**(1): 19-22.
Parisi, V. (2001). "Impaired visual function in glaucoma." Clinical Neurophysiology **112**(2): 351-358.
Pease, M. E., F. E. Cone, et al. (2011). "Calibration of the TonoLab tonometer in mice with spontaneous or experimental glaucoma." Invest Ophthalmol Vis Sci **52**(2): 858-864.
Pekny, M. and M. Nilsson (2005). "Astrocyte activation and reactive gliosis." Glia **50**(4): 427-434.
Polansky, J. R., I. S. Wood, et al. (1984). "Trabecular meshwork cell culture in glaucoma research: evaluation of biological activity and structural properties of human trabecular cells in vitro." Ophthalmology **91**(6): 580-595.
Porter, K. M., D. L. Epstein, et al. (2012). "Up-Regulated Expression of Extracellular Matrix Remodeling Genes in Phagocytically Challenged Trabecular Meshwork Cells." PloS one **7**(4): e34792.
Quigley, H. A. and E. M. Addicks (1980). "Chronic experimental glaucoma in primates. II. Effect of extended intraocular pressure elevation on optic nerve head and axonal transport." Investigative Ophthalmology & Visual Science **19**(2): 137-152.
Quigley, H. A., E. M. Addicks, et al. (1981). "Optic nerve damage in human glaucoma. II. The site of injury and susceptibility to damage." Archives of Ophthalmology **99**(4): 635-649.
Quigley, H. A. and A. T. Broman (2006). "The number of people with glaucoma worldwide in 2010 and 2020." British Journal of Ophthalmology **90**(3): 262-267.
Quigley, H. A., S. J. McKinnon, et al. (2000). "Retrograde axonal transport of BDNF in retinal ganglion cells is blocked by acute IOP elevation in rats." Investigative Ophthalmology & Visual Science **41**(11): 3460-3466.
Razeghinejad, M., M. Pro, et al. (2011). "Non-steroidal drug-induced glaucoma." Eye **25**(8): 971-980.
Reiss, G. R., D. A. Lee, et al. (1984). "Aqueous humor flow during sleep." Investigative Ophthalmology & Visual Science **25**(6): 776-778.
Rieck, J. (2013). "The Pathogenesis of Glaucoma in the Interplay with the Immune System." Investigative Ophthalmology & Visual Science **54**(3): 2393-2409.
Ringvold, A. (1980). "AQUEOUS HUMOUR AND ULTRAVIOLET RADIATION." Acta Ophthalmologica **58**(1): 69-82.
Roberts, M. D., I. A. Sigal, et al. (2010). "Changes in the Biomechanical Response of the Optic Nerve Head in Early Experimental Glaucoma." Investigative Ophthalmology & Visual Science **51**(11): 5675-5684.
Robertson, J. V., E. Golesic, et al. (2010). "Ocular Gene Transfer of Active TGF-β Induces Changes in Anterior Segment Morphology and Elevated IOP in Rats." Investigative Ophthalmology & Visual Science **51**(1): 308-318.
Robertson, J. V., A. Siwakoti, et al. (2013). "Altered expression of transforming growth factor beta 1 and matrix metalloproteinase-9 results in elevated intraocular pressure in mice." Molecular vision **19**: 684.

Rojas, B., B. I. Gallego, et al. (2014). "Microglia in mouse retina contralateral to experimental glaucoma exhibit multiple signs of activation in all retinal layers." J Neuroinflammation **11**: 133.
Rönkkö, S., P. Rekonen, et al. (2007). "Matrix metalloproteinases and their inhibitors in the chamber angle of normal eyes and patients with primary open-angle glaucoma and exfoliation glaucoma." Graefe's Archive for Clinical and Experimental Ophthalmology **245**(5): 697-704.
Rosenbaum, J. T., A. Woods, et al. (2011). "Contrasting ocular effects of local versus systemic endotoxin." Investigative Ophthalmology & Visual Science **52**(9): 6472-6477.
Rouland, J.-F., C. E. Traverso, et al. (2013). "Efficacy and safety of preservative-free latanoprost eyedrops, compared with BAK-preserved latanoprost in patients with ocular hypertension or glaucoma." British Journal of Ophthalmology **97**(2): 196-200.
Rudnicka, A. R., S. Mt-Isa, et al. (2006). "Variations in Primary Open-Angle Glaucoma Prevalence by Age, Gender, and Race: A Bayesian Meta-Analysis." Investigative Ophthalmology & Visual Science **47**(10): 4254-4261.
Saadat, F., A. Raji, et al. (2003). "Alteration in matrix metalloproteinases (MMPs) activity in fibroblast cell line by dexamethasone: a possible mechanism in corticosteroid-induced glaucoma." Iranian Journal of Allergy, Asthma and Immunology **2**(3).
Sakimoto, A., M. Sawa, et al. (2009). "Minimum endotoxin concentration causing inflammation in the anterior segment of rabbit eyes." Japanese Journal of Ophthalmology **53**(4): 425-432.
Sanka, K., R. Maddala, et al. (2007). "Influence of Actin Cytoskeletal Integrity on Matrix Metalloproteinase-2 Activation in Cultured Human Trabecular Meshwork Cells." Investigative Ophthalmology & Visual Science **48**(5): 2105-2114.
Sappington, R. M., B. J. Carlson, et al. (2010). "The Microbead Occlusion Model: A Paradigm for Induced Ocular Hypertension in Rats and Mice." Investigative Ophthalmology & Visual Science **51**(1): 207-216.
Sawada, A. and A. H. Neufeld (1999). "Confirmation of the Rat Model of Chronic, Moderately Elevated Intraocular Pressure." Experimental Eye Research **69**(5): 525-531.
Schloetzer-Schrehardt, U., M. ZENKEL, et al. (2001). "Role of transforming growth factor-1 and its latent form binding protein in pseudoexfoliation syndrome." Experimental Eye Research **73**(6): 765-780.
Schlötzer-Schrehardt, U., J. Lommatzsch, et al. (2003). "Matrix Metalloproteinases and Their Inhibitors in Aqueous Humor of Patients with Pseudoexfoliation Syndrome/Glaucoma and Primary Open-Angle Glaucoma." Investigative Ophthalmology & Visual Science **44**(3): 1117-1125.
Schlötzer-Schrehardt, U., M. Zenkel, et al. (2001). "Role of Transforming Growth Factor-β1 and its Latent Form Binding Protein in Pseudoexfoliation Syndrome." Experimental Eye Research **73**(6): 765-780.
Schmidt, G., H. Hausser, et al. (1991). "Interaction of the small proteoglycan decorin with fibronectin. Involvement of the sequence NKISK of the core protein." Biochem. J **280**: 411-414.
Scott, I. U., D. S. Greenfield, et al. (1998). "OUtcomes of primary trabeculectomy with the use of adjunctive mitomycin." Archives of Ophthalmology **116**(3): 286-291.
Scott, P. G., P. A. McEwan, et al. (2004). "Crystal structure of the dimeric protein core of decorin, the archetypal small leucine-rich repeat proteoglycan." Proc Natl Acad Sci U S A **101**(44): 15633-15638.
Seah, S. K., P. J. Foster, et al. (1997). "Incidence of acute primary angle-closure glaucoma in Singapore: an island-wide survey." Archives of Ophthalmology **115**(11): 1436-1440.
Senatorov, V., I. Malyukova, et al. (2006). "Expression of mutated mouse myocilin induces open-angle glaucoma in transgenic mice." The Journal of Neuroscience **26**(46): 11903-11914.

Shah, M., D. M. Foreman, et al. (1995). "Neutralisation of TGF-beta 1 and TGF-beta 2 or exogenous addition of TGF-beta 3 to cutaneous rat wounds reduces scarring." Journal of cell science **108**(3): 985-1002.

Shepard, A. R., J. C. Millar, et al. (2010). "Adenoviral Gene Transfer of Active Human Transforming Growth Factor-β2 Elevates Intraocular Pressure and Reduces Outflow Facility in Rodent Eyes." Investigative Ophthalmology & Visual Science **51**(4): 2067-2076.

Sime, P. J., Z. Xing, et al. (1997). "Adenovector-mediated gene transfer of active transforming growth factor-beta1 induces prolonged severe fibrosis in rat lung." Journal of Clinical Investigation **100**(4): 768.

Snell, R. (1998). Clinical anatomy of the eye. London, Wiley-Blackwell.

Sommer, A., J. M. Tielsch, et al. (1991). "Relationship between intraocular pressure and primary open angle glaucoma among white and black Americans. The Baltimore Eye Survey." Archives of Ophthalmology **109**(8): 1090-1095.

Stahnke, T., M. Löbler, et al. (2012). "Different fibroblast subpopulations of the eye: a therapeutic target to prevent postoperative fibrosis in glaucoma therapy." Experimental Eye Research **100**: 88-97.

Stamer, W., E. Hoffman, et al. (2011). "Protein profile of exosomes from trabecular meshwork cells." Journal of proteomics **74**(6): 796-804.

Stamer, W. D., R. E. Seftor, et al. (1995). "Isolation and culture of human trabecular meshwork cells by extracellular matrix digestion." Curr Eye Res **14**(7): 611-617.

Stamper, R. L. (2011). "A history of intraocular pressure and its measurement." Optom Vis Sci **88**(1): E16-28.

Steely, H. T., S. L. Browder, et al. (1992). "The effects of dexamethasone on fibronectin expression in cultured human trabecular meshwork cells." Investigative Ophthalmology & Visual Science **33**(7): 2242-2250.

Subak-Sharpe, I., S. Low, et al. (2010). "Pharmacological and environmental factors in primary angle-closure glaucoma." British Medical Bulletin **93**(1): 125-143.

Takeuchi, Y., Y. Kodama, et al. (1994). "Bone matrix decorin binds transforming growth factor-beta and enhances its bioactivity." Journal of Biological Chemistry **269**(51): 32634-32638.

Tamada, Y., T. Taniguchi, et al. (2001). "Intraocular pressure-lowering efficacy of latanoprost in patients with normal-tension glaucoma or primary open-angle glaucoma." Journal of Ocular Pharmacology and Therapeutics **17**(1): 19-25.

Tamm, E. R. and R. Fuchshofer (2007). "What Increases Outflow Resistance in Primary Open-angle Glaucoma?" Survey of Ophthalmology **52**(6, Supplement): S101-S104.

Tamm, E. R., P. Russell, et al. (1999). "Modulation of Myocilin/TIGR Expression in Human Trabecular Meshwork." Investigative Ophthalmology & Visual Science **40**(11): 2577-2582.

Tamm, E. R., A. Siegner, et al. (1996). "Transforming Growth Factor-β1 Induces α-Smooth Muscle-Actin Expression in Cultured Human and Monkey Trabecular Meshwork." Experimental Eye Research **62**(4): 389-398.

Tielsch, J. M., J. Katz, et al. (1994). "Family history and risk of primary open angle glaucoma: the Baltimore Eye Survey." Archives of Ophthalmology **112**(1): 69.

Towle, V. L., A. Moskowitz, et al. (1983). "The visual evoked potential in glaucoma and ocular hypertension: effects of check size, field size, and stimulation rate." Investigative Ophthalmology & Visual Science **24**(2): 175-183.

Tripathi, R. C., J. Li, et al. (1994). "Aqueous Humor in Glaucomatous Eyes Contains an Increased Level of TGF-β2." Experimental Eye Research **59**(6): 723-728.

Tsai, J. C., L. Wu, et al. (2005). "Intravitreal Administration of Erythropoietin and Preservation of Retinal Ganglion Cells in an Experimental Rat Model of Glaucoma." Curr Eye Res **30**(11): 1025-1031.

Tsuji, F., K. Sawa, et al. (1997). "The effects of betamethasone derivatives on endotoxin-induced uveitis in guinea pigs." Inflammation Research **46**(12): 486-490.
Tsuruga, H., H. Murata, et al. (2012). "A model for the easy assessment of pressure-dependent damage to retinal ganglion cells using cyan fluorescent protein-expressing transgenic mice." Mol Vis **18**: 2468-2478.
Ueda, J., S. Sawaguchi, et al. (1998). "Experimental Glaucoma Model in the Rat Induced by Laser Trabecular Photocoagulation After an Intracameral Injection of India Ink." Japanese Journal of Ophthalmology **42**(5): 337-344.
Ueda, J., K. Wentz-Hunter, et al. (2002). "Distribution of myocilin and extracellular matrix components in the juxtacanalicular tissue of human eyes." Investigative Ophthalmology & Visual Science **43**(4): 1068-1076.
Ueda, J., K. Wentz-Hunter, et al. (2002). "Distribution of Myocilin and Extracellular Matrix Components in the Juxtacanalicular Tissue of Human Eyes." Investigative Ophthalmology & Visual Science **43**(4): 1068-1076.
Urcola, J. H., M. Hernández, et al. (2006). "Three experimental glaucoma models in rats: comparison of the effects of intraocular pressure elevation on retinal ganglion cell size and death." Experimental Eye Research **83**(2): 429-437.
Vareilles, P., D. Silverstone, et al. (1977). "Comparison of the effects of timolol and other adrenergic agents on intraocular pressure in the rabbit." Investigative Ophthalmology & Visual Science **16**(11): 987-996.
Vidal-Sanz, M., G. Bray, et al. (1991). "Regenerated synapses persist in the superior colliculus after the regrowth of retinal ganglion cell axons." Journal of neurocytology **20**(11): 940-952.
Vittal, V., A. Rose, et al. (2005). "Changes in Gene Expression by Trabecular Meshwork Cells in Response to Mechanical Stretching." Investigative Ophthalmology & Visual Science **46**(8): 2857-2868.
Walshe, T. E., L. L. Leach, et al. (2011). "TGF-β signaling is required for maintenance of retinal ganglion cell differentiation and survival." Neuroscience **189**: 123-131.
Wang, J.-Y., G.-g. Han, et al. (2009). "BMP-7: Therapeutic target for ocular fibrotic disorders." Bioscience Hypotheses **2**(6): 413-416.
Wang, W.-H., J. C. Millar, et al. (2005). "Noninvasive measurement of rodent intraocular pressure with a rebound tonometer." Investigative Ophthalmology & Visual Science **46**(12): 4617-4621.
Weber, I. T., R. W. Harrison, et al. (1996). "Model structure of decorin and implications for collagen fibrillogenesis." Journal of Biological Chemistry **271**(50): 31767-31770.
Weinreb, R., E. Cotlier, et al. (1996). "The extracellular matrix and its modulation in the trabecular meshwork." Survey of Ophthalmology **40**(5): 379-390.
Weinreb, R. N. and P. T. Khaw (2004). "Primary open-angle glaucoma." The Lancet **363**(9422): 1711-1720.
Weinreb, R. N., J. R. Polansky, et al. (1985). "Acute effects of dexamethasone on intraocular pressure in glaucoma." Investigative Ophthalmology & Visual Science **26**(2): 170-175.
Wessendorf, M. W. (1991). "Fluoro-Gold: composition, and mechanism of uptake." Brain Res **553**(1): 135-148.
Wiederholt, M., H. Thieme, et al. (2000). "The regulation of trabecular meshwork and ciliary muscle contractility." Progress in Retinal and Eye Research **19**(3): 271-295.
Wilbanks, G. A., M. Mammolenti, et al. (1992). "Studies on the induction of anterior chamber-associated immune deviation (ACAID) III. Induction of ACAID depends upon intraocular transforming growth factor-β." European Journal of Immunology **22**(1): 165-173.
Williams, P. A., G. R. Howell, et al. (2013). "Retinal Ganglion Cell Dendritic Atrophy in DBA/2J Glaucoma." PloS one **8**(8): e72282.

Wilson, K., M. D. McCartney, et al. (1993). "Dexamethasone induced ultrastructural changes in cultured human trabecular meshwork cells." Curr Eye Res **12**(9): 783-793.
Wong, T. T. L., A. L. Mead, et al. (2003). "Matrix Metalloproteinase Inhibition Modulates Postoperative Scarring after Experimental Glaucoma Filtration Surgery." Investigative Ophthalmology & Visual Science **44**(3): 1097-1103.
Wu, S. and M. Leske (1997). "ASsociations with intraocular pressure in the barbados eye study." Archives of Ophthalmology **115**(12): 1572-1576.
Yamaguchi, Y., D. M. Mann, et al. (1990). "Negative regulation of transforming growth factor-β by the proteoglycan decorin." Nature **346**(6281): 281-284.
Yamaguchi, Y. and E. Ruoslahti (1988). "Expression of human proteoglycan in Chinese hamster ovary cells inhibits cell proliferation."
Yan, W., P. Wang, et al. (2009). "Decorin gene delivery inhibits cardiac fibrosis in spontaneously hypertensive rats by modulation of transforming growth factor-β/Smad and p38 mitogen-activated protein kinase signaling pathways." Human gene therapy **20**(10): 1190-1200.
Yang, J., K. Zhang, et al. (2003). "Serum Matrix Metalloproteinase Levels and Activities in Patients With Glaucoma." Invest. Ophthalmol. Vis. Sci. **44**(5): 102-.
Yoon, P. S. and K. Singh (2004). "Update on antifibrotic use in glaucoma surgery, including use in trabeculectomy and glaucoma drainage implants and combined cataract and glaucoma surgery." Current Opinion in Ophthalmology **15**(2): 141-146.
Yu, S., T. Tanabe, et al. (2006). "A rat model of glaucoma induced by episcleral vein ligation." Experimental Eye Research **83**(4): 758-770.
Yu, X. B., X. H. Sun, et al. (2007). "Increased levels of transforming growth factor-betal and -beta2 in the aqueous humor of patients with neovascular glaucoma." Ophthalmic Surg Lasers Imaging **38**(1): 6-14.
Zavadil, J. and E. P. Böttinger (2005). "TGF-β and epithelial-to-mesenchymal transitions." Oncogene **24**(37): 5764-5774.
Zhang, G., S. Chen, et al. (2009). "Genetic Evidence for the Coordinated Regulation of Collagen Fibrillogenesis in the Cornea by Decorin and Biglycan." Journal of Biological Chemistry **284**(13): 8888-8897.
Zhang, X.-Y., Y.-Q. Xiao, et al. (2013). "Protective effect of pioglitazone on retinal ischemia/reperfusion injury in rats." Investigative Ophthalmology & Visual Science **54**(6): 3912-3921.
Zhao, X., K. E. Ramsey, et al. (2004). "Gene and Protein Expression Changes in Human Trabecular Meshwork Cells Treated with Transforming Growth Factor-β." Investigative Ophthalmology & Visual Science **45**(11): 4023-4034.
Zhong, L. (2013). "A modified chronic ocular hypertension rat model for retinal ganglion cell neuroprotection." Frontiers of Medicine **7**(3): 367-377.